THE ROLE OF PHOTORECEPTORS IN HUMAN SKIN PHYSIOLOGY; POTENTIAL TARGETS FOR LIGHT-BASED WOUND HEALING TREATMENTS

Identification of opsins and cryptochromes and the effect of photobiomodulation on human skin and in cultured primary epidermal keratinocytes and dermal fibroblasts

I. CASTELLANO PELLICENA

Submitted for the Degree of Doctor of Philosophy

Centre for Skin Sciences

Faculty of Life Sciences

University of Bradford

2017

ABSTRACT

Irene Castellano Pellicena

The role of photoreceptors in human skin physiology; potential targets for light-based wound healing treatments.

Keywords: Human skin, keratinocytes, fibroblasts, opsins, cryptochromes, photobiomodulation, light, wound healing.

The positive effect of photobiomodulation in wound healing has previously been reported, however there is a considerable lack of knowledge regarding the molecular mechanisms involved, and no consensus on light parameters. Cytochrome c oxidase (CCO) is established as the main photoreceptor in cells, but light also induces nitric oxide (NO), production of reactive oxygen species (ROS) and activation of ion channels. Emerging new molecular targets include the GPCRs opsins (OPNs) and the circadian clock transcription factors, cryptochromes (CRYs).

Localisation of OPN1-SW, OPN3, OPN5, CRY1 and CRY2 was seen in female facial and abdominal human skin. Furthermore, expression of these photoreceptors was retained in primary epidermal keratinocytes and dermal fibroblasts in culture; both cell types expressed OPN1-SW, OPN3, CRY1 and CRY2, at the mRNA and protein level. OPN2 was only expressed in cultured dermal fibroblasts, while in line with *in situ* expression, *OPN5* was only expressed in cultured keratinocytes. The photoreceptor-expressing cultured epidermal keratinocytes demonstrated a dose- and wavelength- dependent response in both metabolic activity and cell migration in a scratch-wound assay. Specifically, low dose (2 J/cm^2) blue light (447 nm) increased metabolic activity, but it did not impact keratinocyte migration. In contrast, high dose (30 J/cm^2) blue light had no effect on metabolism, but inhibited migration of epidermal keratinocytes. Red light (655 nm) at 30 J/cm^2 stimulated metabolic activity but did not modulate migration, while a higher dose of 60 J/cm^2 had no effect on keratinocyte metabolic activity.

In order to study OPN3 and CRY1 function, they were silenced in keratinocytes using siRNA; additionally 8 μM KL001 was used to stabilize CRY1. KL001 inhibited migration, and induced *KRT1* and *KRT10*, an effect which was abrogated by knockdown of OPN3. Interestingly, knockdown of OPN3 upregulated *CRY1* expression, while KL001 upregulated *OPN3* expression, indicating a regulation by OPN3 of the molecular epidermal clock. Low levels of blue light increased early differentiation of epidermal keratinocytes, which was mediated by OPN3 and circadian clock mechanisms. However, low levels of blue light decreased keratinocyte DNA synthesis, which was mediated by circadian clock independently of OPN3. Translation of parameters *ex vivo* showed increasing re-epithelialisation and induction of *OPN3* and *CRY1* expression following exposure to 2 J/cm^2 of blue light; however high doses of blue light inhibited re-epithelialisation. Red light, also increased re-epithelialisation, but had no effect on *OPN3* or *CRY1* expression.

In conclusion, photoreceptors are expressed in human skin and they mediate DNA synthesis, migration and differentiation of epidermal keratinocytes. Furthermore, low dose of blue light interacts with OPN3 to induce epidermal differentiation, through the regulation of the circadian clock. A better understanding of the molecular mechanisms behind the photobiomodulation response *in vitro* will help to develop light based therapies for human wound healing. Interestingly, selected light parameters translated to human *ex vivo* skin showed a beneficial effect of low doses of blue (2 J/cm^2) and red (30 J/cm^2) light in re-epithelialisation.

RESUMEN

Irene Castellano Pellicena

El papel de los fotoreceptores en la fisiología de la piel humana; potenciales dianas para terapias de luz para la regeneración de heridas

Palabras clave: regeneración de heridas, fotoreceptores, ritmo circadiano, opsinas, criptocromo, fotobiomodulación, terapias basadas en luz, piel

El efecto beneficioso de la fotobiomodulación para regeneración de heridas se ha mostrado anteriormente, sin embargo, los mecanismos moleculares implicados no están completamente estudiados y existe una falta de consenso en los parámetros de luz que se deben aplicar para el tratamiento de regeneración de heridas. El citocromo c oxidasa es uno de los principales fotoreceptores que existen en las células, aunque la luz también es capaz de producir óxido nítrico y especies oxidativas al oxigeno así como de activar canales iónicos. Nuevas dianas moleculares emergentes incluyen los receptores acoplados a proteínas G (RAPG) opsinas (OPNs) y los factores de transcripción criptocromos (CRYs), que forman parte del ritmo circadiano.

OPN1-SW, OPN3, OPN5, CRY1 y CRY2 se localizaron en piel femenina facial y abdominal. Además, la expresión de éstos fotoreceptores se mantuvo en queratinocitos epidérmicos y fibroblastos dérmicos primarios en cultivo; ambos tipos celulares expresaron OPN1-SW, OPN3, CRY1 y CRY2, a nivel de mARN y proteína. OPN2 sólo se expresaba en cultivos de fibroblastos dérmics, mientras que en línea con la expresión en piel *in situ,* OPN5 sólo se expresaba en cultivos de queratinocitos epidérmicos. Los queratinocitos, los cuales expresan fotoreceptores, mostraron una respuesta dependiente de dosis y longitud de onda en actividad metabólica y migración celular. En concreto, dosis bajas (2 J/cm^2) de luz azul (447 nm) aumentaron la actividad metabólica en queratinocitos, pero no su capacidad de migración. Por otro lado, dosis altas (30 J/cm^2) de luz azul no tuvieron ningún efecto en actividad metabólica, pero redujeron su migración. La luz roja (655 nm) a 30 J/cm^2 estimuló la actividad metabólica pero no produjeron ningún efecto en la migración de los

queratinocitos, mientras que una dosis más alta, de 60 J/cm^2, no afectó su actividad metabólica.

El silenciamiento de OPN3 y CRY1 se realizó usando la tecnología de siARN para estudiar la función de ambos fotoreceptores en queratinocitos: además, 8 µM de KL001 se usó para estabilizar CRY1. KL001 inhibió la migración e indujo la expresión de *KRT1* y *KRT10.* Estos efectos fueron anulados tras la rápida reducción de OPN3. Resulta interesante ver cómo tras knockdown OPN3, se indujo la expresión de *CRY1*, mientras que KL001 indujo la expresión de *OPN3*, indicando una regulación por parte de OPN3 del reloj circadiano molecular de la epidermis. Niveles bajos de luz azul incrementaron la diferenciación de queratinocitos epidérmicos, lo cual era mediado por PON3 y el reloj circadiano molecular. Sin embargo, bajos niveles de luz azul disminuyó la síntesis de ADN en queratinocitos epidérmicos, efecto mediado por el reloj circadiano molecular independientemente de OPN3. La transmisión de parámetros *ex vivo* mostró un incremento en re-epitelización de la epidermis y un incremento en la expresión de *OPN3* y *CRY1* tras la exposición a 2 J/cm^2 de luz azul; sin embargo, altas dosis de luz azul, inhibió en grado de re-epitelización de heridas *ex vivo*. La luz roja también mostró un incremento en re-epitelización de heridas, sin embargo no mostró cambios en la expresión de *OPN3* o *CRY1*.

En conclusión, se encuentra la expresión de fotoreceptores en piel humana. Estos fotoreceptores son capaces de controlar la síntesis de ADN, la migración y la diferenciación de queratinocitos epidérmicos. Además, una dosis baja de luz azul active OPN3 e induce la diferenciación de éstas células, a través de la acción del ritmo circadiano. Un mayor conocimiento de los mecanismos moleculares que están detrás de la respuesta a la fotobiomodulación *in vitro* ayudará a desarrollar terapias de luz para regeneración de heridas. Curiosamente, los parámetros seleccionados en éste estudio se usaron para la traducción a un modelo humano de regeneración de heridas *ex vivo*, lo cual mostró el efecto beneficioso de una baja dosis (2J/cm^2) de luz azul y de luz roja (30 J/cm^2) en el nivel de re-epitelización de heridas.

ACKNOWLEDGEMENTS

I would like to express my sincere gratitude to all those people who make this project possible. I would like to first offer my especial thanks to my PhD supervisor, Dr. M. Julie Thornton for giving me the opportunity to study thoroughly the unknown world of skin biology which has become my field of expertise during the last four years. I also would like to thank Prof. Vladimir Botchkarev, to be my second support within the Center for Skin Sciences (CSS). Philips Research, NL deserves a special mention, especially Dr. Natallia E. Uzunbajaba for all her suggestions, feedback, discussions and enthusiasm and Bianca Raafs for all the help and support in the biolabs, HTC 34 and 11.

I would like to express my gratitude to the Marie Curie actions which granted the CLaSSiC project. Its structure and organisation helped me growing professionally much more than I could have ever imagined. This grant was also the reason of how my way ended up divided into two extremely different towns, Bradford and Eindhoven.

Additionally, my especial thanks are extended to Charles, Serena, Jing Qin, Igor and Charlie, for the stressed, unfair, tense, funny and remarkable moments lived together. There was no other way to go through a PhD in Bradford but with you on my side. I have also gained an awesome international family in Eindhoven, Ajay, Namitha, Juan, Remon, Kata, Mohammed, Ahmet, David, Svetlyn and Ervin, thank you all. They are the biggest present I got during this PhD.

Finalmente, me gustaría agradecer a mi familia y amigos todo el apoyo emocional que he recibido desde la distancia durante los últimos cuatro años. Gracias mama, papá y abuelos, por la ayuda y educación que me habéis dado durante toda mi vida. Habéis sido un modelo a seguir. Gracias Carlos, por tus múltiples visitas que nos han ayudado a crecer como hermanos a pesar de la distancia. Todos vosotros habéis hecho posible que hoy reciba mi título de doctora (PhD) en el Reino Unido. ¡Gracias!

TABLE OF CONTENTS

LIST OF FIGURES

LIST OF TABLES

ABREVIATIONS

α-SMA	α-Smooth Muscle Actin
λ	Wavelength
7TM	Seven transmembrane receptor
A	Area
ATP	Adenosine triphosphate
BMAL1	Brain and muscle ARNT (arylhydrocarbon receptor nuclear translocator)-like protein 1
CAMKII	Ca^{2+}/calmodulin-dependent protein kinase II
Ca^{2+}	Calcium
cDNA	Complementary Deoxyribonucleic Acid
CHK ½	CSK-homologous kinase ½
CKI	Casein kinase I
CLOCK	Circadian locomotor output cycles kaput
CNS	Central nervous system
CP	Committed Progenitor
CREB	cAMP response element-binding protein
CRY	Cryptochrome
CTCF	Corrected Total Cell Fluorescence
Cu	Copper
DAPI	4',6-diamidino-2-phenylindole (DAPI)
Dex	Dexamethasone
DMEM	Dulbecco's Modified Eagle Medium
DMSO	Dimethylsulfoxide
DNA	Deoxyribonucleic Acid
ECM	Extracellular Matrix
EDTA	Ethylenediaminetetraacetic acid
EdU	5-ethynyl-2'-deoxyuridine
EMT	Epithelial-mesenchymal transition
EPU	Epidermal Proliferative Units
FA	Focal Adhesion

FACIT	Fibril Associated Collagens with Interrupted Triple helices
FAD	Flavin Adenine Dinucleotide
FBS	Fetal Bovine Serum
GAG	Glycosaminglycan
GPCR	G Protein-Coupled Receptor
ICC	Immunocytochemistry
ID	Integrated Density
IFE	Interfollicular Epidermis
IgG	Immunoglobulin G
IL-1	Interleukin-1
IR	Infra-red
KRT	Keratin
KCN	Potassium Cyanide
LD	Longdaysin
LED	Light-emitting diode
LLLT	Low-Level Laser Therapy
MET	Mesenchymal-epithelial transition
MMP	Matrix metalloproteinase
mRNA	Messenger ribonucleic acid
NF-κB	Nuclear factor kappa of activated B cells
NFAT	Nuclear transcriptions factor of activated T-cells
NIR	Near-infrared
NTRC	Non-target siRNA control
OPN	Opsin
PBS	Phosphate buffered saline
PCL	Polycation liposome
PCR	Polymerase Chain Reaction
Pen/Strep	Penicillin/Streptomycin
PER1, 2, 3	Period circadian protein homologue 1, 2 and 3
PFGM	Primary Fibroblasts Growth Media
PFSM	Primary Fibroblasts Starvation Media
PKGM	Primary Keratinocytes Growth Media

Plg	Plasminogen
PMN	Polymorphonuclear
R	Constitutively inactive state
R*	Constitutively active state
RHO	Rhodopsin
ROR	Retinoic acid receptor-related Orphan Receptor
ROS	Reactive Oxygen Species
RPE	Retinal pigment epithelium
RT-PCR	Reverse transcriptase polymerase chain reaction
RT-qPCR	Reverse transcriptase quantitative polymerase chain reaction
SC	Stem Cell
SCN	Suprachiasmatic Nucleous
SD	Standard Deviation
TA	Transit-Amplifying
TAE	Tris-Acetate-EDTA
TE	Trypsin/EDTA
TGF-β1	Transforming growth factor beta 1
TNS	Trypsin neutralising solution
TRPV1	Transient receptor potential vanilloid type 1 receptor
TTX	Tetrodotoxin
UV	Ultraviolet

1 Introduction

1.1 Skin structure and its appendages

The skin is the largest organ in the human body covering a surface of between 1.5 and 2m^2 and containing several appendages such as hair follicles, sebaceous glands, sweat glands and nails. The main functions of the skin are to provide a protective water-proof barrier, which prevents the underlying structures from damage either because of injury or microbes; it is also responsible for the sensory system, e.g. pain, temperature and touch, and regulating the body temperature (Waugh and Grant 2010).

The skin is structured in three main layers (Figure 1-1): the epidermis is the most superficial one; beneath the basal layer of the epidermis is a basement membrane, which separates it from the next layer, called the dermis, and finally below the dermis, the hypodermis is found. This is a layer of subcutaneous fat just before the inner structures of the fascia (Fuchs and Raghavan 2002).

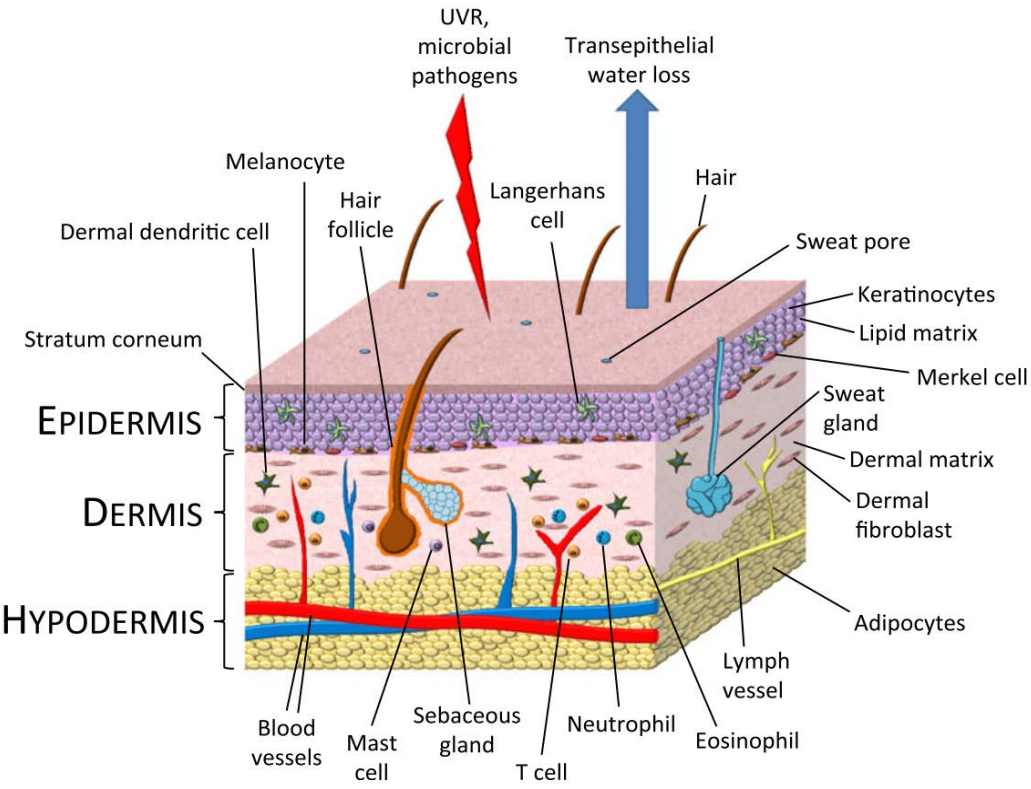

Figure 1-1: Skin structure.

Representation of the three main layers of the skin, the epidermis, the dermis and the hypodermis and the different appendages and cell types present. Taken from (Kendall and Nicolaou 2013).

1.1.1 The epidermis

The epidermis is the outer part of the skin and its thickness varies throughout the different parts of the human body. It is a self-renewing stratified, squamous, keratinizing epithelium first described by Marcello Malpigui (1628-1694). It is mainly composed of keratinocytes derived from the embryonic ectoderm and arranged in different layers to form a stratified epithelium. Within each layer, cells have different shapes depending on their differentiation stage. The more differentiated they are, the higher up they are within the epidermis

(Montagna et al. 1992). Furthermore, dendritic cells such as melanocytes, Langerhans cells and Merkel cells, in addition to immune cells such as lymphocytes, are also present in the epidermis (Figure 1-1). Melanocytes are responsible for melanin production, which is a protective pigment transferred to surrounding keratinocytes (Singh et al. 2010; Tarafder et al. 2014). Langerhans cells are specialized immune cells whose function is to develop a quick response against antigens in contact with the skin (Romani et al. 2010). Merkel cells are neuroendocrine cells primarily localized in the basal layer of the epidermis, but are also found in the outer root sheath of hair follicles. They are more prevalent in touch-sensitive areas such as hands and in hairy skin (Boulais and Misery 2008).

The outer layer of the epidermis is the horny layer also known as the stratum corneum, which functions as a barrier to the environment. It is made up of flattened corneocytes which are terminally differentiated keratinocytes (Figure 1-2). They are non-nucleated cells and their cytoplasm has been replaced by fibres of keratin. Below this layer, there is the compact transitional layer or stratum lucidum only present in areas of thick skin such as palmar and plantar skin. Finally, the stratum malpighii is found in all types of skin and it is divided in three layers: the granular layer or stratum granulosum; the spinous layer or stratum spinosum, where keratinocytes remain attached to each other; and the basal layer from where undifferentiated keratinocytes rapidly divide and start to migrate to the upper layers (Figure 1-2). This is a heterogeneous mixture of cells with both differentiating and proliferative keratinocytes, stem cells, Langerhans cells, Merkel cells and melanocytes. Furthermore, the basal layer

connects the epidermis with the dermis through anchoring fibrils; type IV, VII collagen (Burgeson 1993), laminin and fibronectin proteins are its main protein component (Montagna et al. 1992).

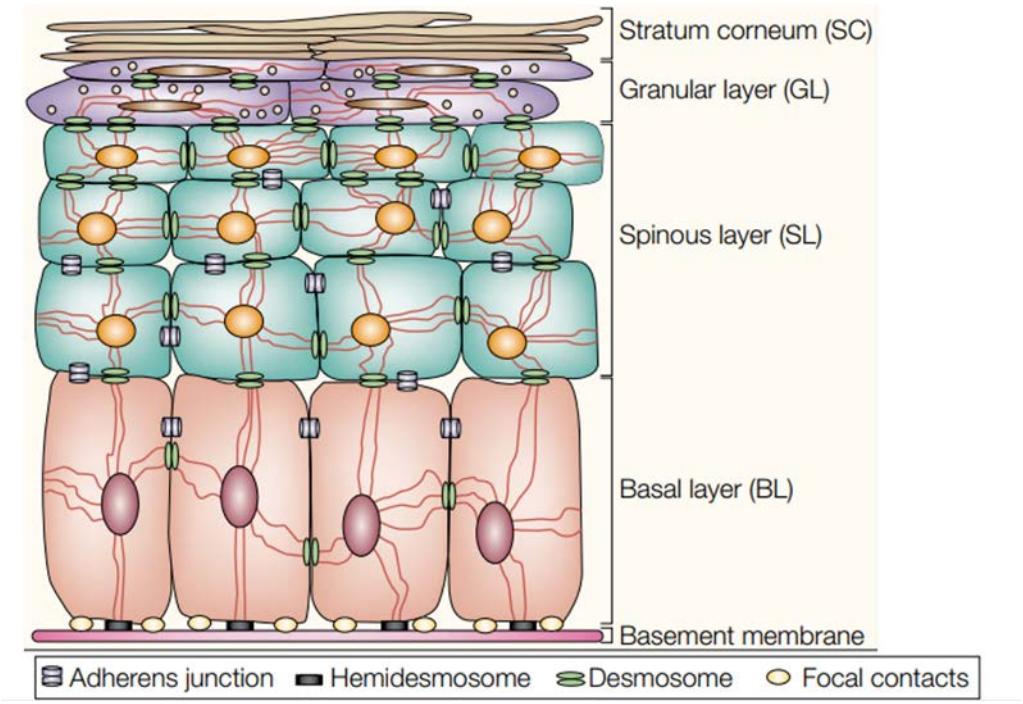

Figure 1-2: Representative image of the epidermis of human skin.

Basal layer keratinocytes are attached to the basement membrane through hemidesmosomes and focal contacts. The next layer of the epidermis is the spinous layer, which shows adherent junctions and desmosomes, followed by the granular layer which only uses desmosomes for cell-cell junctions. Finally the stratum corenum is composed of corneocytes. Taken from Fuchs and Raghavan, (2002).

Postmitotic human keratinocytes start to differentiate in the basal layer and it takes them around 31 days to move upwards and around 45 to become a non-viable cell of the stratum corneum and completely desquamate in human skin (Senoo 2013). The process of differentiation of keratinocytes consists of changes in cell size and shape, changes in the properties of the cell

membranes, appearance, reorganization or loss of different organelles, synthesis and modification of structural proteins such as keratins and dehydration (Montagna et al. 1992). The protein family of keratins (KRT) consists of more than 20 polypeptides which can be found throughout the epidermis depending on the differentiation state of the keratinocytes; for instance, basal cells express lower-molecular-weight keratins (e.g. KRT8, 13, 14, 15, 18) that are associated with proliferation, whereas the more differentiated the cells are, the higher the molecular weight of their keratins such as K1, 2, 10 and 11, which provide biomarkers for suprabasal keratinocytes (Sun et al. 1983).

The basal layer serves both as a physical boundary for the epidermis and as a platform rich in extracellular matrix proteins and growth factors, which promote proliferation. Different kinds of keratinocytes can be found in the basal layer; on the one hand, basal keratinocytes are primarily found along the sides of the rete ridges that connect the epidermis with the dermal surface therefore, their cytoplasm exhibits extensions or serrations towards the dermis; on the other hand, epidermal stem cells are located at the base of the rete ridges (Fuchs and Raghavan 2002).

1.1.1.1 Epidermal homeostasis

Skin homeostasis is the physiological process that maintains a constant number of cells in renewing the skin (Blanpain and Fuchs 2009). Different models of self-renewal have been proposed over the years (Figure 1.3, A). A hypothesis which divides the skin tissue into “epidermal proliferative units”

(EPUs) is one of the oldest and most accepted (Mackenzie 1970) (Figure 1-3, A). This theory establishes that a single slow cycling stem cell sustains each EPU dividing asymmetrically to produce another stem cell and a transit-amplifying (TA) cell. Morphological and proliferation studies in murine skin were the ones to establish this theory (Mackenzie 1970), which was also supported later by other authors (Potten 1974). However, “the single progenitor model” (Senoo 2013) has since arisen to explain the homeostasis of the skin in a simpler way (Figure 1-3, B). It is based on two factors; the fraction of proliferative cells in the basal layer and the probability of an asymmetric cell division occurring. A track of single-cells *in vivo* was made using genetic labelling in mouse tail epidermis, showing that stem cells from the basal layer give rise directly to committed spinous cells without going through a transient amplifying phase (Clayton et al. 2007). In spite of its simplicity, there are keratinocytes with different long-term proliferative potentials (Jones and Watt 1993), which made scientists either revert back to the stem cell/TA cell theory, or join both theories such as Mascré, Dekoninck et al. (2012) who demonstrated the existence of two different types of progenitors within a hierarchical organization with different functions during homeostasis in tail IFE skin of mice: the slow-cycling stem cells (SC) and the rapidly cycling committed progenitor (CP) cells sharing an asymmetric self-renewal mechanism where a balance between proliferation and differentiation is achieved (Mascre et al. 2012) (Figure 1-3, C). A recent review by Alcolea and Jones (2014) that focused on linage-tracing studies concluded that the IFE is mainly maintained by cells termed progenitors in the basal layer, which are equally likely to become either another

progenitor or a differentiating cell; furthermore, rare slow cycling cells are also proposed to be present in the IFE. They are epidermal SCs which are able to become stem cell daughters, or progenitor cells similar to the transient amplifying cells proposed back in 1970 by Mackenzie, and seem to especially play a role in skin repair after injury (Alcolea and Jones 2014). However, knowledge about skin homeostasis in humans is lacking due to the limitations of working with human skin *in vivo.* Special care has to be taken when talking about any of these homeostatic models in human skin.

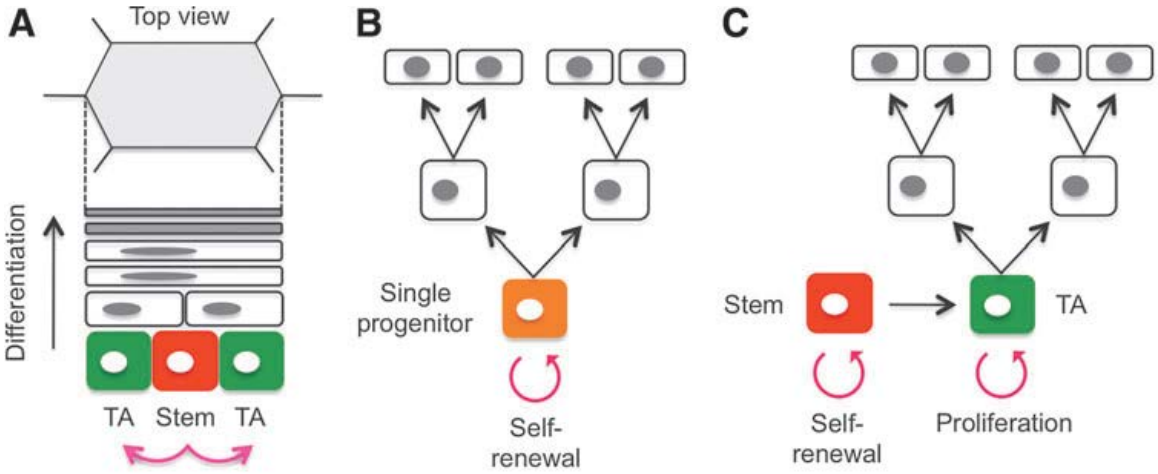

Figure 1-3: Different theories to explain skin homeostasis in mouse skin.

(A) Epidermal proliferative unit model. (B) Single progenitor model. (C) Stem/TA cell hierarchy model. From Senoo (2013).

As previously discussed, there are hair follicle stem cells in human skin, so that not only epidermal stem cells ensure skin homeostasis. Murine studies demonstrated that after wounding 25-50% of cells in the repaired IFE come from the hair follicle (Levy et al. 2007). This is a highly regulated process which stops once the wound is healed and there is no further requirement for tissue regeneration (Levy et al. 2007; Blanpain and Fuchs 2009). However, it has

been shown that wound repair also takes place in hairless skin suggesting the involvement of other skin cells in wound repair (Senoo 2013). The SCs and TA cells from the basal layer of the epidermis are relatively undifferentiated cells with a slow cycle, which are easily available on demand to repair any kind of damage; for example, after injury (Lavker and Sun 1982). Despite their contribution to the IFE, the role of SCs and TA cells from the basal layer of the epidermis in wound healing has not been studied in detail.

1.1.2 The dermis

At the dermal-epidermal junction, a basement membrane follows the contour of the epidermal basal cells separating both physically and functionally the epidermis from the dermis (Yurchenco 2011). The dermis is the connective tissue of the skin, which contributes to its structural and mechanical function protecting the body from injury. It is formed by different filamentous proteins such as collagen and elastic fibres surrounded by the extracellular matrix. Collagen fibres are able to bind water which gives tensile strength to the skin, however this property declines with age resulting in the appearance of wrinkles in aged skin (Waugh and Grant 2010). The most important cell found in the dermis is the fibroblast. In addition, nerves, vascular and lymphatic networks and skin appendages are supported in the dermal cellular matrix (Richmond and Harris 2014).

The dermis is divided in two layers; close to the epidermis there is the papillary dermis where fibroblasts are more abundant (Geerligs 2009). A high percentage of the papillary dermal matrix is formed by ground substance,

whereas it has a small distribution of elastic and collagen fibrils. Furthermore the orientation of these fibres is vertical to allow them to connect with the dermal-epidermal junction. Bellow the papillary dermis, a thicker layer called the reticular dermis is found where fibres are already horizontally oriented. This layer can extend its capacity up or down protecting vessels and cells against mechanical insults (Geerligs 2009). Papillary and reticular fibroblasts in culture have a different gene expression pattern, which can be related to their different behaviour within the skin (Janson et al. 2012).

Collagen is the most abundant extracellular protein in the dermis. Classic ultrastructurally recognizable cross-banded collagen fibrils in the dermis contain collagens I, III and V, but the microfibrillar collagen VI, as well as collagen XIV, which is part of the FACIT (Fibril Associated Collagens with Interrupted Triple helices) collagen subfamily, are also found in the dermis (Gelse et al. 2003). Furthermore, multiplexis collagens XV and XVI are produced by fibroblasts of the dermis (Gelse et al. 2003). Collagen I is the major component of the fibrils, and the amount of the other types of collagen varies.

Dermal fibroblasts are the most abundant cell in the dermis. They are responsible for synthesizing the fibres and ground substance of the extracellular matrix, but they can also remove them by the secretion of several proteolytic enzymes. Dermal fibroblasts are also involved in the synthesis of some parts of the basement membrane.

During the tissue repair processes dermal fibroblasts differentiate into myofibroblasts encouraging contraction of the wound (Rockey et al. 2013).

Furthermore, they are involved in the increase of the amount of collagen III content during wound healing (Bolognia et al. 2003).

Immune cells are also found in the dermis such as macrophages, lymphocytes and mast cells; in particular mast cells are known to develop different functions; vasoactive and smooth muscle-contracting activities, secretion of chemotactic factors, proteolysis and anticoagulation (Richmond and Harris 2014). They are extremely important for inflammatory reactions and they release diverse important substances following degranulation. They are commonly found in close proximity to fibroblasts. Cell-to-cell communications between them enables mast cells to modulate collagen production by dermal fibroblasts (Abe et al. 2000).

1.1.3 Skin appendages: the hair follicle and sebaceous gland

The hair follicle is a unique organ found in the skin of mammals. Hair follicles are formed by a down-growth of epidermal cells into the dermis (Waugh and Grant 2010) and their main functions are physical protection and thermal insulation, although they are also responsible for camouflage in some mammals, and for the disposal of sweat and sebum (Stenn and Paus 2001). They also contribute to the sensory and tactile senses of the skin. However, in humans hair also has a very important social and psychological impact (Schneider et al. 2008).

Therefore, there is a need for continuous hair renewal during life (Alonso and Fuchs 2006). In order to replace hairs, the hair follicle cycles continuously, going through periods of growth and rest (Stenn and Paus 2001). The hair

follicle has a permanent upper segment, which comprises the follicular infundibulum and isthmus and a non-permanent lower segment, where the lower follicle and bulb are found (Figure 1-4). The fibre of terminal hairs is made of keratin filaments surrounded by a sulfur-rich matrix (Whiting 2004). The bulb of the hair follicle (Figure 1-4) is closely associated with blood vessels, the source of nutrition; therefore cells from the bulb are highly proliferative. As they divide and then differentiate, they move upwards and loose their proximity to the blood vessels, ending in death and keratinisation (Waugh and Grant 2010).

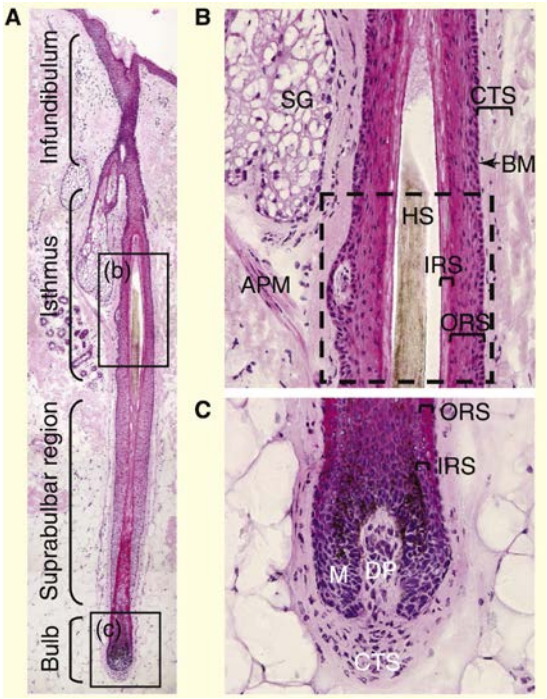

Figure 1-4: The hair follicle structure.

(A) H&E staining of the human anagen hair follicle, showing the permanent structures (infundibulum and isthmus) and the anagen associated components (suprabulbar region and the bulb). (B) The isthmus at high magnification, which is formed by the connective tissue sheath (CTS), the basal membrane (BM), the outer root sheath (ORS), which is the most external one, the inner root sheath (IRS) and finally the hair shaft (HS). The square dashes show the approximate location of the bulge, the stem cell niche of the hair follicle, SG indicates

sebaceous gland, a structure attached to the hair follicle and APM indicates arrector pili muscle. (C) The bulb region at high magnification composed by the dermal papilla (DP), the connective tissue sheath (CTS) and the matrix (M). Adapted from Schneider *et al.,* (2008).

Hair follicles contain the most important stem cell niche in the skin regarding the number of quiescent stem cells and they are essential for hair renewal processes (Hsu et al. 2014). They are found in the bulge region, which express the surface marker CD200 and have a quiescent state (Figure 1-4). A more proliferative population of SCs can be also found below the bulge, in the outer root sheath of the anagen hair follicle and it is characterised by the expression of CD34 (Garza et al. 2011).

Ectodermal-mesodermal interactions are very important for hair development. All the epithelial compartments of the hair follicle, in addition to the sebaceous glands and the apocrine glands, are formed from ectodermal hair follicle stem cells (Schneider et al. 2008). However, the dermal papilla and the dermal sheath, also known as connective tissue sheath are derived from the mesoderm. The dermal papilla is responsible for the induction of hair growth. It is formed by a cluster of mesenchyme-derived cells enclosed within the epidermal matrix producing the necessary signals to regulate hair growth (Kishimoto et al. 2000).

Other structures can be found attached to the hair follicle. The small bundles of smooth muscle fibres of the arrector pili attached to the hair follicle can contract to erect the hair in situations of stress, fear, or cold, because they are connected and stimulated by sympathetic nerve fibres (Waugh and Grant

2010). Furthermore, the sebaceous duct unit is also continuous and empties into the hair canal (Figure 1-4) (Schneider et al. 2008).

1.2 Wound repair

When the skin barrier is disrupted, the wound healing process is essential for skin recovery and repair, but it is a very complex process. It involves different cells, signals and molecular pathways taking place in a regulated and co-ordinated manner.

This process has been typically described by the initiation of immediate events such as coagulation and hemostasis followed by three important phases; the inflammatory phase, the proliferative phase and the remodelling phase (Diegelmann and Evans 2004). However, during these phases many cellular and molecular processes take place at the same time, which means that the difference between phases is not clearly separated, and that some processes from two different phases can overlap (Figure 1-5).

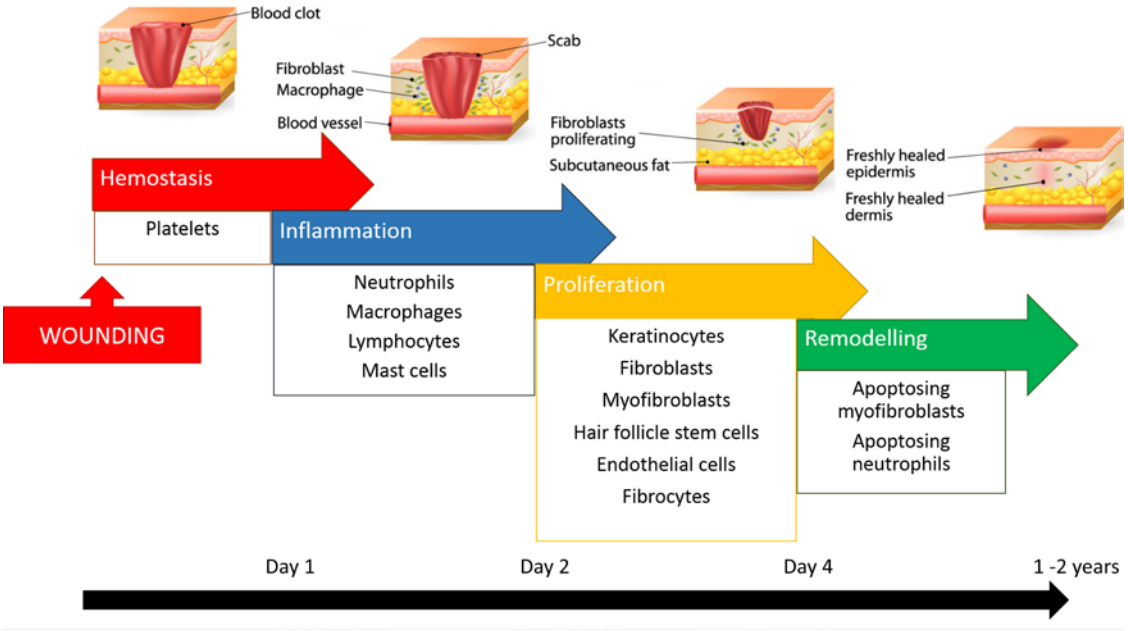

Figure 1-5: The four stages of normal wound healing in time.

Overlap between the four stages, hemostasis, inflammation, proliferation and remodelling. Cells involved in each of the wound healing stage are indicated. Adapted from (Diegelmann and Evans 2004).

1.2.1 The wound healing stages

1.2.1.1 The immediate events

Immediately after injury two processes take place in order to stop bleeding and avoid blood leaking; coagulation is the formation of a clot over the wound providing a matrix over which keratinocytes can migrate. This clot consists of platelets embedded in a mesh of cross linked fibrin fibres where they can release cytokines and growth factors and activate the complement cascade. The amount of fibrin and size of the clot will be determined not just by coagulation, but also by its balance with endothelial cells, thrombocytes and fibrinolysis (Velnar et al. 2009). These first signals are responsible for triggering the whole wound healing sequence of events (Martin 1997). At the same time,

hemostasis occurs, consisting of an intense vasoconstriction for the first 5 to 10 minutes followed by active vasodilatation 20 minutes after injury to ensure blood supply once the clot is formed (Stadelmann et al. 1998).

1.2.1.2 The inflammatory phase

While the fibrin clot is being formed and platelets migrate to the wound the inflammatory phase is also initiated. During this phase, inflammatory cells are recruited to the wound site and initiate a healing cascade mediated primarily by cytokines including platelet-derived factors and macrophage-derived factors.

First of all, a vasomotor-vasopermeability response is essential to permeabilise the site of trauma, leading to an influx of a variety of leukocytes, which migrate to the wound site by chemotactic migration. They kill bacteria and remove devascularised tissue fragments and debris. Furthermore, the first three hours are critical to avoid infection because it is when the wound is least protected. Adequate tissue oxygen tension is important for leukocytes to kill bacteria via oxidative intracellular mechanisms (Eming et al. 2007).

Neutrophils are one of the first leukocytes to infiltrate to the wound site. Neutrophils are attracted to the wound by chemoattractive agents such as TGF-β, complement components (mostly C3a and C5a) and formylmethionyl peptides secreted by either bacteria or platelets 24 to 36 hours after injury, (Velnar et al. 2009). Diapedesis is the process by which neutrophils and other inflammatory cells migrate from the blood vessels through the endothelium to the wound site. Once in the wound site, neutrophils release reactive oxygen species (ROS) and lysosomal enzymes such as proteases and matrix

metalloproteinase (MMP) including collagenases, gelatinases and elastases to destroy foreign bacteria and material after phagocytosis (Shaw and Martin 2016).

Monocytes are attracted to the wound site by clotting factors, complement components, cytokines, and collagen or elastin breakdown products. Once in the wound they mature into macrophages 48 to 72 hours after wounding, during the late inflammatory phase (Velnar et al. 2009). Furthermore, they are able to act at low pH so their lifespan is longer than that of the neutrophils, thus providing an abundant reservoir of growth factors and other chemoattractive mediators to the wound site to activate skin cells around the wound margin.

Mast cells are another type of resident leukocytes in the skin and they have a key role during different stages of wound healing (Koh and DiPietro 2011).

Although inflammation during normal wound healing lasts for 2 to 5 days, the immune response continues for the whole wound healing process. Lymphocytes, B and T cells, are the responsible for this adaptive immune response, which is a delayed but more specific immune response. Lymphocytes are the last type of immune cells to enter into action. They are attracted by interleukin-1 (IL-1), complement components and immunoglobulin G (IgG) breakdown products 72 hours after wounding (Velnar et al. 2009). B cells, which are antibody secreting cells, are also able to produce cytokines and growth factors, present antigens on its cell membrane and regulate T cell activation and differentiation (Landen et al. 2016). On the other hand, T cells also produce

growth factors while functioning as immunological effector cells. In particular, regulatory T cells are involved in the attenuation of the interferon-γ production and accumulation of macrophages to regulate tissue inflammation (Sorg et al. 2017). This is mediated through the activation of the epidermal growth factor receptor pathway in order to enable the regeneration process of the wound.

1.2.1.3 The proliferative phase

The formation of granulation tissue is essential for the wound healing process. Dermal fibroblasts at the wound edges start the production and deposition of fibronectin which binds fibrin creating scaffolding on which fibroblasts can migrate into the wound (Stadelmann et al. 1998). The proliferation of dermal fibroblasts to this scaffold leads to the development of granulation tissue, which will therefore enable re-epithelialization. After increase of DNA replication, migration and metabolic activity of fibroblasts during the first two days after wounding, dermal fibroblasts start proliferating (Stadelmann et al. 1998). Resting fibrocytes of regional connective tissue and perivascular adventitia, and in haired skin, dermal sheath cells from the hair follicles are the source of fibroblasts (Jahoda and Reynolds; Jahoda and Reynolds 2001).

Changes in expression of certain receptors, such as integrins allow fibroblasts to migrate into the clot. Integrins from part of specialized cell surface structures called focal adhesions (FAs) which mediate the adhesion between the extracellular matrix (ECM) and the actin cytoskeleton of fibroblasts (Zaidel-Bar et al. 2007). They are regulated by different signals from the surrounding matrix and growth factor milieu. Specifically, integrins binding collagen receptors are down-regulated, while integrins which bind fibrin, fibronectin and

vitronectin are all up-regulated (Martin 1997) to allow migration of fibroblasts to the wound site.

After migration, fibroblasts are responsible for glycosaminoglycans (GAGs) and collagen production (Shaw and Martin 2016). GAGs form an amorphous gel called “ground substance” useful for collagen fibres to be deposited and aggregated. Collagen type I and III start to be produced at high levels, increasing the wound tensile strength, reaching at maximum levels at the end of the first week. It has been shown that type III collagen accumulation precedes that of type I in wound repair, and the final type I/III collagen ratio in the skin is of vital importance for the healing process (Dale et al. 1996). For example, when comparing the normal skin ratio, which is 4:1, with hypertrophic and immature scars, there is a dramatic change. Hypertrophic and immature scars show a 2:1 proportion of type I/III collagen (Stadelmann et al. 1998).

Due to the higher metabolic need of cells during the proliferative phase, and the lack of vascularisation in the wound site, angiogenesis is critical during this phase of wound healing; therefore new capillary growth also takes place (Velnar et al. 2009).

Re-epithelialization is required to close the wound with a layer of keratinocytes. In the basal layer, this process involves mobilization, migration, mitosis and cellular differentiation of keratinocytes from the surrounding epidermis.

After wounding, cell contact inhibition is lost, which induces the keratinocytes that are immediately adjacent to the wound margin to migrate.

This process is called epithelial-mesenchymal transition (EMT), where epithelial cells that are in contact with a basement membrane, change to a mesenchymal cell phenotype by activating different biochemical changes related to an enhanced migratory capacity, invasiveness, resistance to apoptosis and production of ECM proteins (Kalluri and Neilson 2003). During wound healing, keratinocytes undergoes type 3 EMT as part of the repair process which has already been started by fibroblasts and immune cells. Unlike EMT in fibrosis, EMT in wound healing is associated with inflammation; once inflammation has been resolved and the wound site is covered by keratinocytes again, the reverse MET occurs (Kalluri and Weinberg 2009). During EMT, downregulation of hemidesmosomes occurs to enable keratinocyte migration and new fibronectin-recognising integrins (e.g. α5β1, αvβ1 and αvβ6) are expressed (Koivisto et al. 2014).

In addition, fibroblasts in the dermis relocalise their collagen receptors to grasp hold of the provisional wound matrix and the underlying wound dermis. Proteases are also expressed at this stage in order to cut a path through the fibrin clot to allow keratinocytes to migrate and plasminogen (Plg) urokinase-type (uPA) and the tissue-type (tPA) are upregulated to activate plasmin. This scenario makes it possible for keratinocytes to advance through the border as the rate of mitosis increases in cells distant from the wound site (Haensel and Dai 2017).

The phenotype of repairing epidermis shows a very particular pattern of expression of KRTs. Activation of both KRT16 and KRT17 happens immediately

after wounding and is required for re-epithelialisation (Patel et al. 2006), while they are almost absent in normal human skin. Furthermore, KRT14, normally expressed in the basal layer of the epidermis, is unregulated in the new epithelial tissue.

Once both edges of the wound meet, the keratinocytes stop migrating due to cell contact inhibition signalling. Then, they undergo mesenchymal-epithelial transition (MET) and the protein expression profile of basal keratinocytes returns to normal and allows them to be able to differentiate again and restore the barrier function of the epidermis (Stadelmann et al. 1998).

Once homeostasis has been achieved and the barrier has been restored, the maturation phase takes places, which consists of collagen reorganization and GAG degradation. This period of remodelling can last for up to 2 years (Stadelmann et al. 1998).

1.2.1.4 The remodelling phase

The remodelling phase normally starts four days after wounding when some fibroblasts start to differentiate into myofibroblasts expressing high levels of α-smooth muscle actin (α-SMA) after stimulation by transforming growth factor beta 1 (TGF-β1) and the mechanical stimuli generated from resisting wound contraction forces (Sorg et al. 2017). Myofibroblasts ensure attachments via adherent molecules that attach them to each other as well as to the wound margins leading to wound closure (Velnar et al. 2009).

Once the wound contraction forces are relaxed again, cell surface fibronectin is released and the myofibroblast cell surface receptors become desensitized, which means they cannot respond to growth factors in the surrounding tissue. However, the exact molecular mechanism of this process remains unknown (Stadelmann et al. 1998). Finally, myofibroblasts undergo apoptosis, even when growth factors are added to the wound of a rat model (Burgess et al. 1990).

An increase in the expression of α-SMA in mechanically scratched monolayers of human dermal fibroblasts has been described (Pomari et al. 2015), and also in other mesenchymal cells from different body locations such as rat hepatic stellate cells (Rockey et al. 2013).

1.2.2 Metabolic activity in wound healing

Wound healing is a highly energy demanding process. During wound healing there is a need of high proliferation rate, production of extracellular matrix as well as the prevention of infection. Furthermore, different metabolites play an essential role during cell signalling (André-Lévigne et al. 2017). Metabolism refers to the pathways required for the production or consumption of energy from different sources, from carbohydrates and lipids, as well as proteins during starvation periods. Catabolism is the set of pathways used for the production of energy by the living cells. Aerobic respiration metabolise carbohydrates through glycolysis and the pentose phosphate pathway in the cytosol which produce pyruvate which are then used by the citric acid cycle in the mitochondria creating reducing species such as NADH and NADPH. Fatty

acids can be the source of energy by the production of acyl CoA derivatives, which go through beta oxidation in the mitochondria generating short carbon chain regulatory intermediates such as succinate. Finally, the reducing species create an electron gradient which is used by oxidative phosphorylation in the electron transport chain of the mitochondria to generate the energy molecule, ATP. All these processes, glycolysis in the cytosol and citric acid cycle and electron transport in the mitochondria, are able to produce ATP (Griffiths et al. 2017).

The adenine nucleotides ADP and ATP are used by skin cells to promote those biological processes needed for regeneration. Specifically, ATP was found to induce epithelial cell migration *in vitro* (Dignass et al. 1998). Furthermore, the reducing species, NADPH, created during catabolic processes such as glycolisis, are not only used by the oxidative phosphorylation process but they can also act as cofactors of ROS-generating NADPH oxidase enzymes as well as several antioxidant enzymes which control the redox state of the cell. Metabolically active cells show an irrefutable relationship between metabolism and cellular redox state (Griffiths et al. 2017). Finally, metabolic activity has a huge impact in the immune response immediately after wounding. The first responder cells of the innate immune response, neutrophils, are largely dependent on glycolysis while in immune cells in the absence of any demand rely mainly on oxidative phosphorylation (Griffiths et al. 2017).

1.2.3 Acute vs. chronic wound healing in the skin

Although the normal process of wound healing is well documented, it is not clear why a normal wound may develop into a chronic non-healing wound where complete healing does not take place, and what the cellular and molecular differences between them are. A number of different types of chronic wounds may arise and a significant proportion of the population may suffer from them resulting in a highly cost condition to manage by the healthcare providers (Guest et al. 2017).Therefore, a deeper understanding of chronic wounds is essential in order to find an effective and patient friendly treatment, such as home-used light based devices, which have been shown to have the potential to improve wound healing due to stimulatory effects on proliferation and migration of different skin cell populations, including keratinocytes, fibroblasts and immune cells (Chabert et al., 2015)

There are a number of features which characterize chronic wounds and differentiate them from normal wounds and their healing process. The epidermis of tissue surrounding chronic wound was shown to be very different from intact epidermis (Figure 1-6).

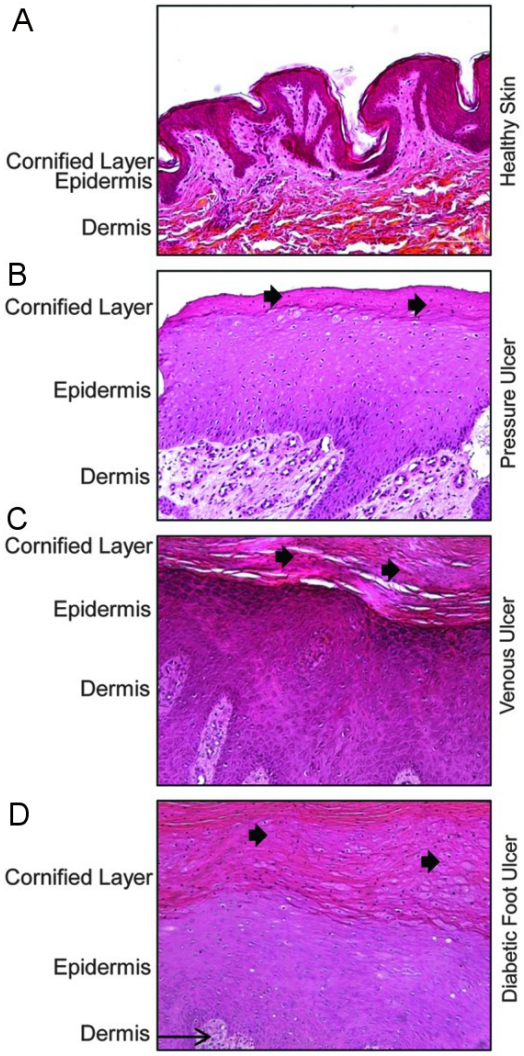

Figure 1-6: Histology of epidermis of healthy human skin and ulcers.

(A) Healthy human skin, (B) preassure ulcer skin, (C) venous ulcer skin and (D) diabetic foot ulcer skin. Adapted from Pastar *et al.,* (2014).

Proliferative keratinocytes are found in the basal layer of the epidermis which ensure skin homeostasis in normal skin (Figure 1-6, A), however, a hyperproliferative epidermis is found in many different chronic wounds such as pressure ulcers (Figure 1-6, B), venous ulcers (Figure 1-6, C) and diabetic foot ulcers (Figure 1-6, D) where keratinocytes undergo mitosis not only in the basal layer but also in the suprabasal (Pastar et al., 2014). Activation of c-myc was

proposed to be involved in this response characteristic of chronic wounds (Stojadinovic et al., 2005) as a downstream target of β-catenin.

Furthermore, another difference between both types of wounds is found in the volume of granulation tissue present, which is bigger in chronic than acute wounds but more important is the poor quality of this granulation tissue (Stadelmann et al., 1998). In order for normal wound healing to proceed, this granulation tissue must contain capillaries that vascularise the tissue, and it must be rich in different types of cells, such as fibroblasts and myofibroblasts, inflammatory cells, endothelial cells and pericytes. As the healing process advances, cells are removed from this tissue by undergoing apoptosis, and the granulation tissue is converted to an acellular and a vascular matrix of collagen (Stadelmann et al., 1998). A low quality granulation tissue at the beginning of the process may result in the development of chronic wounds. On a more frequent basis, failure of the development of granulation tissue during wound healing in a timely manner can lead to a high degree of cellularity in the granulation tissue at the later stages of wound healing, such as myofbroblasts, neutrophils or lymphocytes, which may result in chronic wounds. These wounds may eventually heal with abundant scar tissue (Stadelmann et al., 1998).

Finally, wound contraction is required to reduce the size of the wound and close the defect; however in chronic wounds this process takes place indiscriminately and leads to a disorganized structural integrity, loss of function and cosmetic deformity in the wound site (Pastar et al., 2014).

1.3 Photobiomodulation: a deep understanding of the role of light in the skin

Photobiomodulation is emerging as a clinical application for skin disorders, including wound healing but the lack of understanding of the molecular targets impedes identification of effective therapeutic parameters (Mignon et al. 2016). Before addressing the question of how skin cells are able to interact with low levels of light, it is essential to understand the properties of light and its propagation within different biological structures in human skin.

1.3.1 Can the skin interact with light?

Since the skin acts as a barrier between the human body and the environment it is continuously exposed to any kind of environmental factor, including light.

Light is commonly used to refer to the visible part of the electromagnetic spectrum. It covers a wavelength range from 400 (violet) to 780 (red) nm. Furthermore, the neighbouring parts of this spectrum of electromagnetic radiation can also be seen with the help of some optical devices, and the skin is also exposed to them. Ultraviolet (UV) light which is close to blue light, ranges from wavelengths of 100 to 400 nm and infrared (IR) light (0.78-2000 μm) is found at the opposite end of the light spectrum, just after red light (Table 1-1) (Altshuler and Tuchin 2009).

Type of radiation		Wavelength (λ)
Ultraviolet (UV)	**UVC**	100-280 nm
	UVB	280-315 nm
	UVA	315-400 nm
Visible light	**Violet**	400-450 nm
	Blue	450-490 nm
	Cyan	490-520 nm
	Green	520-560 nm
	Yellow	560-590 nm
	Orange	590-620 nm
	Red	620-780 nm
Infrared (IR)	**Near IR**	0.8-2.5 µm
	Middle IR	1.5-50 µm
	Far IR	50-2000 µm

Table 1-1: Electromagnetic radiation from UV to IR including visible light spectra.

When light interacts with human skin, part of the radiation is reflected back due to the different refractive index in comparison to the atmosphere (Lister et al. 2012). The rest is able to penetrate the skin. The effects that this penetration may cause depend on wavelength, intensity and exposure of the light. High irradiance and low exposure times leads to photomechanical or ablative mechanisms, while medium irradiance and medium exposure times produce

photothermal responses. Both mechanisms are able to stop skin functionality. However, when the energy is low enough not to cause these negative consequences (low irradiance and long exposure times), scattering and photoabsorption take place inside the skin (Boulnois 1986). Different molecules called chromospheres (Young 1996; Altshuler and Tuchin 2009) are responsible for absorbing light in the skin; these include protoporphyrin IX, melanin, riboflavin, oxyhemoglobin, bilirubin and β-carotene (Figure 1-7). Heme groups of blood cells and water (Mahmoud et al. 2008) strongly absorb IR light at wavelengths greater than 1100 nm (Huang et al. 2009).

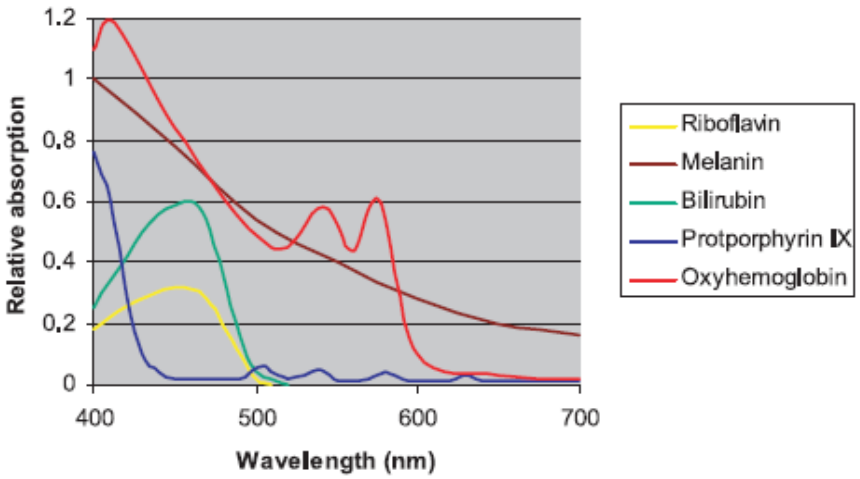

Figure 1-7: Absorption spectra of different skin chromophores.

Adapted from Mahmoud *et al.,* (2008).

In addition, some molecules called photoreceptors or photoacceptors are known to absorb light undergoing any kind of photochemical reaction (Lister et al. 2012). In the world of photobiology this is the most interesting and useful phenomenon as it is the one which can be used to produce molecular controlled effects in cells. Photoreceptors are especially important for plants as most of their functions are regulated by light. In humans, two members of the G protein

coupled receptor (GPCR) family, opsin 1 (OPN1) and opsin 2 (OPN2) or rhodopsin (RHO), are the main photoreceptors as they are present in the eye and are involved in vision (Terakita 2005). Since the skin is the human organ in which more surface area is exposed to light, it makes sense to hypothesise that photoreceptors (either known or unknown ones) are also present in skin cells. An understanding of the correct light parameters that modulate such receptors will be a step forward towards understanding the skin's response to light, and whether its effects can be harnessed for therapeutic benefits.

The use of light for medical applications has previously mainly focused on the use of low-level laser therapy (LLLT). This treatment uses light in the red or near-IR region of the electromagnetic spectrum and a power of up to 500 mW. It can be either continuous or pulsed light with a low energy density, normally between 0.04 and 50 J/cm^2 which means no heat, sound or vibrations are produced (Huang et al. 2009). However, a new term has arisen to include a wider range of wavelength in the visible light spectra; photobiomodulation (Mignon et al. 2016).

Human cell models have been used to analyse cell biology, protein expression and percentage of closure after a scratch in primary fibroblasts and keratinocytes, showing beneficial effects when using red light (Chabert et al. 2015). Interestingly, hypertrophic scar derived fibroblasts from human donors were irradiated with red light at 660 nm and IR (880 nm) (Webb et al. 1998; Webb and Dyson 2003). These studies demonstrated that red light induced an increase in number of cell count for both normal dermal and hypertrophic scar

derived fibroblasts during the first five days following irradiation at both 2.4 and 4 J/cm2 (Webb et al. 1998). However the NIR exposure reported the opposite effect, showing a significant decrease in cell number on day five for normal fibroblasts, and on day 4 for hypertrophic fibroblasts with the same radiant exposure (Webb and Dyson 2003). In parallel to this observation, the beneficial outcomes of red light was also reported for human diabetic fibroblasts, showing a higher degree of migration in comparison with both NIR irradiated and non-irradiated fibroblasts (Houreld and Abrahamse 2010).

Animal studies have also been used to test the effect of light on wound healing *in vivo.* One of the most interesting studies was done on epidermal barrier recovery in mice, where red light increased the rate of epidermal barrier recovery in comparison with both white light and dark conditions (Denda and Fuziwara 2008). They further suggested that phosphodiesterase 6 may be involved in this effect (Goto et al. 2011).

Clinical studies on the effect of light on wound healing have also been reported. A double-blind randomized placebo controlled trial (14 patients and 23 leg ulcers) was performed to assess the outcome of combined 660 and 890 nm light-emitting diode (LED) therapy (Minatel et al. 2009). The LED treated group demonstrated faster healing and more granulation tissue production at day 30 than the placebo group. Furthermore, 58.3% of the treated wounds were healed at day 90 in comparison to only one placebo ulcer which was healing by this time (which corresponds approximately to 9%) (Minatel et al. 2009). Nevertheless, these clinical trials have obvious limitations as wounds can differ

quite a lot one from each other; they normally have different causes, time of healing and outcomes. Therefore, well-designed clinical trials are a requirement to comprehensively validate light-based therapies for wound healing (Beckmann et al. 2014).

Notwithstanding studies using blue and violet light in photobiomoulation are growing, and they seem to be very promising as OPNs mainly absorbing light at these wavelengths, but the effects appear to be different to the use of red light. Irradiation with blue light has reported a reduction in the proliferation of primary epidermal keratinocytes at doses above 33 J/cm^2, with an increase in apoptosis only at extremely high doses 100 J/cm^2 (Liebmann et al. 2010). On the other hand, low doses of blue light, below 4 J/cm^2, increased proliferation of outer root sheath hair follicle keratinocytes (Buscone et al. 2017) and metabolic activity in primary fibroblasts (Mignon et al. 2017) after one light treatment; however, multiple light treatments resulted in a decrease of metabolic activity of dermal fibroblasts even at very low doses (Mignon et al. 2017). Blue light (5 J/cm^2) stimulated markers of early differentiation in epidermal keratinocytes, such as KRT1 and KRT10, but only high doses of blue light (66 and 100 J/cm^2) induced the involucrin (INV) marker of late differentiation (Liebmann et al. 2010). Blue light has also been reported to delay the epidermal barrier recovery in mice (Denda and Fuziwara 2008). Reduction in proliferation and metabolic activity at non-toxic doses has also been observed in primary dermal fibroblasts (Oplander et al. 2011; Taflinski et al. 2014). In a scratch-wound assay, although low doses of blue light (2, 5 and 10 J/cm^2) did not modulate migration of human

primary dermal fibroblasts, higher doses (55 J/cm^2) inhibited migration (Masson-Meyers et al. 2016).

A reduced of proliferation and enhanced differentiation of epidermal keratinocytes after blue light irradiation (Liebmann et al. 2010) makes this wavelength very promising for the treatment of psoriasis. Furthermore, it has been proposed that blue light reduce cytokine and interleukin release (Masson-Meyers et al. 2016). All these characteristics also makes blue light appealing for the treatment of other conditions such as fibrotic skin conditions and the prevention of keloids and hypertrophic scars. However, very low doses of blue light might follow another mechanism, which is still to be uncovered.

As previously discussed, the efficacy of light treatment for skin disorders and wound healing has been assessed in the laboratory using cell and animal models, as well as in human clinical trials. However there are still challenges to overcome regarding the relevance of the models used, and the selection of light parameters (Liebmann et al. 2010; Mignon et al. 2017). Although it is clear that light has an effect on biological organisms, not all types of light will have a beneficial outcome. Therefore, it is very important to select the correct light parameters for wound healing regarding wavelength, irradiance (W/cm^2) and radiant exposure (J/cm^2). Secondly, it is very important to use a relevant model for the study of light treatments. The closer the model is to the real clinical situation, the better. New *in vitro* wound healing models are becoming more popular as 3D culture technology advances. Reconstructive skin and full

thickness human skin *ex vivo* models are already in used by different research laboratories (Stephens et al. 2013).

All these facts have to be taken into account when choosing a model to perform experiments; primary human fibroblasts or keratinocytes, 3D skin models and *ex vivo* wound healing models may be the most convenient to use, but avoiding cell lines as their characteristics can differ significantly with respect to the *in vivo* situation (Katayama et al. 2015).

1.3.2 Possible mechanisms of action of light in human skin: an overview of skin photoreceptors

Direct targets for photobiomodulation include cytochrome c oxidase (Karu 1999), photolysis of nitrozated proteins to generate nitric oxide (Liebmann et al. 2010; Oplander et al. 2013), ROS production (Opländer et al. 2011; Khan and Arany 2015; Nakashima et al. 2017) and light activation of calcium ion channels (Wang et al. 2016). Emerging photoreceptors in humans are opsins (OPNs) (Tsutsumi et al. 2009; Haltaufderhyde et al. 2015) and cryptochromes (CRYs) (Hoang et al. 2008) (Figure 1-8).

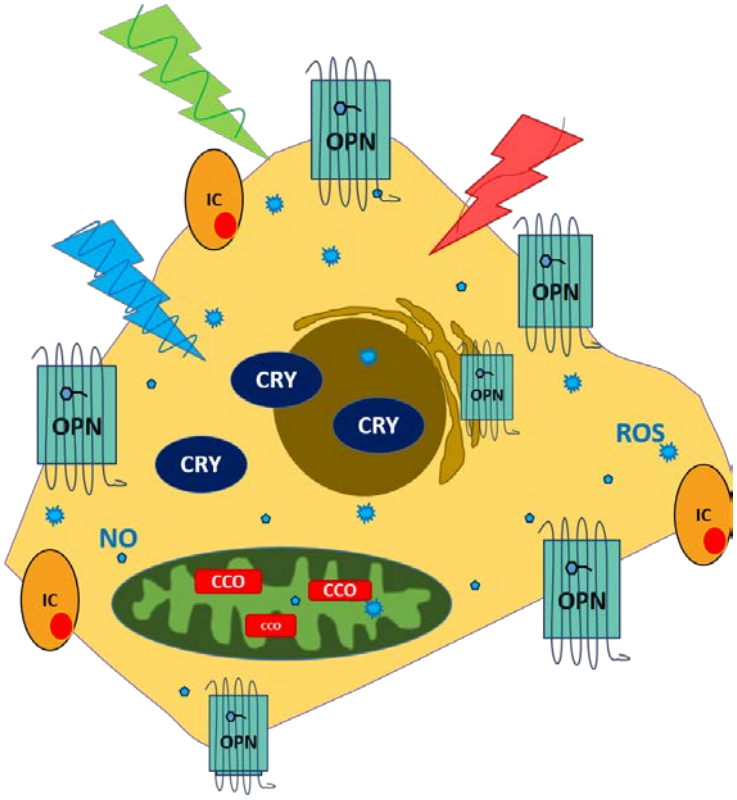

Figure 1-8: Photoreceptors present in epidermal keratinocytes.

OPN: opsin, CRY: cryptochrome, CCO: cytochrome c oxidase, ROS: reactive oxygen spices, NO: nitric oxide and IC: ion channels. Image self-drawn.

1.3.2.1 Cytochrome c oxidase

Nowadays, the most commonly accepted mechanism of action of photobiomodulation or low-level-light therapy (LLLT) is through cell metabolism (Hamblin et al. 2006; Huang et al. 2009; Chung et al. 2012; Prindeze et al. 2012) with cytochrome c oxidase (CCO) the proposed photoreceptor (Karu 1999; Karu and Kolyakov 2005).

Following this theory, it has been established that LLLT is able to excite an electron within the cytochrome c oxidase structure, stimulating the transfer of electrons through the respiratory chain. This leads to an increase of the proton

electrochemical potential, increasing adenosine triphosphate (ATP) synthase activity and increasing cell metabolism (Prindeze et al. 2012). As a consequence, cell proliferation, migration and adhesion are also enhanced and cell apoptosis is prevented (Karu 1999). It has been reported that an overall shift in the cell redox potential may in turn induce transcriptional changes (activation of NF-β and other transcription factors) explaining the effects on growth factor production, extracellular matrix deposition, cell proliferation and cell motility, which are all important during wound healing (Hamblin and Demidova 2006). Finally, NO is able to bind to CCO via the heme center. Photoactivation of CCO is able to dissociate NO, allowing increase in respiration and ATP formation again (Huang et al. 2009).

In order to study the direct interaction of light with cytochrome c oxydase, some work has been done related to action and absorption spectra. An action spectrum is the rate of a physiological activity plotted against wavelength of light and an absorption spectrum is a spectrum of radiant energy whose intensity at each wavelength is a measure of the amount of energy at that wavelength that has passed through a selectively absorbing substance. Karu and Kolyakov (2005) showed a relationship between the action spectra of proliferation and DNA content in HeLa cells (epithelial cervix cancer cell line) regarding its interaction with light and the absorption spectra of the most important structures of cytochrome c oxidase.

This study was the starting point to consider this molecule as the main photoreceptor for photobiomodulation. Cytochrome c oxidase is a

transmembrane protein of the inner mitochondrial membrane involved in the electron transfer within the respiratory chain. It accepts electrons from cytochrome c and gives them to oxygen, the last electron acceptor to form a water molecule (Figure 1-9). The most important intermediates involved in electron transfer within this protein are copper A (Cu_A), heme a, heme a3 and $Cu_{B,}$ and its redox state determines the redox state of cytochrome c oxidase which can be either oxidized or reduced (Karu and Kolyakov 2005).

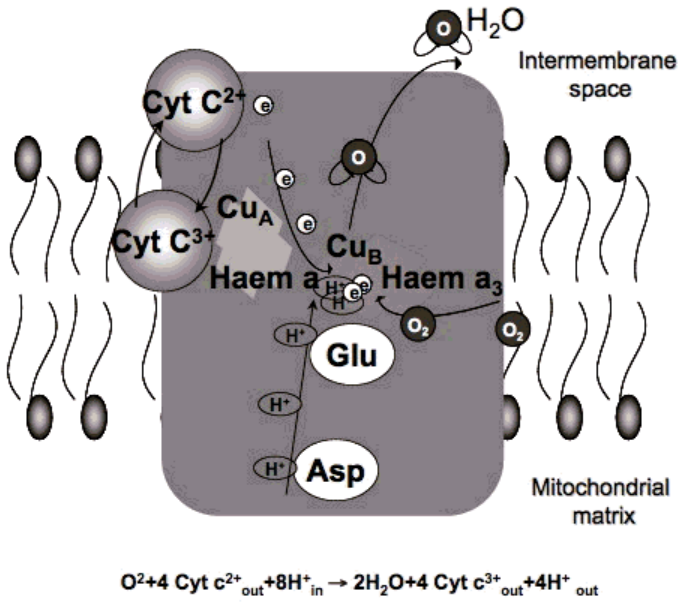

Figure 1-9: Structure and biochemical reactions of cytochrome c oxidase.

Adapted from Hamblin and Demidova (2006).

Limitations are also present especially when trying to match both action and absorption spectra because the biological effect measured may just be an indirect consequence of the application of light. Four peaks were found within the visible to IR wavelength light, which were identified with the absorption spectra of Cu_A, heme a, heme a_3 and Cu_B separately, but not with the absorption spectra of cytochrome c oxidase. In fact when analyzing both its

oxidised and reduced form, the two biggest peaks are found in other regions; the first one in the blue region and another one around 600 nm (Karu and Kolyakov 2005). Both forms are able to absorb radiation through other regions of the electromagnetic radiation meaning that cytochrome c oxidase could be excited with any kind of light within the visible or IR spectrum. However, apart from Karu and colleagues (2005) little has been reported in this field, so it has not yet been demonstrated whether CCO is the photoacceptor for visible/IR radiation. To overcome the limitations of action spectra studies, testing directly the activity of the putative photoreceptor comparing both light exposed and non-exposed conditions is required. Only one study reported by Wong-Riley and colleagues (2005) showed the role of CCO in response to light in neutrophils. They showed how pretreatment with red light completely reverted the effect of tetrodotoxin (TTX), a voltage-dependent sodium channel blocker, which blocks neuronal impulse activity, decreasing ATP demand and down-regulating cytochrome c oxidase activity. Furthermore, this pretreatment with red light also increased the efficacy of cytochrome c oxidase when using potassium cyanide (KNC) an irreversible inhibitor of cytochrome c oxidase (Wong-Riley et al. 2005). These discoveries, together with the comparison of absorption and action spectra already explained, give more solid evidences supporting the role of cytochrome c oxidase as a photoreceptor.

1.3.2.2 The opsins

Cell signalling is an important event which enables cells to communicate with each other and with the environment. This way, they are prepared to

respond to environmental changes or perturbations. Membrane receptors have the role of transmitting the signal to intracellular signal transduction cascades, altering cell behaviour. Fundamentally, the components of a signalling transduction pathway are first, the signal and the receptor and subsequently, the transduction, the effector and the final response (Alberts et al. 2007)

There are three main cell surface receptors: ion-channels, GPCRs and enzyme-linked receptors (Alberts et al. 2007). G-protein-coupled receptors or seven transmembrane receptors (7TMs) are the biggest cell surface receptor family comprising a 3-4% of the whole human genome (May et al. 2007). OPNs are GPCRs which can be stimulated by light through a covalent binding to a vitamin A derived chromophore which is normally 11-cis-retinaldehyde (Ebrey and Koutalos 2001).

When the receptor protein is activated, it can join a G protein complex which includes three subunits α, β and γ. One of these three subunits of the G protein complex, the α subunit hydrolyses GTP to GDP; and in doing so the βγ complex is activated as well (Alberts et al. 2007). Downstream enzymes activated by G proteins catalyse the production of molecules which act as secondary messengers. Many downstream signalling pathways can be activated by GPCRs. The phosphatidylinositol pathway through phospholipase C is considered to be one of the most important GPCR pathways (Pierce et al. 2002), being mediated by Gq proteins. Another G protein, G13 is also activated by GPCRs and transmit the signal through Rho downstream signalling pathway.

Although GPCRs can bind a broad variety of different ligands, their primary structure, as well as their tertiary structure is are highly conserved (Strader et al. 1995). All these proteins share a structure of seven hydrophobic segments that are the transmembrane-spanning α-helices, most commonly known as TM domains. These seven domains are separated by extra- and intracellular hydrophilic loops, with an extracellular N-terminus and an intracellular C-terminus. Due to the variety of GPCRs, they divide into three distinct subfamilies based on sequence differences, which are principally found beyond the TM domains (Pierce et al. 2002).

The class A subfamily includes OPN2 or RHO and β2 adrenergic receptor-like receptors. It is the largest of the three GPCRs subfamilies (Gether 2000). The class B subfamily includes glucagon/calcitonin receptor like receptors. Finally, metabotropic glutamate-like receptors represent the class C subfamily (Figure 1-10) (Vauquelin and Van Liefde 2005).

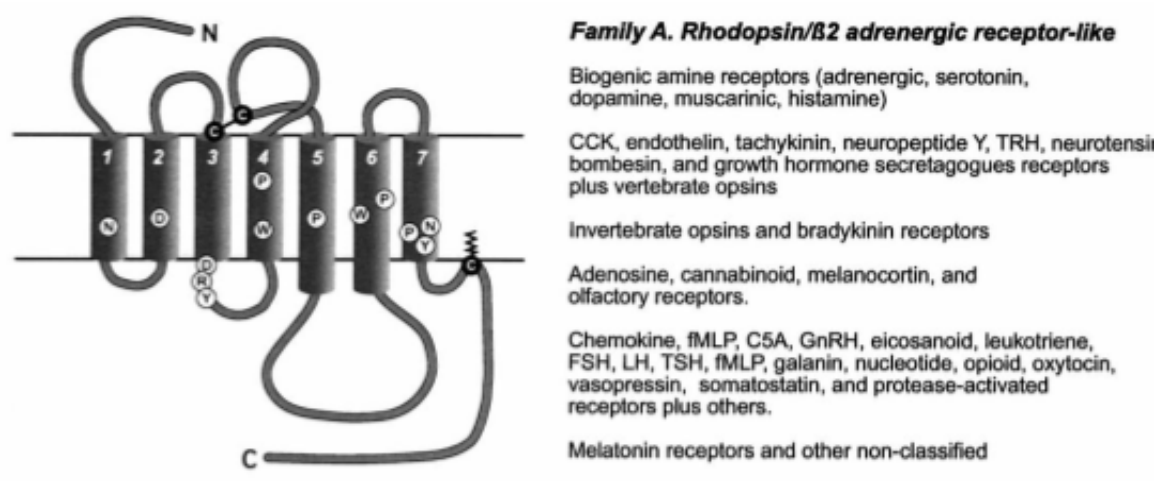

Figure 1-10: Families A of GPCRs.

Adapted from Gether, (2000).

Mammalian OPN2 or RHO, one of the better studied GPCRs, is present in rod cells within the retina and plays a remarkable role in vision in dim and dark light (Bourne and Meng 2000). OPNs in general and OPN2 in particular, bind covalently to the photochromophore retinal both in the dark (inactive) state and after photoactivation (Bourne and Meng 2000). The absorption of a photon by the 11-*cis* retinal isomeric form causes a conformational change and produces the all-*trans* retinal which enables the visual pigment rhodopsin to undergo a conformational change to become active (R*). This signal leads to a depolarization of the cell membrane and in the context of vision, it will reach the cell membrane of retinal neurons (Dell'Orco 2013). 11-*cis*-retinal acts as an inverse agonist, blocking the constitutive activity of the receptor which can be activated only by light (Gether 2000).

However, other OPNs are also expressed in mammals. OPN1-short wavelength (OPN1-SW) has its maximum absorption spectra in the violet-blue range, but the peak for OPN1-middle/long wavelength (OPN1-M/LW) is at higher wavelengths, in the green part of the spectra. OPN2 can be excited by blue-green light. In humans, OPN1 and OPN2 (rhodopsin) are the main photoreceptors in the eye. They transduce the light signal through the G protein transducin or Gt. Transducin, in turn, activates the cGMP-dependent phosphodiesterase, which hydrolyzes cGMP, thus reducing its concentration and leading to the closure of sodium channels in the outer segment membrane (F). Following isomerization and release from the opsin proteins, all-trans retinal is reduced to all-trans retinol and travels back to the retinal pigment epithelium to be ‘recharged’. Finally, peropsin was found in the retinal pigment epithelium

(RPE) of the mammalian eye where it can act as a retinal photoisomerase (Terakita 2005).

Non-visual OPNs have also been identified; OPN3 or encephalopsin activates the Gi/Go pathway and has its absorption peak at 460 nm of the light spectra, OPN4 or melanopsin transduces the light signal through Gq protein and OPN5 or neuropsin, a UV-R sensitive photoreceptor, activates Gi proteins (Poletini et al. 2015). Each of them has its maximum absorption spectra at a different wavelength, being able to respond to different light parameters and activating a different G protein related downstream pathway, which will induce different biological responses.

Following the work of Miyashita, Moriya *et. al.* (2001) describing the presence of OPN2 and cone opsins in murine melanocytes, Tsutsumi *et al.* (2009) confirmed the presence of rhodopsin-like proteins and opsin-like proteins throughout the human epidermis from the face, and a reconstructed skin model using both reverse transcription polymerase chain reaction (RT-PCR) and immunohistochemistry (IHC). OPN2 was observed throughout most of the epidermis except the basal layer. Furthermore, the presence of two different types of OPNs was confirmed. The first one, stimulated by a shorter wavelegth, OPN1-SW was found in the upper layer of the epidermis, and OPN1-M/LW opsin-like protein, stimulated by a longer wavelength, was localized to the basal layer of the epidermis. Furthermore, while they confirmed this finding in total RNA from facial human skin by RT-PCR, any of these photoreceptors were not found in primary human keratinocytes derived from neonatal foreskin in culture.

Subsequently, a recent study on the role of violet light in primary cultures of human epidermal keratinocytes derived from neonatal foreskin found expression of OPN2 by immunocytochemistry (ICC) and western blot (Kim et al. 2013). Finally, a detailed study by Haltaufderhyde, K. *et al.* (2015) using primary human epidermal melanocytes derived from neonatal foreskin, and purchased primary human keratinocytes (Lifeline Cell Technology; they do not give details from the origin of these keratinocytes) demostrated the presence of *OPN1-SW*, *OPN2, OPN3 and OPN5* mRNA in both cell types as well as *OPN4* in melanocytes while *OPN1-M/LW* was not detected in either.

Strong evidence for the photosensitivity of OPNs to light in tissues other than the eye is now emerging (Kojima et al. 2011; Wicks et al. 2011; Kim et al. 2013; Koyanagi et al. 2013; Sikka et al. 2014; Toh et al. 2016; Buscone et al. 2017; Regazzetti et al. 2017). It has been shown that OPN-like receptors have an important role in light reception and signal transduction through a G protein and the polycation liposome (PCL)-mediated pathway, which mobilizes calcium (Ca^{2+}) following UVA exposure which induced dose-dependent melanin production by human melanocytes (Wicks et al. 2011). More specifically, OPN2 played a role in the effect of UV in mediating differentiation of human epidermal keratinocytes derived from neonatal foreskin (Kim et al. 2013).

Focusing on non-visual OPNs, OPN3 has been shown to be a photoreceptor in lower animals such as pufferfish and mosquito. It has been shown the role of OPN3 to interact with light in vertebrates (Koyanagi et al. 2013). In line with this, Buscone *et al.,* (2017) have recently reported that OPN3

downregulates proliferation of human hair follicle outer root sheath cells in culture; furthermore, blue light was inducing proliferation of outer root sheath cells, effect which was abrogated after silencing of OPN3. Melanopsin or OPN4 has been highly studied in the context of circadian clock. It has been identified as a circadian clock photoreceptor in mammals, which means it is able to entrain the circadian clock in several mammal tissues (Panda et al. 2002; Hankins et al. 2008). Apart from its circadian function, OPN4 was shown to specifically respond to blue light in mice mediating the blue-light vasorelaxation response of blood vessels in mice (Sikka et al. 2014). Human and mice OPN5 were able to respond to UV (380nm) light through Gi mice signalling pathway. This was leading to the formation of a new OPN5 photoproduct absorbing blue light (Kojima et al. 2011). Finally, peropsin was also studied in human skin and it contributed to the UV light-induced Ca^{2+} release in a retinal-dependent way in N/TERT-1 keratinocyte cell line (Toh et al. 2016). These findings reveal a role for OPNs in a very important function of the skin, melanin production, as well as hair follicle cell proliferation.

Even though there is new evidence for the role of OPNs in non-photoreceptive tissues, their specific function still needs to be explored in more detail. Further explanation about the circadian clock will be made in the next section, however, the idea of non-visual OPNs mediating circadian clock photoentrainment by their interaction with light in peripheral tissues is gaining momentum (Poletini et al. 2015; de Assis et al. 2016), and highlights the importance of the circadian clock in skin physiology and wound healing (Plikus

et al. 2015). Therefore, non-visual OPNs are emerging as interesting targets for wound healing light-based therapies.

1.3.2.3 Cryptochrome

Cryptochromes are one of the three groups of proteins that belong to the family of photolyases/cryptochromes. This diverse gene family shares the presence of two photoactive molecules within their structure throughout all the biological kingdoms (Chaves et al. 2011), the chromophores flavin adenine dinucleotide (FAD) and pterin (Hsu et al. 1996). These chromophores are able to absorb blue light which give the role of blue light receptors to the photolyase/cryptochrome family.

Furthermore, photolyases act as light-dependent DNA repair enzymes; while on the other hand, cryptochromes (first identified in *A. thaliana* (Ahmad and Cashmore 1993)) are signalling molecules involved in circadian clock regulation in both plants and animals (Chaves et al. 2011). They are also regulated by external light signals, which can lead to circadian photoentrainment in plants and some animals such as Drosophila (Chaves et al. 2011). Despite the presence of FAD and pterin in mammalian CRY, their role as blue light receptors in mammals has not yet been established (Lucas and Foster 1999) (Figure 1-11).

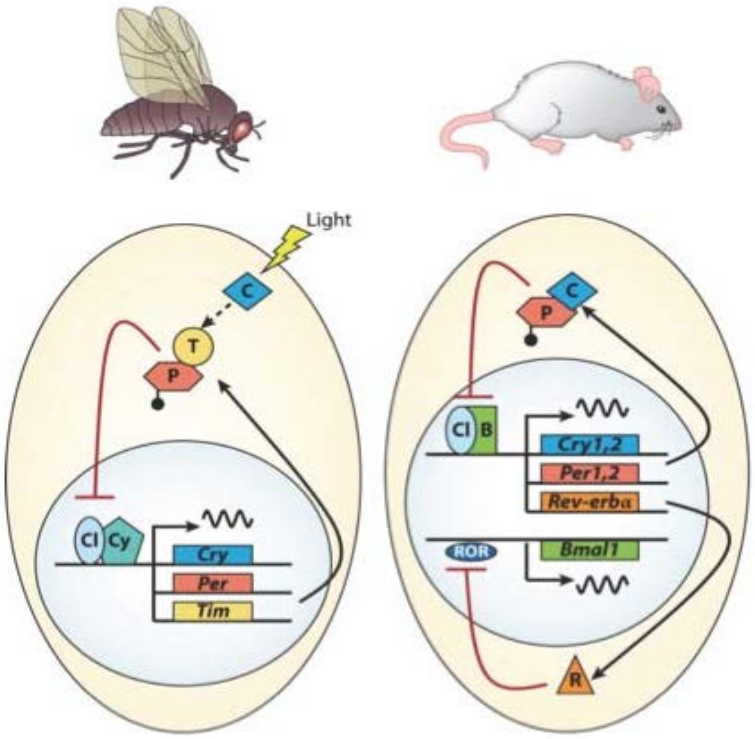

Figure 1-11: Molecular clock of drosophila and mouse.

C or Cry: Cryptochrome; P or Per: Period; T or Tim: Timeless; Cl, Clock; B or Bmal1: Brain and muscle ARNT (arylhydrocarbon receptor nuclear translocator)-like protein 1; R or Reb-erbα; Cy, Cycle. Adapted from (Chaves et al. 2011).

Nowadays, the role of CRYs in the circadian clock molecular machinery in different animals including humans has been accepted (Zhao et al. 2014). As a consequence of exposure to daily cyclic variation of light and dark, circadian rhythms have been observed through all biological kingdoms, as a highly conserved system. These circadian rhythms produce oscillations at the molecular, physiological and behavioural level of organisms and it confers on them a selective advantage (Sancar 2000). In humans, its molecular pathway is based on two main feedback loops cryptochrome/period (CRY/PER) and REV-ERBs/retinoic acid receptor-related orphan receptor (ROR) which are connected by aryl hydrocarbon receptor nuclear translocator like (ARNTL) or

BMAL1 and clock circadian regulator (CLOCK) (Figure 1-12) (Geyfman and Andersen 2009).

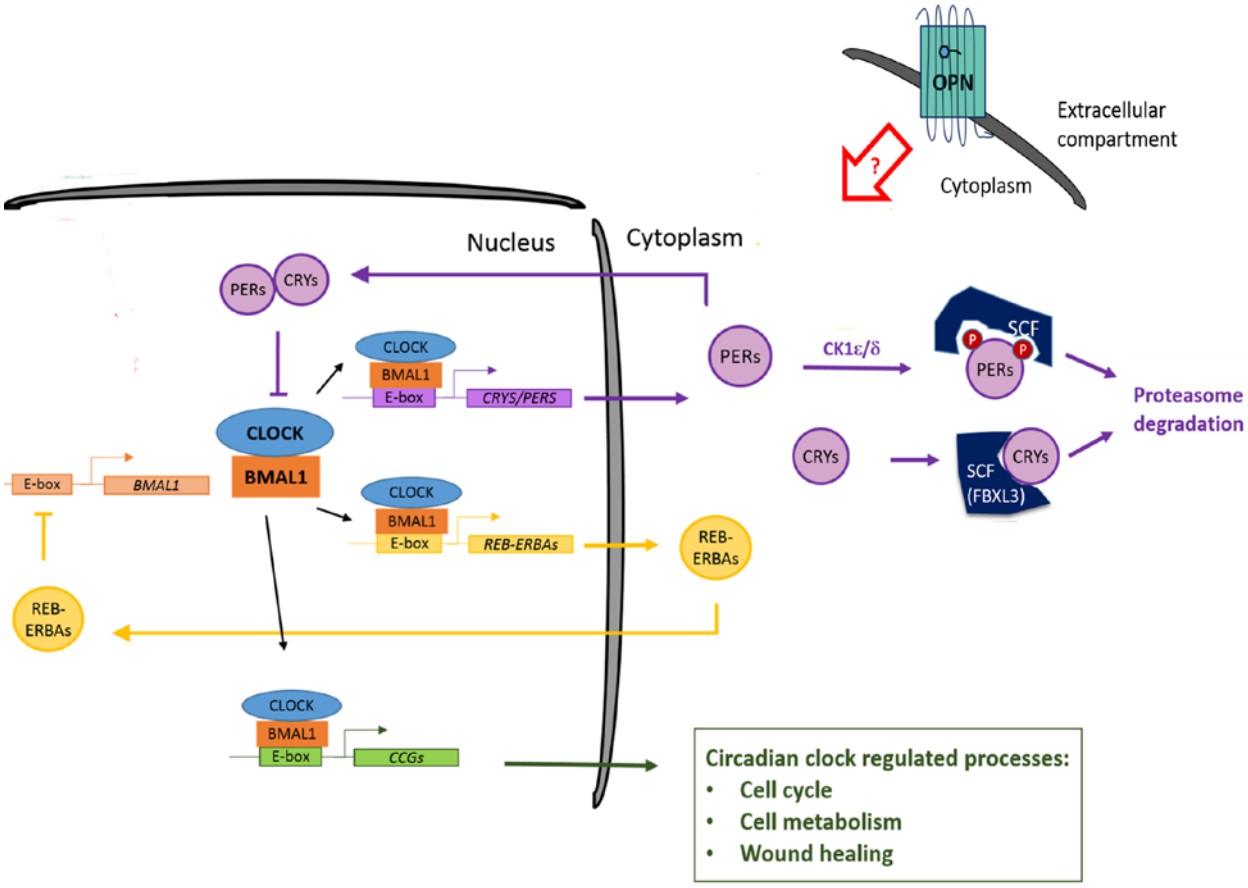

Figure 1-12: The peripheral circadian clock in human skin.

Possible implication of OPNs in the modulation of circadian clock is suggested with a red question mark. Pointed arrow means activation and stopped arrow means inhibition.

The importance of the circadian clock in the cell cycle regulation has been already established (Plikus et al. 2015). Although the mechanism of action is not completely understood, it has been established that the circadian clock regulates several cell cycle check point genes such as *wee1* and *Cyclin Dependent Kinase Inhibitor 1A (CDKN1A)* (Plikus et al. 2015). Furthermore, molecules such as the mammalian TIM and non-POU domain-containing

octamer-binding protein (NONO) interact with both circadian proteins and cell cycle proteins (Kowalska et al. 2013). The connection between both circadian clock and cell cycle processes is of interest in wound healing research, especially when the focus is on chronic wounds where cell regulation is completely lost. Kowalska *et al.,* (2013) have shown that Nono knockout mice display an impaired wound healing response; these animals were characterised by delayed epidermal regeneration, loss of dermal organization and decreased collagen deposition in the wound site.

Regarding the photoreceptor function of cryptochromes, the two human Cryptochrome proteins CRY1 and CRY2 were first identified as *Drosophila* (6-4) photolyase homologues, but they lacked both the ability to bind to damaged DNA and to repair thymidine photoproducts, which led to the conclusion that these two genes may act as blue-light receptors (Hsu et al. 1996). Subsequently, numbers of studies have been done to elucidate both the expression and function of these two proteins. The dual function of mammalian CRYs as circadian clock regulators and photoreceptors was also suggested due to their structural similarity with non-mammalian CRYs (Vitaterna et al. 1999), however no strong evidence has yet been shown and arguments have been proposed against human CRY ability to respond to blue light (Foster and Helfrich-Förster 2001). The different role of CRYs within the circadian clock of mammals in comparison to plants or other animals is clear. While, for example in Drosophila, cry is not part of the core molecular mechanism of the circadian clock, but acts more like a gate that interacts with timeless (tim) and gives an input to the molecular loops to function, while in mammals CRY is part of one of

the two feedback loops that maintain cellular rhythmicity (Figure 1-11). This difference can be more important than the highly similar protein structure when addressing the question of mammalian CRY as the circadian clock photo entrainment molecule (Foster and Helfrich-Förster 2001). However, it is still a fact that CRY contains two chromophores inside its protein structure that may not transduce in a change of protein conformation, but may be involved in the production of ROS as a stress signalling mechanism (Hoang et al. 2008).

There are only limited studies that demonstrate that the human CRY1 and CRY2 proteins are able to interact with light. Hoang, Schleicher et al. (2008) used the action spectra approach to measure the level of oxidized flavin in insect living cells transfected with human CRY1; showing that human CRY1 undergoes light-dependent proteolysis after blue light exposure when expressed in living flies (Hoang et al. 2008). This is the most promising finding supporting the role for cryptochromes as photoreceptors in humans. However, whether this degradation is the result of a direct effect of the light on hCRY molecule or wheather other mechanisms are involved is not clear. Furthermore, non-irradiated controls at every time point were not included for comparison, and the light-dependent function of hCRY within human cells was not addressed.

Peripheral clocks are found in all organs in the human body. Specifically, *PER1* and *CLOCK* mRNA were found in human skin (Zanello et al. 2000). These data were confirmed and consolidated by showing the mRNA expression of *BMAL1 and TIM* in human skin (Bjarnason et al. 2001). Furthermore, *PER1*

and *BMAL1* followed a circadian behaviour (Bjarnason et al. 2001). Human primary skin cells were shown to express CRYs and to maintain circadian oscillations in culture; primary keratinocytes from neonatal foreskin showed mRNA oscillations for most of the clock genes after synchronisation with chelated FBS, including *BMAL1, REB-ERBAα, , REB-ERBAβ, PER1, PER2, PER3, CRY1* and *CRY2* (Janich et al. 2013). Primary dermal fibroblasts from the anterior pubic region also showed oscillations in culture of *BMAL1, PER1, PER2, CRY1* and *CRY2* after synchronisation with dexamethasone (Lippert et al. 2014). Furthermore, gene silencing of CRY1 in epidermal keratinocytes resulted into increase on late differentiation and reduced in colony formation, while *PER2* was significantly unregulated (Janich et al. 2013). This shows the relevance of CRY1 in epidermal keratinocytes proliferation and differentiation *in vitro*.

In order to study the role of CRYs and OPNs in the context of the circadian clock, it is important to understand how this molecular pathway can be modulated. Several pharmacological tools have been identified to regulate the CRY/PER feedback loop; KL001 was found to block one of the enzymes required for CRYs degradation, stabilising the protein while longdaysin (LD) dowregulates the degradation of PERs (Hirota et al. 2012) (Figure 1-12). KL001 was used to study corneal wound healing and was shown to slow down the re-epithelialisation process in mice (Xue et al. 2017), suggesting the use of interventional strategies to regulate biological rhythms to improve corneal healing.

1.4 Aim and objectives

Expression of the photoreceptors OPNs in human skin and latest findings about their implication in diverse functions of the skin such as melanin production and hair follicle cell proliferation open a new field to explore a range of opportunities for the development of new light-based therapies specifically targeting OPNs with differennt light parameters. Furthermore, photosensitivity of human CRY to blue light has also opened the possibility of regulating the peripheral circadian clock of human skin using photobiomodulation.

The first aim of this study was to investigate the expression of OPNs and CRYs in human skin from different anatomical regions and to establish whether primary epidermal keratinocytes and dermal fibroblasts retain expression in culture. Then, to investigate the effect of different light parameters on epidermal keratinocytes in terms of their metabolism and migration in a scratch wound assay by using gene silencing of OPNs and CRYs , establishing their role in normal conditions and after blue light exposure. Finally, to develop an *ex vivo* human skin wound healing model to determine whether light inrradiation can improve re-epithelialisation.

Objectives:

- Localisation of visual OPNs, OPN1-SW and non-visual OPNs, OPN3 and OPN5 photoreceptors as well as the circadian clock CRY1 and CRY2 in human skin *in situ*.

- Confirmation of mRNA and protein expression of OPNs and CRYs in primary epidermal keratinocytes and dermal fibroblasts *in vitro* to validate further use as a model to investigate the effect of light on cellular responses.

- Determine the optimal light parameters to modulate epidermal keratinocyte metabolism, migration, DNA synthesis and differentiation.

- Establishing a role for photoreceptors in epidermal keratinocyte DNA synthesis, migration and differentiation with low levels of blue light irradiation following gene knock down by siRNA transfection (targeting OPN3 and CRY1) in combination with KL001 treatment.

- Investigate the effect of light on wound healing using an *ex vivo* human wound healing model to evaluate the efficiency of selected light parameters in re-epithelialisation, and the expression of photoreceptors in the new epithelial tissue formed.

2 MATERIALS AND METHODS

Ethical approval to carry out this study was granted by the Chair of the Biomedical, Natural and Physical Sciences Research Ethics Panel at the University of Bradford on the 24th of October 2014.

2.1 Human skin samples

Skin samples from healthy patients undergoing facelift plastic surgery or abdominoplasties were obtained with informed consent. The skin tissue was immediately placed in transporting media until it was processed no longer than 12 h later.

Transporting media was made as follows: Minimum Essential Medium (MEM), GlutaMAX supplement (GIBCO, UK) was supplemented with 10% foetal calf serum (FCS) (GIBCO), 250 Units/ml penicillin and 250 µg/ml streptomycin (Pen/Strep) (GIBCO), 7.5 µg/ml of amphotericin B and 6.15 µg/ml of sodium deoxycholate, both contained in fungizone antimycotic (GIBCO) and 2 mM of L-alanyl-L-glutamine dipeptide in 0.0085% of NaCl or glutaMAX (GIBCO) and stored at 4˚C.

After reception, skin tissue was placed in a 60 mm tissue culture dish (Starstedt) with PBS (Figure 2-1, 1) and fat tissue was removed using scissors. Then, the skin was cut into small squares (≈1cm^2); some of the pieces were embedded in OCT for further histological analysis of *in vivo* skin (section 2.2.5) and the rest was used for primary epidermal keratinocyte and dermal fibroblast cell extraction (section 2.2.2).

2.2 Establishment of primary cells

2.2.1 Cell culture solutions

2.2.1.1 Primary epidermal keratinocyte growth media

Primary keratinocyte growth media was made up using keratinocyte growth media 2 (PromoCell, UK) supplemented with 0.004 ml/ml of bovine pituitary extract, 0.125 ng/ml of epidermal growth factor (recombinant human), 5 µg/ml of insulin (recombinant human), 0.33 µg/ml of hydrocortisone, 0.39 µg/ml of epinephrine, 10 µg/ml of tranferrine holo (human), 0.06 mM of $CaCl_2$ 100 Units/ml penicillin and 100 µg/ml streptomycin (Pen/Strep) (GIBCO) and 2.48 µg/ml fungizone (GIBCO). Keratinocyte growth media 2 was kept at 4 ˚C and all supplements at -20 ˚C. Once media was supplemented, it was stored at 4 ˚C for no longer than one month.

2.2.1.2 Primary dermal fibroblast growth media

Primary fibroblast growth media was made up using Dulbecco's modified Eagle's medium (DMEM) with L-glutamine (Sigma-Aldrich) supplemented with 10% foetal bovine serum (FBS) (GIBCO), 100 Units/ml penicillin and 100 µg/ml streptomycin (Pen/Strep) (GIBCO), 2.5 µg/ml of amphotericin B and 2.05 µg/ml of sodium deoxycholate, both contained in fungizone antimycotic (GIBCO). DMEM was kept at 4 ˚C and FBS, Pen/Strep and fungizone at -20 ˚C. Once fibroblast medium was prepared, it was kept at 4 ˚C for no longer thatn one month.

2.2.1.3 Primary cells freezing media

Cryo-SFM (Promocell) was used to freeze primary human keratinocytes. Fibroblasts were frozen in media prepared using 80% of fibroblasts growth media (2.2.1.2), 10% FBS (GIBCO) and 10% dimethyl sulfoxide (DMSO) (Sigma-Aldrich).

2.2.2 Cell extraction

After cleaning and cutting the skin tissue as described above (Figure 2-1, 1), into small pieces, they were placed in 5.2 U/ml of dispase (GIBCO) in PBS with 100 Units/ml penicillin and 100 µg/ml streptomycin (Pen/Strep) (GIBCO) and 2.5 µg/ml of amphotericin B and 2.05 µg/ml of sodium deoxycholate, both contained in fungizone antimycotic (GIBCO) and kept at 4 ˚C overnight.

Working under the dissecting microscope (Leica), the epidermis was peeled using forceps and kept in primary keratinocyte growth media (2.2.1.1) in ice. The remaining dermis was placed in fibroblast growth media (2.2.1.2), which was also kept in ice (Figure 2-1, 2). Once all the skin tissue was processed, the epidermis was trypsinised with 3 ml of 0.05% Trypsin/EDTA (GIBCO, Netherlands) for 5 to 10 minutes at 37 ˚C and vortexed (Figure 2-1, 4). After removing the excess epidermis, trypsin neutralising solution (TNS) (Lonza, UK) was added (equal volume as trypsin) and the suspension was centrifuged for 5 min at 600 g. The pellet was dissolved in keratinocyte growth media (2.2.1.1) and cultured in T75 flasks (Corning, UK) at approximately 25,000 cells/ml (Figure 2-1, 5).

Between 6 and 12 pieces of dermis were placed in a T75 flask (Corning) with the papillary dermis facing down (Figure 2-1, 6) and once it had stuck to the flask, 5 ml of fibroblast growth media (2.2.1.2) was added. Both primary keratinocytes and fibroblasts were incubated at 37 ˚C and 5% CO_2 and maintained by changing the media every other day until they reached 80-90% confluence (Figure 2-1, 7) when they were either passaged or frozen in liquid nitrogen.

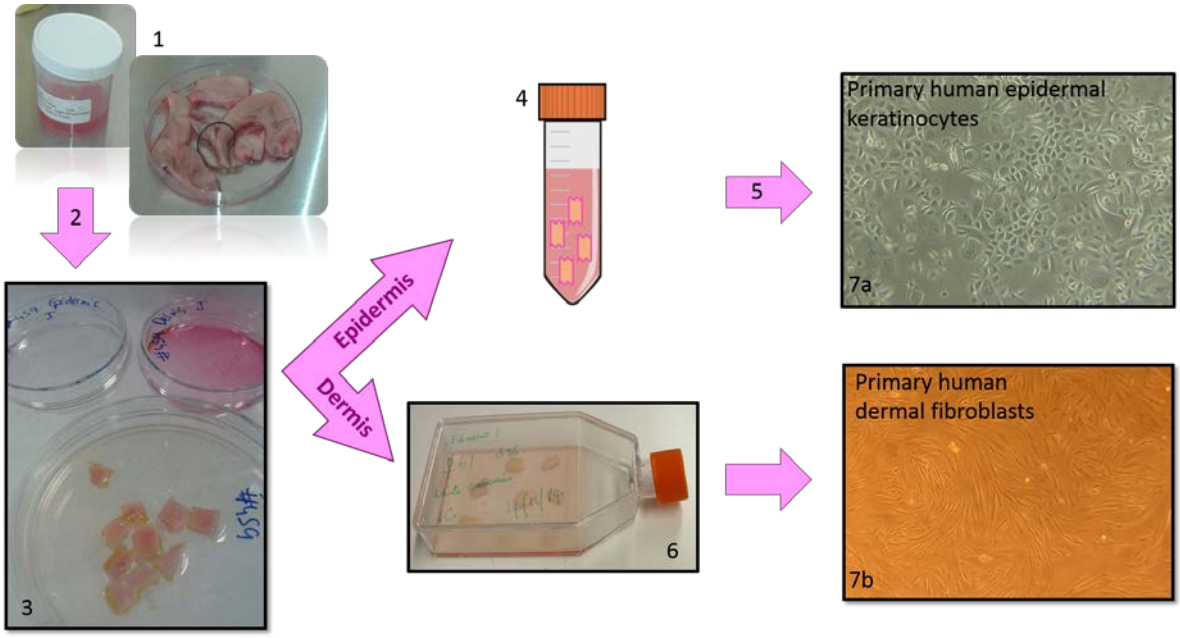

Figure 2-1: Workflow of primary fibroblasts and keratinocytes extraction from human skin.

1 - Reception of post-surgery skin; clean, remove fat and cut into small pieces. 2 - Incubate overnight in 5.2 U/ml of dispase. 3 - Peel the epidermis from the dermis. 4 – Trypsinise the epidermis (5 to 10 mins at 37 ˚C), vortex and remove pieces of epidermis. Add equal volume of TNS and centrifuge for 5 mins at 1000 rpm. 5 – Resuspend the pellet in keratinocyte growth media and culture cells in a T75 flask. 6 – Culture dermis explants in fibroblast growth media in a T75 flask . 7a – Incubate primary keratinocytes at 37 ˚C 5% CO_2. 7b – Incubate primary keratinocytes at 37 ˚C 5% CO_2.

2.2.3 Cell maintenance and passaging

Cells were maintained at 37 ˚C and 5% CO_2 in a humidified incubator. Both primary keratinocyte growth media (2.2.1.1) and fibroblast growth media (2.2.1.2) were changed every other day until cells reached confluence. Special care had to be taken with primary keratinocytes; they had to be passaged at 80% confluent to avoid differentiation.

2.2.3.1 Primary epidermal keratinocytes

Once primary keratinocytes had reached 80% confluence, they were washed with PBS twice. Then, 0.5 mM of ethylenediaminetetraacetic acid (EDTA) (GIBCO) was added (Table 2-1) and cells were incubated for 4 min at 37 ˚C to disrupt cell-cell interactions. After removing EDTA, 0.05% Trypsin/EDTA (GIBCO) was added for 2 mins at 37 ˚C (Table 2-1). Under the phase contrast microscope cells were checked for detachment from the flask and a double volume of TNS was added (Table 2-1).

Volumes added of	**T25 flask**	**T75 flask**
0.05 mM EDTA	1.5 ml	2.5 ml
0.05% Trypsin/EDTA	1 ml	2 ml
TNS	2 ml	4 ml
Fibroblasts growth media (for trypsin neutralisation)	2 ml	4 ml

Table 2-1: Keratinocyte and fibroblast passaging.

Cells were transferred to a 15 ml Falcon tube (Starstedt, UK) and cell number and viability quantitated using an improved Neubauer haemocytometer (Hawksley, UK). The cell suspension was mixed with trypan blue solution 0.4% (Sigma-Aldrich) (1:1) and 10 µl was added into the haemocytometer. The total number of cells and the non-viable cells (blue colour) in the 4 corners and the middle compartments were counted. Cells in the bottom and left grids were taken into account, discarding cells in the upper and right grids of the compartments. The average number of cells was calculated and multiplied by 2 (dilution factor) and by 10^4 (0.1 mm depth) to calculate the cell concentration (number of cells per ml). This information was used to plate cells at the desired cell density. Cells were centrifuged at 400 g for 5 mins; the supernatant was removed and the pellet was re-suspended in keratinocyte growth media (2.2.1.1) and the cells were plated at the desired cell density. For routine passaging, cells were split at a ratio of 1:3.

2.2.3.2 Primary dermal fibroblasts

Similar to primary keratinocytes, monolayers of primary fibroblasts were washed twice with 1x PBS after reaching 80-90% confluence. Then, 0.05% Trypsin/EDTA (GIBCO) was added for 5 mins at 37 ˚C. Under the phase contrast microscope it was checked whether cells had detached from the flask. Tapping the bottom of the flask helped in the detachment process. A double volume of fibroblast growth media (2.2.1.2) which contained 10% FBS was added to neutralise the trypsin and the cell suspension was transferred to a 15 ml Falcon tube. Cells were counted as previously described for primary

keratinocytes and centrifuged at 400 g for 5 mins. The supernatant was removed and the cell pellet was re-suspended in fibroblast growth media (2.2.1.2) and plated at the desired cell density. For routine passaging, cells were split at a ratio of 1:3.

2.2.4 Freezing and thawing cells

Correct freezing and defrosting processes are critical for cell viability. The freezing process has to be done slowly, while defrosting has to be done quickly. Once confluence was reached, cells were processed as previously described up to the point of centrifugation (see 2.2.2). After centrifugation, the supernatant was discarded and the cells were re-suspended in 1 ml of either fibroblasts freezing media or Cryo-SFM freezing media (see 2.2.1.3) or transfer to CryoPure tubes (Sarstedt) labelled with the sample tracking number, gender and age of the patient, passage number, date and size of flask. The CryoPure tubes were placed in liquid nitrogen vapour for 24 h before transferring into liquid nitrogen.

When the cells were required, culture flasks were labelled and filled with either warmed fibroblast growth media (2.2.1.2) or keratinocyte growth media (2.2.1.1). Cells were taken from liquid nitrogen and immediately thawed under hot water. Then, the cell suspension was added to its flask and incubated at 37 ˚C and 5% CO_2 for 24h to allow cells to attach before the medium was changed.

2.3 The expression of photoreceptors in human skin *in situ* by immunofluorescence

Human female skin samples from face and abdomen were obtained from facelift (n=1) or abdominoplasty surgeries respectively (n=5) from females after ethical approval was given (Table 2-2). Samples were snap frozen embedded in OCT medial and kept at -80 °C.

Body site	Age
Face (F)	63
Abdomen (A)	**59**
	Unknown (U)
	51
	44
	55

Table 2-2: Human skin donor details used for immunofluorescence.

Cryosections of 7 to 10 µm thickness were cut with a Cryostat (Cryotome™ FSE Cryostats, Thermo Scientific), mounted on Superfrost+ glass microscope slides (Thermo-scientific, Netherlands) and store at -80 °C. Cryosections were air-dried at room temperature for 10 minutes and then fixed in either 4% paraformaldehyde (PFA) (Sigma-Aldrich, Netherlands) or cold acetone (Sigma-Aldrich, Netherlands) for 10 minutes as indicated in table 2-3. Then, sections were washed 3 times with PBS and permeabilisation step was

done for nuclear antibodies (CRY1 and CRY2) with 0.1% triton (Sigma-Aldrich, Netherlands) for 10 minutes. 100 µL of blocking solution (table 2-3) was added to the sections before incubating for 1h at room temperature. Double staining was done with desired antibody (table 2-3) and 1:200 KRT14 antibody (Abcam, ab51054 or ab7800). Sections were incubated with the primary antibody in blocking solution at 4 °C overnight. One section per slide was incubated with blocking solution only as negative control. Sections were washed with 0.05% tween in PBS three times for 10 minutes each before incubating with the secondary antibodies Alexa-488 (Abcam, ab150073) and Alexa-647 (Abcam, ab150115) at a 1:200 dilution for 1h at 37 °C. Sections were washed again with 0.05% tween in PBS three times for 10 minutes each before mounting using VECTASHIELD® Mounting Media with 4',6-diamidino-2-phenylindole (DAPI) (VECTOR laboratories). The cell lines HeLa and MCF-7, kindly provided by Christa Dam (Philips Research) were used as positive controls.

	Fixation		Blocking		Primary antibody		Primary antibody dilutions	
	IHC and ICC		IHC	ICC	IHC	ICC	IHC	ICC
OPN1-SW	Cold acetone: -20 °C for 10´		5% BSA + 5% Donkey Serum	5% BSA	ab5407 (Millipore)		1:200	
OPN3	Cold acetone: -20 °C for 10´		5% BSA + 5% Donkey Serum	5% BSA	ab66742 (Abcam)	ab75285 (Abcam)	1:100	1:100
OPN5	Cold acetone: -20°C for 10´		5% BSA + 5% Donkey Serum	5% BSA	ab199668 (Abcam)		1:200	1:500
CRY1	4%PFA: RT for 10´		5% BSA		ab54649 (Abcam)		1:200	1:400
CRY2	4%PFA: RT for 10´		5% BSA		PA5-13125 (Thermo Fisher Scientific)		1:100	
KRT 10	NA	4%PFA: RT for 10´	NA	3% BSA	NA	ab150075 (Abcam)	NA	1:200

Table 2-3: Immunofluorescence protocol for immunohistochemistry (IHC) of skin and immunocytochemistry (ICC) of primary cell cultures.

NA indicates not applicable.

2.4 Expression of photoreceptors in human primary skin cells in culture by RT-qPCR and immunofluoresence

After cell expansion (section 2.2.3), primary keratinocytes and fibroblasts were plated in 6-well plates (Greiner bio-one, UK) at a density of 50,000 to 100,000 cells per well for RNA extraction, or in Millicell EZ slide 8-well glass chamber slides (Merck, UK) at between 5,000 and 10,000 cells per well for immunocytochemistry (ICC) in the appropriate growth media. After reaching 80 to 90% confluence, cells were washed with 1x PBS twice and the media was either changed to fibroblast media supplemented with 2% FBS or to keratinocyte media without EGF and fungizone. After 24h, the RNA from 6-well plates was harvested and pooled for qPCR of photoreceptor mRNA expression and cells in chamber slides were fixed in 4% PFA or in cold acetone for ICC of photoreceptor expression.

2.4.1 Total RNA expression by RT-qPCR

RNA was extracted from primary female human epidermal keratinocytes (n=4 donors) and primary female human dermal fibroblasts from facial skin (n=2), scalp (n=2), breast (n=3) and abdominal skin (n=1). A human immortalized keratinocyte cell line NCTC 2544 (gift from Dr. Thornton) was included as a control. The age of the patient, passage number and sample name is specified in table 2-4 and 2-5. RNA from human fetal normal eye tissue (Biochain, UK) was purchased to use as positive control.

Body site	Age	Passage	Sample
Cell line	NCTC	-	NCTC
Face (F)	61	4	EK-F61*
	53	3	EK-F53•
	53	3	EK-F53▲
	49	5	EK-F49

Table 2-4: Primary human epidermal keratinocyte samples used for photoreceptors RNA expression by qRT-PCR.

EK denotes epidermal keratinocytes. *, • and ▲ denotes derived from the same donor in Table 2-5.

Body site	Age	Passage	Sample
Face (F)	61	4	DF-F61*
	53	3	DF-F53•
	53	3	DF-F53▲
	57	4	DF-F57
Scalp (S)	56	4	DF-S56
	51	4	DF-S51
Breast (B)	48	7	DF-B48
	44	4	DF-B44
	34	5	DF-B34
Abdomen (A)	55	6	DF-A55

Table 2-5: Primary human dermal fibroblast samples used for photoreceptors RNA expression by RT-qPCR.

DF denotes dermal fibroblasts. * denotes derived from the same donor. *, • and ▲ denotes derived from the same donor in Table 2-4.

2.4.1.1 RNA extraction and quantification

Primary cell total RNA extraction was performed with the RNeasy Mini Kit (QUIAGEN, UK) according to the RNeasy Mini Handbook protocol (QUIAGEN 2012). All the processes were performed using TipOne filter tips (STARLAB, UK) which are sterile and certified RNase, DNase, DNA and pyrogen free were used to avoid again RNA degradation and/or DNA contamination. 10 µl/ml of β-mercaptoethanol (Sigma-Aldrich) was added to Buffer RLT provided by the kit and added straight away to the cell monolayer pipetting up and down for not more than one minute. Then, the suspension was transferred to a 1.5 ml microcentrifuge tube where 350 µl of 70% ethanol was added to the lysate and mixed by pipetting. Up to 700 µl of the cell extract was transferred to the RNeasy spin column and centrifuge at 13000 rpm for 15 sec at 4 ˚C. This step was repeated if the total volume exceeded 700 µl. Subsequently, on-column DNase digestion was performed using the RNase-free DNase set (QUIAGEN 2012) to remove possible DNA contamination of the sample. Following appendix D (QUIAGEN 2012), 350 µl of buffer RW1 was added to wash the RNeasy spin column and centrifuged at 13000 rpm for 15 s at 4 ˚C. 80 µl of 0.34 U/µl of DNase I in buffer RDD was added to the RNeasy spin column to eliminate any DNA contamination. Samples were incubated for 15 min at room temperature. Then, the column was washed with 350 µl of buffer RW1 again and centrifuged at 13000 rpm for 15 s at 4 ˚C. Then, 500 µl of RPE buffer was added and centrifugation took place at 13,000 rpm, 15 s, 4 ˚C first. After discarding flow-through, this step was repeated changing the centrifugation conditions to 2 mins (same speed and temperature). RNeasy spin column was

placed in a new collection tube and it was centrifuged again for 1 min at 13,000 rpm and 4 ˚C to eliminate any residual of buffer RPE in the column. Finally, the RNA was collected; the RNeasy spin column was placed in a new 1.5 ml collection tube (RNAse free) supplied in the kit and 25 to 30 µl of RNase-free water was added to the membrane of the spin column, which was centrifuged at 13,000 rpm for 1 min at 4 ˚C. This step was repeated using the RNase-free water, where the RNA was eluted to increase the final RNA concentration.

RNA quantification was analysed using a NanoPhotometer (IMPLEN). One microliter of nuclease-free water provided in the RNeasy Mini Kit was used as a blank. One microliter of RNA was added to the NanoDrop which gave the concentration in ng/µl and the RNA quality by the A260/280 and 260/230 ratios, which should be around 2 and 2.2 respectively.

The human universal reference total RNA (Clontech) and total RNA human foetal normal tissue - whole eye (Biochain, UK) were used to verify quality and specificity of primers and they were also used as positive controls for photoreceptor expression.

2.4.1.2 cDNA synthesis

The high capacity cDNA reverse transcription kit with RNase inhibitor from Applied Biosystems (UK) was used for cDNA synthesis by reverse transcription following the manufacturer's instructions. The amount of total RNA used was 500 ng per 20 µl reaction. To perform the reverse transcription, the reactions were put in a thermal cycler where the conditions where set up as follows: pre-

heating at 25 ˚C for 10 min, anneling at 37 ˚C for 120 min and strand synthesis at 85 ˚C for 5min and holding at 4 ˚C.

2.4.1.3 qPCR

SYBR Green (Applied Biosystems) was used for RT-qPCR experiments, with 10µl final volume reactions. The samples were kept on ice and TipOne filter tips were used throughout. Two master mixes were prepared; one for cDNA dilution into nuclease-free water (0.03 µl/µl final concentration) and the second one for SYBR Green reagent (1:2) and primer mix (1µM final concentration) (Sigma-Aldrich) (Table 2-7). Primers were either chosen from publication or self-designed using an on-line tool called GenScript real-time PCR (TaqMan) primer design (GenScript 2002). Self-complementarity of the primers was checked using another on-line tool, oligonucleotide properties calculator (Kibbe 2007) and Primer-BLAST (Ye et al. 2012) to ensure primer specificity to the target RNA. Primers for amplification of photoreceptors are specified in Table 2-7. While working with SYBR Green, lights were switched off to avoid light interaction with this reagent. Reactions were loaded in PCR plates (STARLAB) which were spun down for 20 sec at 4 ºC before they were introduced into the qPCR machine (Applied Biosystems).

Gene	Primer sequence	Amplicon (bp)	Design	T (ºC)
OPN1-SW	Forward: 5'CGCCAGCTGTAACGGATACT3'	144	GeneScript (NM_001708.2)	63.1
	Reverse: 5'CCGAAGGGCTTACAGATGAC3'			
OPN2	Forward: 5'AGGAACACGAGGATTCTTGC3'	166	GeneScript (NM_000539.3)	62.2
	Reverse: 5'GCGAGGGTCTGAGAGGATAG3'			
OPN3	Forward: 5'CAATCCAGTGATTTATGTCTTCATGATCAGAAAG3'	125	Haltaufderhyde et al., (2015)	63.1
	Reverse: 5'GCATTTCACTTCCAGCTGCTGGTAGGT3'			
OPN5	Forward: 5'CTAGACGAAAGAAGAAGAAGCTGAGACC3'	119	GeneScript (NM_181744.3)	63.1
	Reverse: 5'GCGGTGACAAAAGCAAGAGA3'			
CRY1	Forward: 5'TAAGAGGCTTCCCTGCAAAA3'	230	Lin et al., (2014)	63.1
	Reverse: 5'GCCTCCATTCCCATTAGGAT3'			
CRY2	Forward: 5'AGGAGAACCACGACGAGA3'	288	Lin et al., (2014)	61.2
	Reverse: 5'TCCGCTTCACCTTTTTATAC3'			
GAPDH	Forward: 5'TATAAATTGAGCCCGCAGCC3'	143	GeneScript (NM_002046.5)	61.2, 62.2 and 63.1
	Reverse: 5'CGACCAAATCCGTTGACTCC3'			

Table 2-6: qPCR primers for photoreceptor amplification.

The Genex software (Biorad) was used for quantification, which was done using the Ct ($Ct^{\Delta\Delta}$) equation method and normalised to the housekeeping gene GAPDH. The final relative expression results were plotted and analysed with Prism (GraphPad, San Diego, CA, USA).

2.4.2 Protein expression by immunocytochemistry

Primary keratinocytes and dermal fibroblasts used for immunocytochemistry of photoreceptors are listed in table 2-8. All samples come from female donors. Age of donor, passage number and sample name are specified in table 2-8.

Cell type	Body site	Age	Passage	Sample
Primary keratinocytes	**Face (F)**	64	3	EK-F64
		61	4	EK-F61
		53	4	EK-F53
Primary fibroblasts	**Face (F)**	57	4	DF-F57
	Scalp (S)	53	4	DF-S53
		51	4	DF-S51
	Breast (B)	48	7	DF-B48

Table 2-7: Primary human epidermal keratinocytes and dermal fibroblasts used for photoreception protein expression analysis by ICC.

EK denotes epidermal keratinocytes. DF denotes dermal fibroblasts.

Cells were grown as indicated in section 2.2.3. Once the desired confluence was reached, the media was changed to EGF and fungizone free for keratinocytes or 2% FBS for fibroblasts and the cells were fixed after 24 h. For

fixation, cells were washed with PBS twice and 4% PFA for 10 min at room temperature or acetone for 10 min at -20 ˚C was added to the Millicell EZ slide where cells were growing. Single staining only was done as described for immunohistochemistry (section 2.2.5). Little differences in the protocol were detailed in table 2-3.

2.5 *Ex vivo* wound healing model

An ex vivo wound healing assay was adapted from (Stojadinovic and Tomic-Canic 2013) but the round wounds described were substituted to straight wounds as described by (Rizzo et al. 2012). Skin samples from healthy patients undergoing abdominoplasty surgery were obtained with informed consent. Tissue was processed within the first 8h after surgery. Tissue was washed in 1x PBS twice, and the fat was removed using scissors. The tissue was again washed twice in 1x PBS and placed in the lid of a 60 mm tissue culture dish (Sarstedt). Using the dissecting microscope (Leica), a double blade scalpel (1 mm gap) made in house (Philips Research) was used to make two incisions in the epidermis and the upper part of the papillary dermis (Figure 2-2, 2). Using forceps and scissor, the epidermis was cut so that a wound was created (Figure 2-2, 3). With a scalpel, small rectangles were cut around the wound; a metal plate with marked lines was used to help make reproducible cuts. The final result was a 60 to 80 mm^2 rectangular wound surrounded by epidermis at both sides (Figure 2-2, 4). Total area of the wounded skin samples were approximately 65 cm^2 and they were placed on a Netwell insert (6 well Netwell mesh inserts, CORNING) in a 6-well plate with 2 ml of phenol red free complete

DMEM. Wounds were cultured at the air-liquid interface to recreate *in vivo* conditions for up to 124 hours (around 5 days).

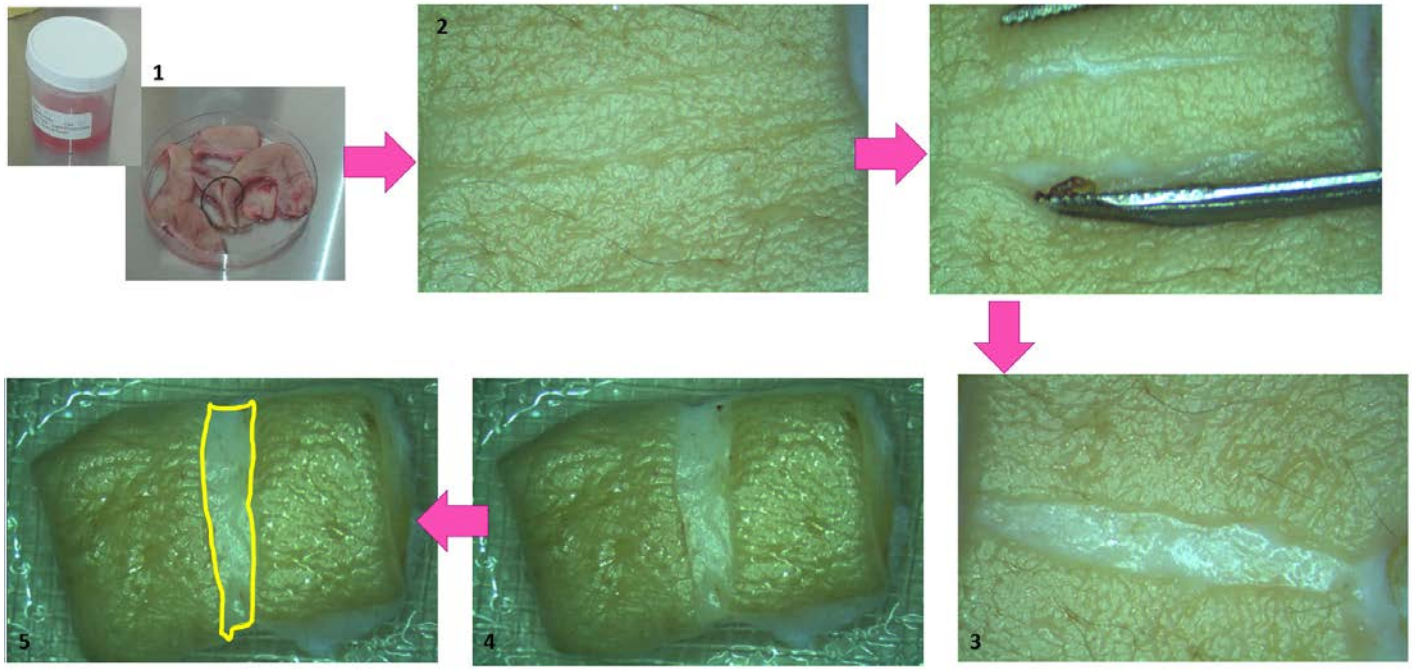

Figure 2-2: *Ex vivo* wound healing model using abdominal skin.

1. Reception of post-surgery abdominal skin. Skin was cleaned and fat was removed. 2. Two incision were made with a scalpel of ≈1cm width. 3. The epidermis between the two incisions made was removed using forceps and scissors. 4. Wounds were cultured in the air-liquid interface and pictures were taken twice a day for 6 days. 5. The wound area of each picture was analysed using Image J.

2.6 Light treatment of cells and wounds

Two different light devices were used to irradiate cells and *ex vivo* wound cultures depending on the requirements of the experiment.

2.6.1 Sirius-24

A custom light-based device was designed and developed in Philips Research (High Tech Campus, Eindhoven, The Netherlands) to study the effect of different wavelengths of light in cells *in vitro*; Sirius -24. It was designed as a two-box device where different LEDs were grouped in 6 different wavelengths, the first box was called blue box (Figure 2-3, A) and the second box was the red box (Figure 2-3, B). It was developed in house by Charles Mignon to work with 24 well plates (Mignon et al. 2017). One LED is designed to be in place to homogenously irradiate each well of the plate (Figure 2-3).

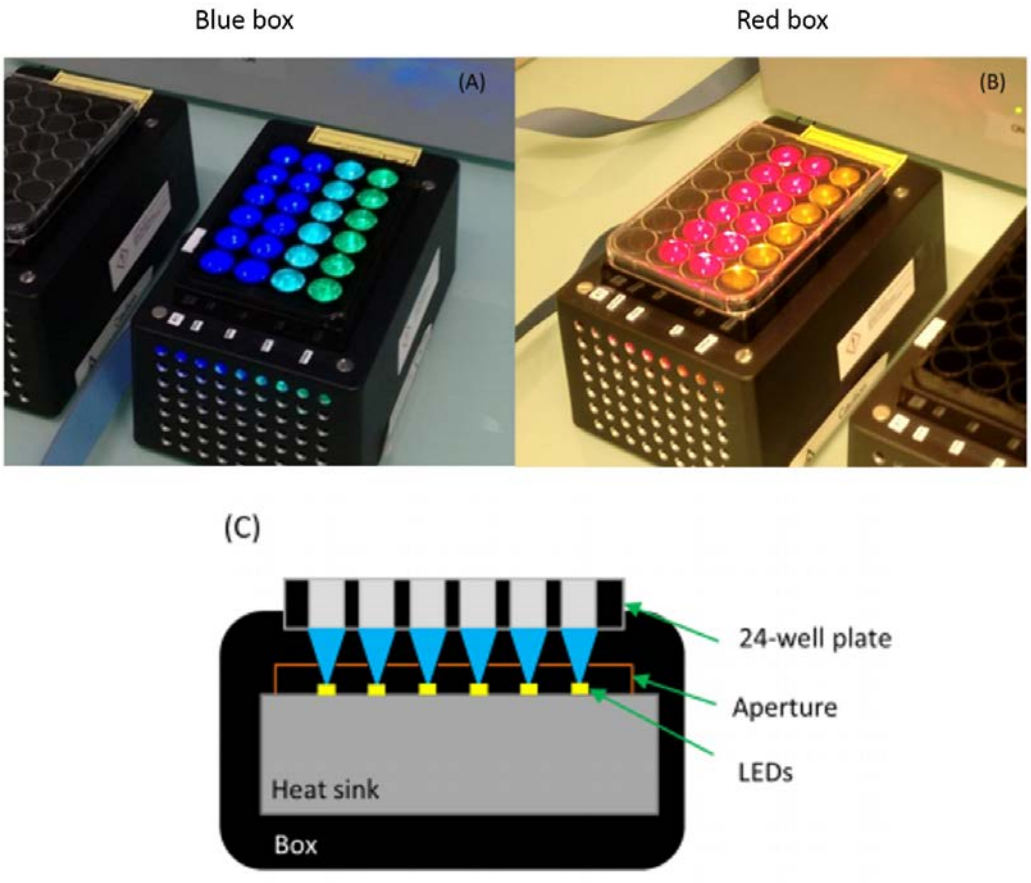

Figure 2-3: Light device Sirius-24 used for screening of parameters in epidermal keratinocytes.

Adapted from Mignon *et al.*,(2017).

The blue box (Figure 2-2, A) holds three wavelengths; two rows are illuminated by blue light (447 nm) and the other two by cyan light (505 nm) and green light (530 nm) respectively. The red box (Figure 2-2, B) holds longer wavelengths; one row is illuminated by yellow light (591 nm), another two with red light (655 nm) and the last row is illuminated with near infrared (NIR) light (850 nm). Each row can be controlled separately with a software program so that one row can always be the non-irradiated control.

2.6.2 Blue and red light panels

Two other devices were used once a certain light parameter was selected for further experiment after the screening of wavelength and irradiance effects. Identical LEDs were in place to deliver a flat and homogenous illumination over the area of a multiple well plate for cell culture (104 cm2). This device was designed to illuminate the cell culture from the top, therefore, to avoid reflection plates were placed on a transparent stage which was on top of a black surface (Figure 2-4). One device emitted blue light (453 nm ± 16 nm). This device has previously been used for *in vivo* and *in vitro* and experiments (Velnar et al. 2009; Kleinpenning et al. 2010; Liebmann et al. 2010; Mignon et al. 2017). A very similar light-based device was used to study the effect of red light. This time the wavelength peak was 656 nm. Both wavelengths were almost the same as the ones used by Sirius-24.

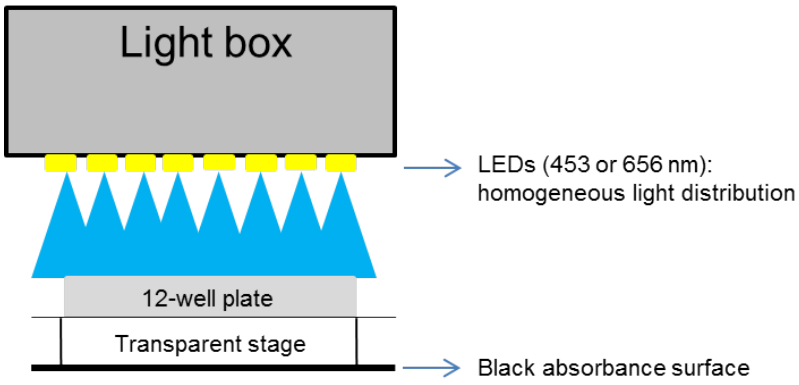

Figure 2-4: Light panel device to homogenously irradiate a multiple well plate.

2.7 Metabolic activity of epidermal keratinocytes assessed by Alamar Blue® assay. Screening of light parameters.

Metabolic activity of epidermal keratinocytes was assessed to screen a wide range of visible to infrared light parameters (Table 2.9). Black frame 24 well-plates (Porvair, Netherlands) were used to avoid light propagation between different light treated groups. Epidermal keratinocytes at 80% confluence were treated in EGF free, fungizone-free keratinocyte media to prevent an excessive proliferation which is triggered by EGF and avoid any interferences of fungizone in the behaviour of the keratinocytes. Media was refreshed after irradiation. Irradiation was used using Sirius-24 (Section 2.2.8.1). Details of light parameters used are shown in Table 2-9. Alamar Blue® assay (Thermo Fisher Scientific) was used to assess metabolic activity of keratinocytes. It is based on the redox state of its active ingredient, resazurin which is a blue non-fluorescent dye. After reduction of resazurin by the living cell, it becomes resorufin, a highly fluorescent pink-colored molecule (Rampersad 2012). Alamar Blue® was added to the cell culture 22 h after irradiation and fluorescence intensity was measured

after 2 h in a plate reader at 37 ºC (FLUOstar Omega II, BMG Labtech) (excitation: 544 nm, emission: 590 nm).

Group	Wavelength (nm)	Irradiance (mW/cm^2)	Radiant exposure (J/cm^2)	Time (sec)
Control	None	None	None	Same as treated
Blue light	447	50	2	40
			30	600
Cyan light	505	30	2	67
		30	30	1000
Green light	530	30	2	67
		30	30	1000
Red light	655	16	3.2	200
		40	30	750
		65	200	3077
Infrared light	850	40	60	1500
		80	250	3125

Table 2-8: Light parameters used to investigate an effect on the metabolic activity of epidermal keratinocytes.

Absorbance values were exported into Microsoft Excel (2010) and relative metabolic activity of light treated epidermal keratinocytes to non-irradiated

keratinocytes from each respective plate was calculated. Mean values from four different patients were used for two-way ANOVA statistical analysis (Section 2.2.12).

2.8 Scratch-wound assay to analyse migration of human primary epidermal keratinocytes after blue and red light irradiation

After cell expansion (section 2.2.3) (Figure 2.5 – 1), epidermal keratinocytes were plated in 12-well plates at 100,000 cells per well (Figure 2.5 – 2). After two days cells had reached 80% confluence and the media was changed to EGF free, funguizone free media (Figure 2.5 – 3). After 24 h, a scratch assay was performed (Figure 2.5 – 4). Four 10 µL tips were inserted into a scratch device built in house (Philips research) to scratch cell monolayers in 12-well plates. Two parallel scratches were also done to increase the area of cells affected by this perturbation. Afterwards, cells were washed twice with PBS and 1 ml of fresh media was added to each well. Four to eight replicates were carried out in for each of the conditions studied (non-irradiated, 2 J/cm^2 of blue light, 30 J/cm^2 of blue light and 30 J/cm^2 of red light). Only selected light parameters were studied, therefore, the panel light-based devices (section 2.2.7.2) were used for this experiment.

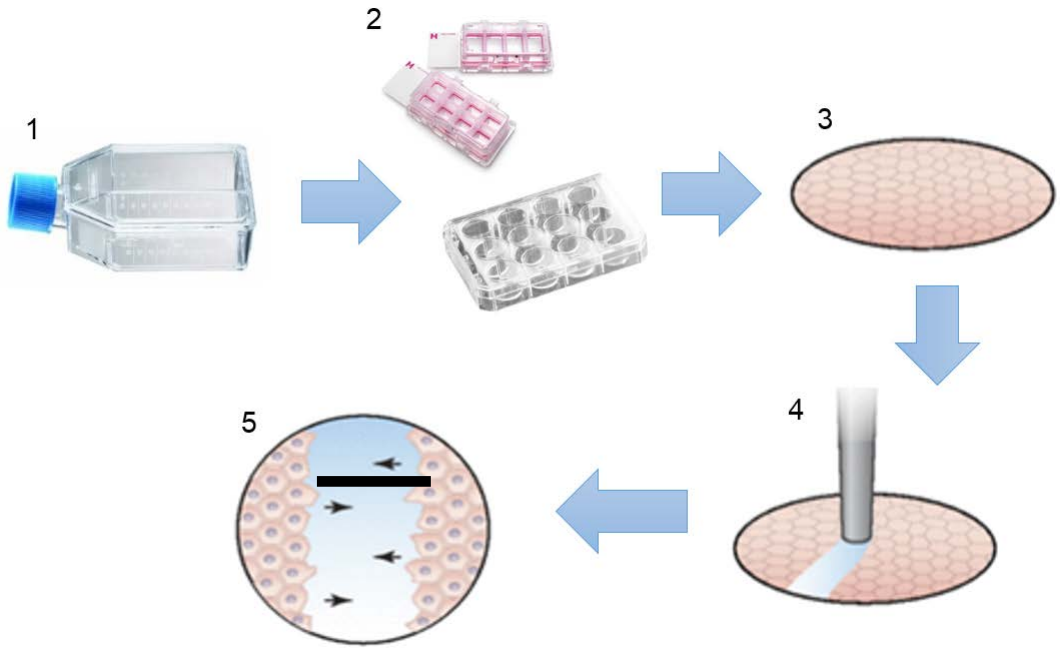

Figure 2-5: Scratch-wound assay.

1. Primary cell culture for cell expansion. 2. Cells were seeded into 6 or 12-well plates. 3. Cells were grown to confluence and pretreated for 24h. 4. Scratch was made with a 2-10 µl pipette tip using scratch device (Philips Research) in 12-well plates 5. Pictures of the scratch were taken at specific time points after cells were scratched.

After the scratch-wound was made and before the light treatment was applied four pictures per scratch were taken at the center of the well. A stereoscopic microscope at 10x magnification with a Nikon Coolpix digital camera was used to take the images. This was repeated at 12h and 21h after the initial scratch-wound/light treatment.

The scratch-wound area was analysed using Image J software. The speed of closure in the scratch-wound was analysed in Microsoft Excel; i.e. area at 12h (A_{12h}) or 21h (A_{21h}) minus the starting area (A_{0h}) was divided by the number of hours after scratching (12 or 21 respectively). The relative speed of closure was calculated by dividing the light-treated groups by the mean of the control

non-treated groups. Results from three donors (three independent experiments) were plotted in GraphPad (GraphPad, San Diego, CA, USA) and two-way ANOVA statistical analysis was performed (Section 2.2.12).

2.9 Physiological significance of OPN3 and CRY1 in primary epidermal keratinocytes and dermal fibroblasts

2.9.1 Synchronisation of dermal fibroblasts

Primary fibroblasts were cultured in 6-well plates (Greiner bio-one) until they reached 80% confluence and then washed twice with 1x PBS before the media was changed to either primary fibroblast media supplemented with 10% FBS, serum free medium or serum free medium supplemented with 250 nM of dexamethasone in 0.0025% ethanol (vehicle control) for 24h. The RNA was extracted at 4 and 24 h after synchronisation, converted into cDNA and clock gene expression was analysed by qPCR as described in section 2.2.6.1. Primers used are listed in table 2-10.

Gene	Primer sequence	Amplicon size (bp)	Design/ref.	Annealing T (ºC)
CRY1 (NM_004075.4)	Forward: 5'TAAGAGGCTTCCCTGCAAAA3'	230	Lin et al., (2014)	58.6
	Reverse: 5'GCCTCCATTCCCATTAGGAT3'			
CRY2 (NM_021117.3)	Forward: 5'AGGAGAACCACGACGAGA3'	288	Lin et al., (2014)	58.6
	Reverse: 5'TCCGCTTCACCTTTTTATAC3'			
PER1 (NM_002616.2)	Forward: 5'TGGCTATCCACAAGAAGATTC3'	48	James et al., (2007)	58.6
	Reverse: 5'GGTCAAAGGGCTGGCCCG3'			
PER2 (NM_022817.2)	Forward: 5'TCCAGATACCTTTAGCCTGATGA3'	97	Shih et al., (2005)	62.2
	Reverse: 5'TTTGTGTGTGTCCACTTTCGA3'			

PER3 (NM_001289862.1)	Forward: 5'CCCCTCTCTGTCCTCTGTTG3'	326	GeneScript	62.2
	Reverse: 5'ACTGCCATTGTTGCCTGTAA3'			
BMAL1 (NM_001178.5)	Forward: AAACCAACTTTTCTATCAGACGATGAA	87	Archer et al., (2008)	58.6
	Reverse: 5'TCGGTCACATCCTACGACAAAC3'			
CLOCK (NM_001267843.1)	Forward: 5'TTGTAAGCTGCCTGGGTTTC3'	109	GeneScript	58.6
	Reverse: 5'CTCAGTGTTTGCTGGTGGTG3'			
GAPDH (NM_002046.5)	Forward: 5'TATAAATTGAGCCCGCAGCC3'	143	GeneScript	58.6, 61 and 62.2
	Reverse: 5'CGACCAAATCCGTTGACTCC3'			

U6 (NR_004394.1)	Forward: 5'CTCGCTTCGGCAGCACA3'	94	GeneScript	58.6, 61 and 62.2
	Reverse: 5'AACGCTTCACGAATTTGC3'			

Table 2-9: RT-qPCR primers and conditions for clock genes.

2.9.2 Effect of modulating the circadian clock with KL001 and longdaysin in scratched dermal fibroblasts: changes in expression of circadian clock genes

Primary fibroblasts were cultured in 6-well plates (Greiner bio-one) until they reached 85-90% confluence before washing twice with 1x PBS and synchronising by incubating in serum-free fibroblasts media for 24h. Then, cells were washed twice with 1x PBS and monolayers of cells were scratched as described in section 2.2.9. Cells were either incubated with 0.016 % DMSO (vehicle control), 8 µM of KL001 or 8 µM of longdaysin (LD) in triplicate wells for 24h before RNA was extracted, converted into cDNA and analysed by qPCR as described in section 2.2.6.1. Primers used for different circadian clock genes are listed in Table 2-9.

2.9.3 Scratch assay of synchronised and transfected primary keratinocytes

Primary epidermal keratinocytes at 80% confluency were synchronised with 12% FBS in EGF-free funguizone-free keratinocyte growth media (2.2.1.1) for 2h (Janich et al. 2013) and then washed twice with PBS. 50 nM of smartpool

siRNAs directed against OPN3 or CRY1 (ON-Targetplus, Dharmacon) using Lipofectamine RNAiMax (Invitrogen) according to the manufacturer's specifications were used to transfect epidermal keratinocytes. Eight μM of KL001 in EGF-free funguizone-free keratinocyte growth media (2.2.1.1) was used to treat epidermal keratinocytes. Non-targeting siRNA control (Dharmacon) and 0.016% of dimethyl sulfoxide (DMSO) was used as control. After a 24h incubation, a scratch-wound assay was performed as described previously (section 2.2.10) and the media was replaced with, or without, 8μM of KL001. The RNA was collected 24h after the initial scratch using 350 μl of RLT buffer (Qiagen) with β-mercaptoethanol (Sigma-Aldrich). RNA extraction, cDNA synthesis and qPCR to amplified OPN3, CRY1 and CRY2 were carried out as described in section 2.2.6.1. Keratins (KRTs) primers were also used for qPCR (Table 2-11).

Gene	Primer sequence	Amplicon size (bp)	Design/ref.	Annealing temperature (˚C)
KRT17 (NM_000422.2)	Forward: 5'AGGGAGAGGATGCCCACCTG3' Reverse: 5'GCGGGAGGAGATGACCTTGC3'	107	GeneScript	61.2 or 62.4
KRT14 (NM_000526.4)	Forward: 5'GCCTGTCTGTCTCATCCTC3' Reverse: 5'CTGAAGCCACCGCCATAG3'	76	GeneScript	62.4
KRT1 (NM_006121.3)	Forward: 5'ACTTGACAACTTGCAGCAGG3' Reverse: 5'CAATGATGCTGTCCAGGTCG3'	143	GeneScript	61.2
KRT10 (NM_000421.3)	Forward: 5'AGCATGGCAACTCACATCAG3' Reverse: 5'TGTCGATCTGAAGCAGGATG3'	126	GeneScript	62.4
GAPDH (NM_002046.5)	Forward: 5'TATAAATTGAGCCCGCAGCC3' Reverse: 5'CGACCAAATCCGTTGACTCC3'	143	GeneScript	61.2 or 62.4

Table 2-10: KRTs and GAPDH primers for RT-qPCR and amplification conditions.

2.9.4 Analysis of proliferation and differentiation of epidermal keraitnocytes by the EdU assay and KRT10 staining

Round glass coverslips of 20 mm^2 area (Fisherbrand, The Netherlands) were cleaned in 100% isopropanol and added to 12-well plates. They were washed three times with PBS and coated with 0.5% gelatin (Sigma-Aldrich) in distilled water at 37 ºC for 2h. Coverslips were washed a further 3 times with PBS and sterilised under UV light for 20 minutes before seeding epidermal keratinocytes. Cells were seeded at 200,000 cells per well, so they would be at approximately 80% confluence after 24h. Cells were synchronised with 12% FBS in as described previously and washed twice with PBS. 50 nM of smartpool siRNAs directed against OPN3 or CRY1 (ON-Targetplus, Dharmacon) using lipofectamine RNAiMax (Invitrogen, Netherlands) according to the manufacturer's specifications were used to transfect primary epidermal keratinocytes. 8 μM of KL001 was used to treat parallel cultures of keratinocytes. Non-targeting siRNA control (Dharmacon) and 0.016% of DMSO was used as control and added where necessary. After a 24h incubation, light treatment was performed in two out of four plates using the blue light panel (section 2.6.2). Light parameters were 50 mW/cm^2 for 40 seconds (2 J/cm^2) and the media was replaced with, or without, 8 μM of KL001. The 5-ethynyl-2'-deoxyuridine (EdU) reagent in the Click-iT EdU Alexa Fluor 488 imaging kit (Thermo Fisher Scientific) was also added to the culture media. EdU is a nucleoside analog of thymidine, therefore it is easily incorporated into the DNA of cells in culture during DNA synthesis, showing a very specific staining of the S phase of the cell cycle. Cells were incubated for 10h before fixing with 4%

PFA. EdU staining was done following manufacturer instructions after which ICC of KRT10 was performed. Blocking was done with 3% BSA for 1h at room temperatura. Fixed cells on coverslips were washed three times with PBS and rabbit anti-cytokeratin 10 antibody (ab76318, Abcam) was added at 1:200 dilution overnight. Coverslips were washes three times with PBS and 0.05% tween 20 (Sigma-Aldrich) and Alexa-647 (ab150075) secondary antibody was used at 1:200 dilution for 1h at 37 ºC. After washing three times with 0.05% tween 20 – PBS, two coverslips were mounted (no light vs blue light treated) in one glass slide using VECTASHIELD® Mounting Media with 4',6-diamidino-2-phenylindole (DAPI) (VECTOR laboratories).

Fluorescence imaging was done using a fluorescent microscope/scanner, the 3D HISTECH Panoramic MIDI (3D HISTECH) with a Nikon Eclipse 501 camera. Same acquisition settings were used throughout the imaging process. The software Panoramic viewer was used to take 16 pictures per well. Analysis of positive green (EdU) and red (KRT10) cells related to total (blue) number of cells (DAPI) was done using Image J. This was done by applying the same threshold to different pictures, converting the picture to binary and using the watershed option to differentiate between closed cells. Finally, the option analyse particles was chosen, and analysis was done excluding cells on the edges of the picture. A minimum size of 100 was used to avoid measuring unspecific staining as positive. This was repeated for every channel (blue, red and green). Summation of cells from the 16 pictures was done for each well in Microsoft Excel. % of EdU positive cells and KRT10 positive cells was divided by non-targeting non irradiated control to get relative % numbers. Two way

ANOVA analysis was performed in each cell donor with replicates value of n=4. EdU staining was done in two different donors and KRT10 staining in three donors.

2.10 Effect of blue and red light in an *ex vivo* wound healing model

2.10.1 *Ex vivo* culture, wound size analysis and KRT17 expression

Ex vivo wounds cultured at the air liquid interphase (section 2.2.7) were treated with either blue (2 and 30 J/cm^2 at 50 mW/cm^2), or red (30 J/cm^2 at 40 mW/cm^2) light immediately after wounds were created and every 24h after that. Phenol red-free complete DMEM was used for the *ex vivo* culture to avoid interaction of light with phenol red. The blue and red light panels were used for irradiation (Section 2.2.8.2). Images were taken at 0h, 48h and 120h just before light treatment using the microdissecting microscope (Leica), and the media was changed immediately after every light treatment. This is to be sure that the effect induced by light is a direct effect of this light on tissue and not an indirect effect mediated by the chemicals in the culture media. Wound area was measured using Image J from pictures taken by the microdissection microscope at 0.68 magnification.

Samples were harvested immediately after the wounds were made, and then 4 h after the third (day 2) light treatment. They were snap frozen and embedded in OCT media, and stored at -80ºC. An anti cytokeratin 17 (made in rabbit) primary antibody (ab109725, Abcam, The Netherlands) and an anti

cytokeratin 14 primary (made in mouse) antibody (ab7800, Abcam) were used at a 1:200 dilution. Double immunofluorescence protocol was done as previously described (section 2.2.5).

2.10.2 Laser microdissection, RNA extraction and qPCR of photoreceptors

A cryostat, Microm HM550 (ThermoFisher Scientific), was cleaned with RNase away spray (ThermoFisher Scientific). Cryosections of 7µm thickness were collected at -28^{0}C and placed onto mmi MembraneSlides, RNAse free (Molecular Machines and Industries, USA). Sections were kept in the original container where membrane slides were before use at -80^{0}C to ensure an RNase free environment. Sections were stained with haematoxylin using the mmi H&E staining kit (Molecular Machines and Industries) which is also RNase free, prior to microdissection. The epithelial tongue from *ex vivo* wounds was collected into mmi isolation caps, 0.5 ml diffuser caps (Molecular Machines and Industries). This is a collection tube whose cap contains a membrane. This was done by using a Nikon T2000 laser capture microscope. Images were taken before and after microdissection was performed (Figure 3-17). Laser capture for each sample (up to 10 sections) was performed for a maximum time of one hour to minimise RNA degradation. 350µL of RLT buffer from RNeasy Micro Kit (QIAGEN) was added to the samples, which were kept at -80^{0}C. RNA isolation was performed following the manufacturer's instructions. RNA was finally eluted in 12µL of RNase free water. Arcturus^{TM} RiboAmp® PLUS Kit (ThermoFisher Scientific) was used to amplify RNA. Final RNA concentration was assessed using a NanoPhotometer (IMPLEN).and quality was assessed with Agilent 2100

bioanalyzer (Agilent). The cDNA synthesis was performed as detailed previously (section 2.2.6.1.2). Quantitative PCR was carried out using 0.5 µL of cDNA. *OPN1-SW, OPN3, OPN5, CRY1, CRY2* and *KRT17* mRNA was amplified with previously described primers using the same conditions (Table 2-6 and 2-8). The relative gene expression was calculated as previously described with n=3 wounds from the same donor.

2.11 Statistical analysis

Statistical analysis of the results obtained experimentally is needed to establish differences in the observed data and therefore, reach conclusions. Statistical analysis was done using Prism (GraphPad, San Diego, CA, USA), which allows the performance of different tests based on the data provided.

When comparison is made between two groups, there are two main tests which could be performed; t-test (parametric) is able to compare means while the Mann-Whitney U-test (non-parametric) compares medians (Fowler et al. 1998). Both tests results in a level of significance which is known as p-value. Significant results are those p-values equal of bellow 0.05; * represents p-value ≤ 0.05, ** represents p-value ≤ 0.01 and *** represents p-value ≤ 0.001

In this work, statistical analysis of the means for more than two groups was often needed. The analysis of variance (ANOVA) allows comparison of any number of sample means in one single test so that it is a highly advantageous statistical test to use in biology. One-way ANOVA was used to analyse the effect of one variable over the sample mean of different treatment groups while two-way ANOVA was used to analyse the effects of two independent variables

on a dependent variable (Fowler et al. 1998). Similarly to t-test and Mann-Whitney U-test, p-values indicate level of significance of ANOVA. * represents p-value ≤ 0.05, ** represents p-value ≤ 0.01 and *** represents p-value ≤ 0.001.

The type of statistical test selected for each analysis is clearly specified in each one of the figure's legend within the results section.

3 RESULTS

3.1 Photoreceptors are expressed in human skin

The expression and localisation of different classes of photoreceptors OPNs and CRYs was compared using immunohistochemistry in cryosections of female facial and abdominal skin and in primary cell cultures of epidermal keratinocytes and dermal fibroblasts by quantitative RT-PCR and immunocytochemistry (ICC).

3.1.1 Expression of OPN1-sw, OPN3 and OPN5 in facial and abdominal skin *in situ*

Localisation of OPNs in human skin was both specific and consistent when female skin from facial (n=1) and abdominal (n=3) regions were compared. Double staining was performed with keratin 14 (KRT14) in order to identify the basal layer of the epidermis. KRT14 was visualised with red staining (Figure 3.1).

OPN1SW was expressed throughout the epidermis and dermis of human skin. While expression was more prominent in the suprabasal layer of the epidermis, the epidermal basal layer and the dermal fibroblasts in the dermis also expressed OPN1SW as indicated by the white arrows in figure 3.1, (A and B). In contrast, OPN3 was mainly expressed in the basal layer of the epidermis, although a very low expression could be seen also in the suprabasal layer (Figure 3.1, C and D). In contrast, OPN5 was exclusively localised to the basal layer of the epidermis and was not detected in the dermis (Figure 3.1, E and F).

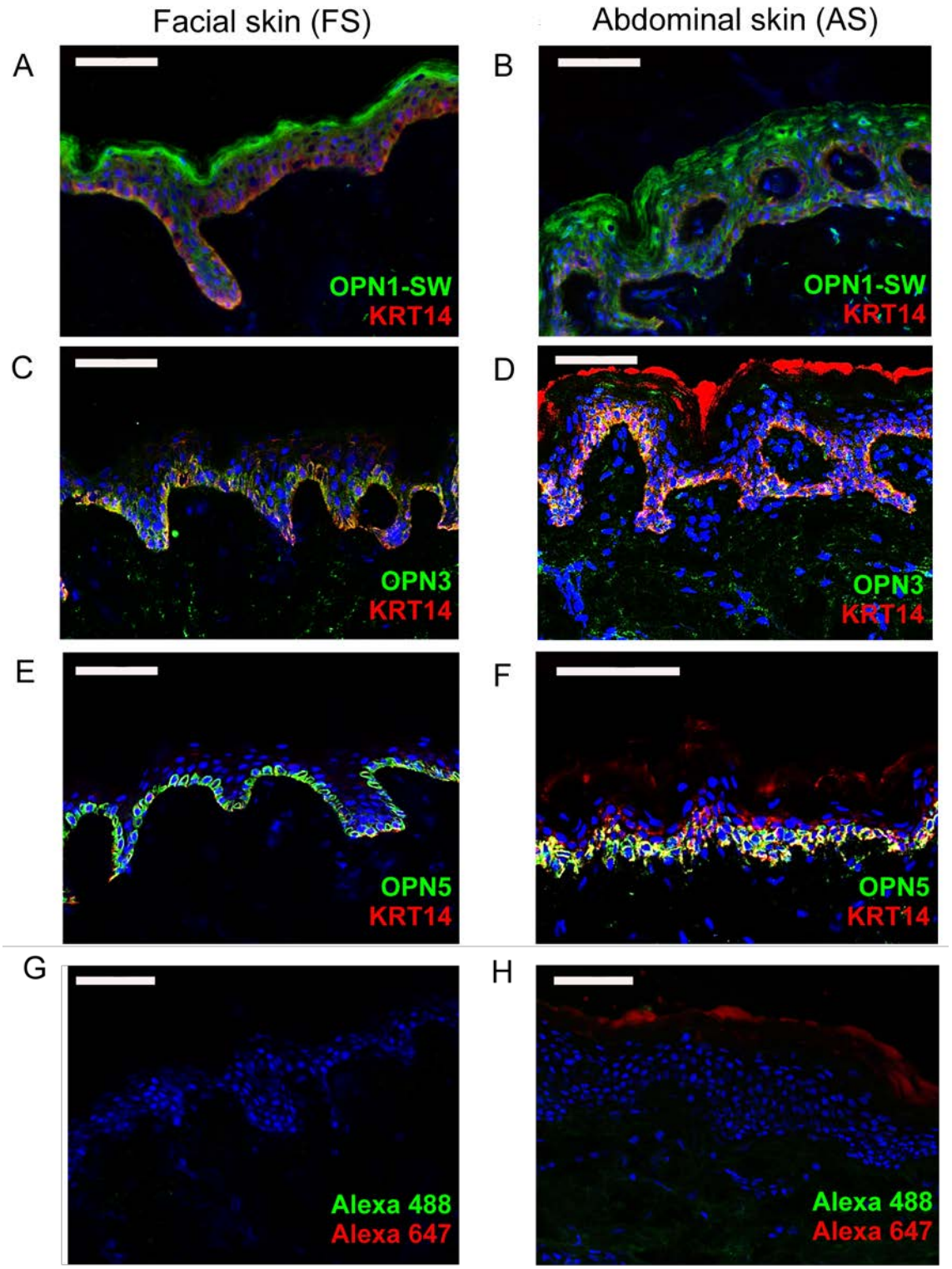

Figure 3-1: Localisation of OPN1-SW, OPN3 and OPN5 in human skin.

Representative images of the localisation of OPN1-SW, OPN3 and OPN5 in facial and abdominal female skin by immunohistochemistry. (A) Localisation of OPN1-SW (green) and KRT14 (red) in facial skin (FS). (B) Localisation of OPN1-SW (green) and KRT14 (red) in

abdominal skin (AS). (C) Localisation of OPN3 (green) and KRT14 (red) in FS. (D) Localisation of OPN3 (green) and KRT14 (red) in AS. (E) Localisation of OPN5 (green) and KRT14 (red) in FS. (F) Localisation of OPN3 (green) and KRT14 (red) in AS. (G-H) Negative control (no primary antibody). Nuclei are counterstained with DAPI (blue). Magnification = 40x. Scale bar = 75 µm.

3.1.2 Expression of CRY1 and CRY2 in facial and abdominal skin *in situ*

Both CRYs were expressed in human female facial and abdominal skin (Figure 3.2). Double staining was performed with KRT14 in order to identify the basal layer of the epidermis. KRT14 was identified by either green staining (A and B) or by red staining (C and D).

Localisation of CRY1 was confined to the nuclei of epidermal keratinocytes in facial skin (Figure 3.2, A); however, expression of CRY1 in abdominal skin did not follow the same pattern. Expression of CRY1 was more prominent in the cytoplasm of epidermal keratinocytes (Figure 3.2, B), and was only seen in two of the three donors. In contrast, CRY2 was localised to the nucleus and cytoplasm of epidermal keratinocytes in both facial and abdominal skin (Figure 3.2, C and D respectively). The dermal compartment of abdominal skin also showed CRY1 and CRY2 expression, but results were inconclusive in facial skin. In addition, the staining did not appear to be very specific in this compartment, due to auto fluorescence of the extracellular matrix of the dermal compartment.

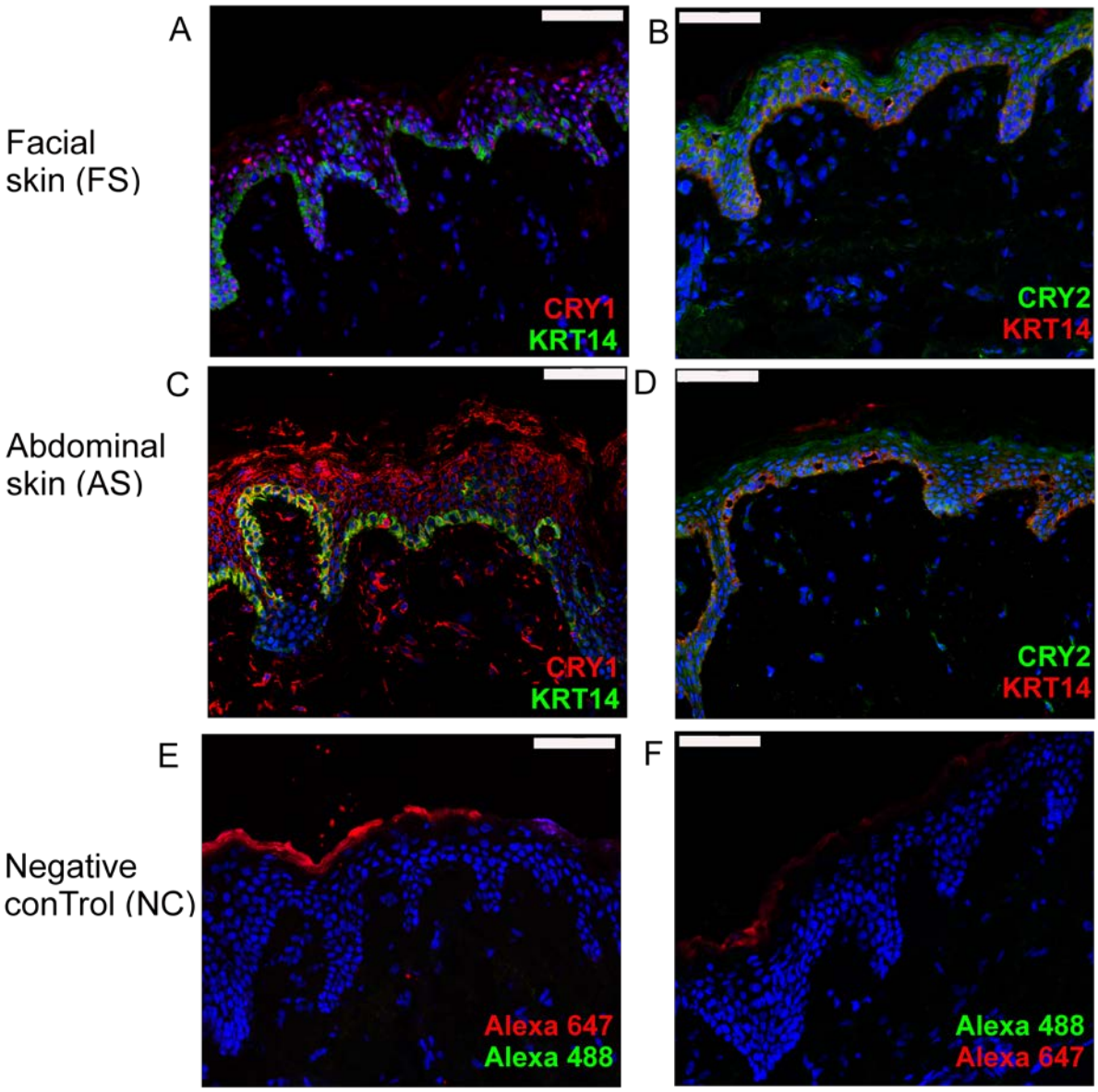

Figure 3-2: Localisation of CRY1 and CRY2 in human skin.

Representative images of the localisation of CRY1 and CRY2 in human female facial skin (FS) and abdominal skin (AS) by immunohistochemistry. (A) Localisation of CRY1 (red) and KRT14 (green) in FS. (B) Localisation of CRY2 (green) and KRT14 (red) in AS. (C) Localisation of CRY1 (red) and KRT14 (green) in FS. (D) Localisation of CRY2 (green) and KRT14 (red) in AS. (E-F) Negative control (no primary antibody). Nuclei are counterstained with DAPI (blue). Scale bar = 75 µM.

3.1.3 Expression of photoreceptors in human primary skin cells in culture

3.1.3.1 OPN1-SW, OPN3, CRY1 and CRY2 were expressed in cultured primary human epidermal keratinocytes and dermal fibroblasts; while OPN2 was only found in dermal fibroblasts and OPN5 in epidermal keratinocytes.

The expression of *OPN1-SW* was verified in primary cultures of human epidermal keratinocytes, and detected for the first time in primary cultures of human dermal fibroblasts. Analysis by RT-qPCR confirmed the expression of *OPN1-SW* mRNA in all the cells analysed; the human keratinocyte cell line NCTC, primary cultures of epidermal keratinocytes derived from facial skin (n=4) and primary cultures of dermal fibroblasts derived from female facial skin (n=3) scalp (n=2), breast skin (n=3) and abdominal skin (n=1) (Figure 3-3, A and B respectively). Human eye RNA was included as a positive control.

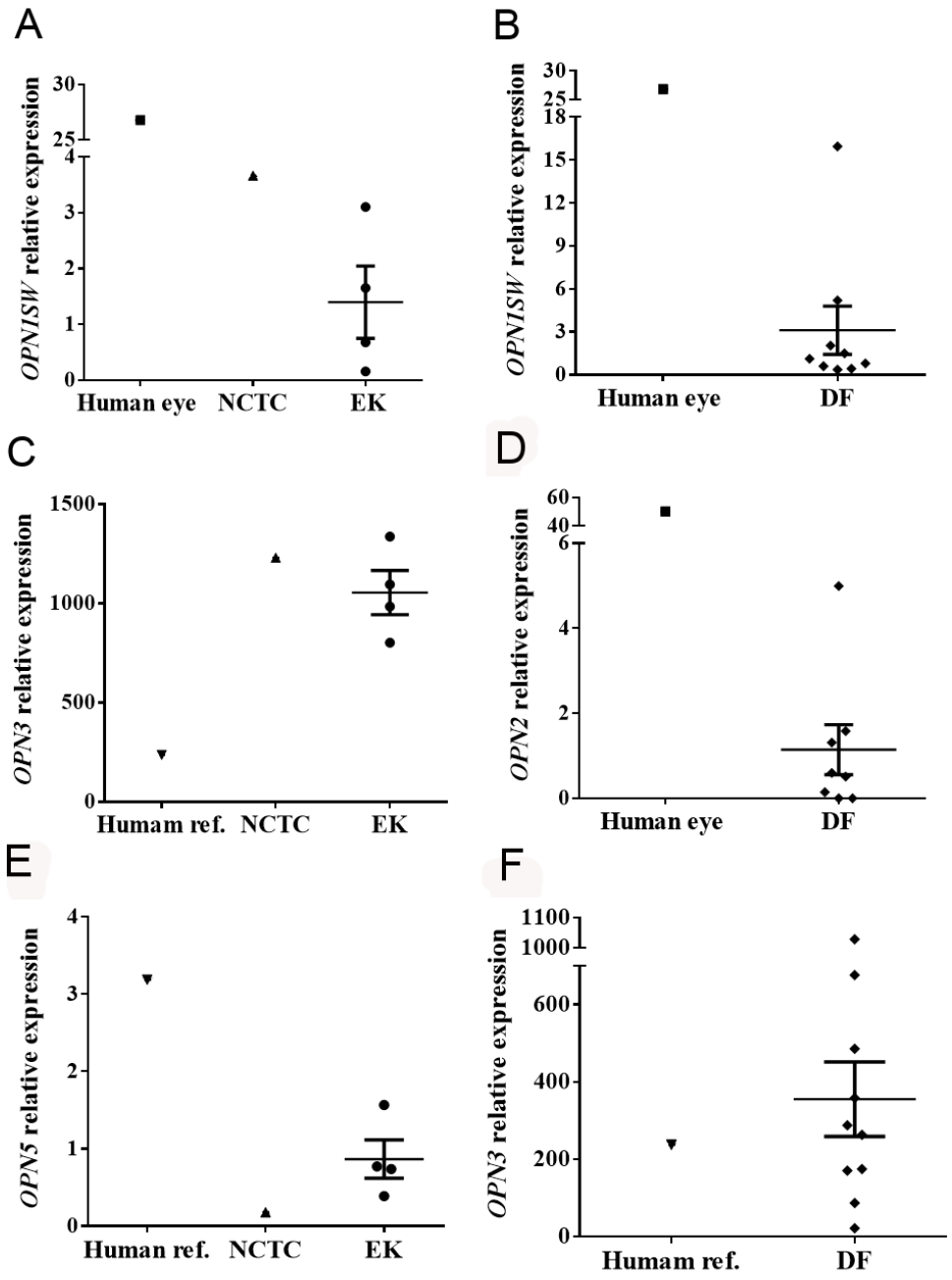

Figure 3-3: The expression of *OPNs* mRNA in primary cultures of human epidermal keratinocytes (EKs) and dermal fibroblasts (DFs).

Relative expression of mRNA in the NCTC cell line (indicated by a triangle) and EKs (indicated by a circle); for *OPN1-SW* (n=4) (A), *OPN3* (n=4) (C), *OPN5* (n=4) (E) ±SEM quantitated by RT-qPCR; Relative expression of mRNA in DFs (indicated by a diamond) for *OPN1-SW* (n=9) (B), *OPN2* (n=8) (D), *OPN3* (n=9) (F), ±SEM quantitated by RT-qPCR; human eye RNA

(indicated by a square) and human reference (ref.) RNA (indicated by an inverted triangle) were the positive controls.

The protein expression of OPN1-SW was confirmed by immunocytochemistry in primary cultures of both keratinocytes (n=3) and fibroblasts (n=3) (Figure 3-4). A negative control where the primary antibody was omitted verified the specificity of the staining (Figure 3-4, G). The localisation of this protein was cytoplasmic in both cell types; in dermal fibroblasts OPN1-SW was polarised in a specific region close to the nucleus (Figure 3-4, B).

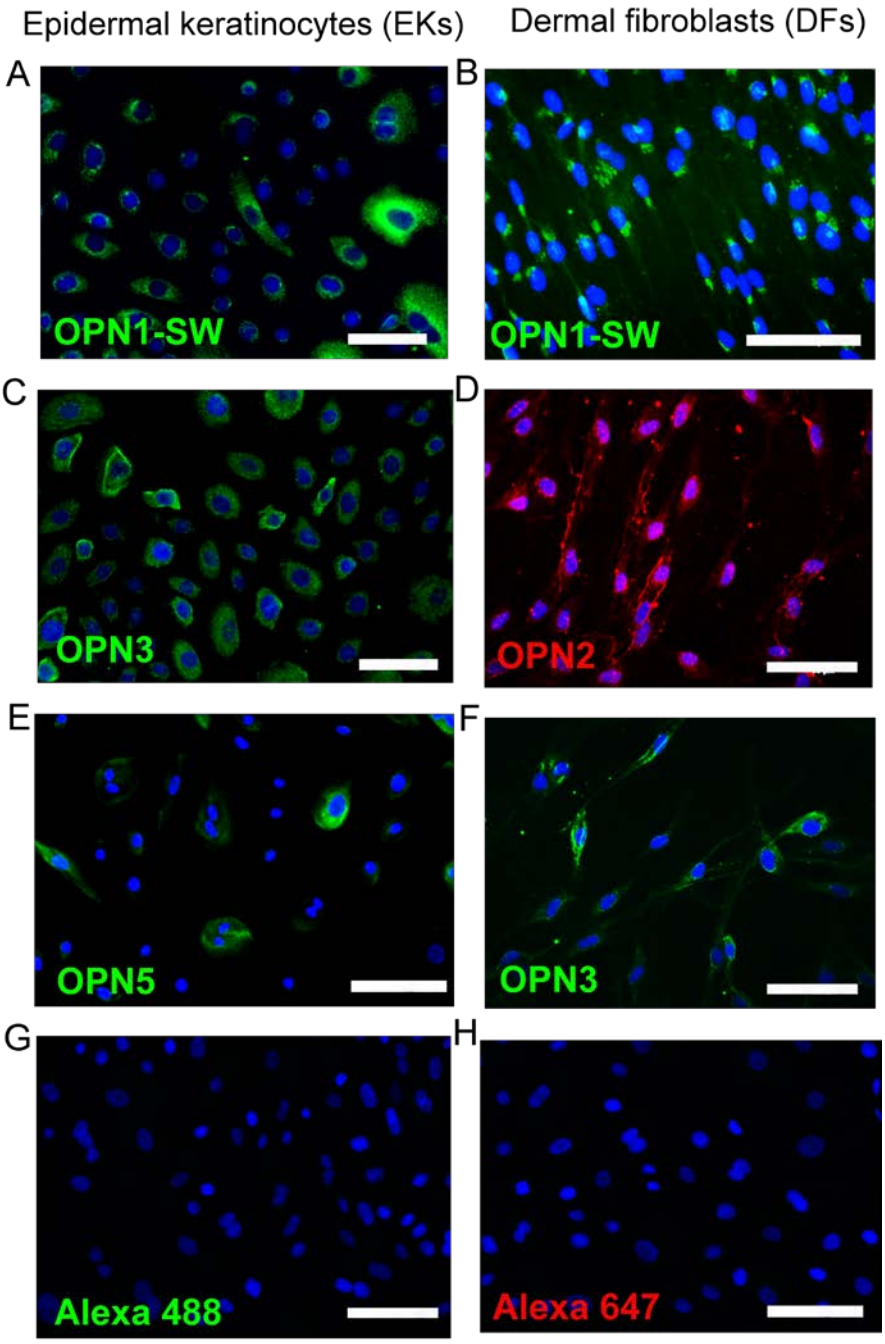

Figure 3-4: The localisation of OPNs in primary cultures of human epidermal keratinocytes (EKs) and dermal fibroblasts (DFs).

Representative images of OPN1-SW (green) (A), OPN3 (green) (C), OPN5 (green) (E), localisation in EKs (n=3) by immunofluorescence. Representative images of OPN1-SW (green) (B), OPN2 (red) (D), OPN3 (green) (F), localisation in DFs (n=3) by immunofluorescence; nuclei are counterstained with DAPO (blue). Scale bar = 75 µm.

The expression of mRNA for *OPN2* in primary keratinocytes (n=2) and fibroblasts (n=8) was analysed by RT-qPCR. Human eye RNA was used as a positive control. *OPN2* was not detected in the primary keratinocytes analysed, but it was present in 6/8 cultures of primary human dermal fibroblasts (n=6/8) (Figure 3-3, D). The exceptions included fibroblasts derived from facial skin (DF-F61) which were derived from the same donor as one of the epidermal keratinocyte cultures (EK-F61) and a second one derived from scalp skin (DF-S56). Immunocytochemistry confirmed that OPN2 was specifically localised in the cytoplasm and in the plasma membrane of dermal fibroblasts (n=3) (Figure 3-4, D).

The expression of mRNA for the non-visual opsin, *OPN3* in primary keratinocytes (n=4) and fibroblasts (n=9) was analysed by RT-qPCR. *OPN3* was expressed in all cell cultures analysed, including the NCTC human keratinocyte cell line NCTC (Figure 3-3, C and F). Human reference RNA was included as a positive control. Immunocytochemistry confirmed that OPN3 was specifically localised in the cytoplasm and plasma membrane of keratinocytes (n=3) and fibroblasts (n=3). (Figure 3-4, C and F respectively).

The expression of mRNA for the non-visual opsin, *OPN5* in primary keratinocytes (n=4) and fibroblasts (n=9) was analysed by RT-qPCR. *OPN5* was expressed in the NCTC cell line and all the primary keratinocytes analysed (n=4) (Figure 3-3, E), however it was not expressed in any of the cultures of dermal fibroblasts n=9 (Table 3-1). Human reference RNA was used as a positive control. Immunocytochemistry confirmed that localisation of OPN5 was

similar to OPN3 in keratinocytes (n=3), and was predominately expressed in the cytoplasm and plasma membrane (Figure 3-4, E).

Talking about the expression of both *CRY1* and *CRY2*, their mRNA expression was confirmed by qPCR in non-synchronised cell cultures of primary epidermal keratinocytes and dermal fibroblasts. All cells analysed i.e. the NCTC cell line, primary keratinocytes (n=6) and primary dermal fibroblasts (n=8) expressed *CRY1* and *CRY2* (Figures 3-5). Positive controls included human reference mRNA and human eye mRNA. The protein expression of both CRYs in cultured cells was confirmed by immunocytochemistry. CRY1 was mainly localised to the nucleus of keratinocytes (n=3) and fibroblasts (n=3) (Figure 3-5, B and D), although one of the keratinocyte cultures (61-year-old female donor) only expressed CRY1 in the cytoplasm. In contrast, CRY2 was mainly localised to the cytoplasm of both cell types (Figure 3-5, F and H respectively).

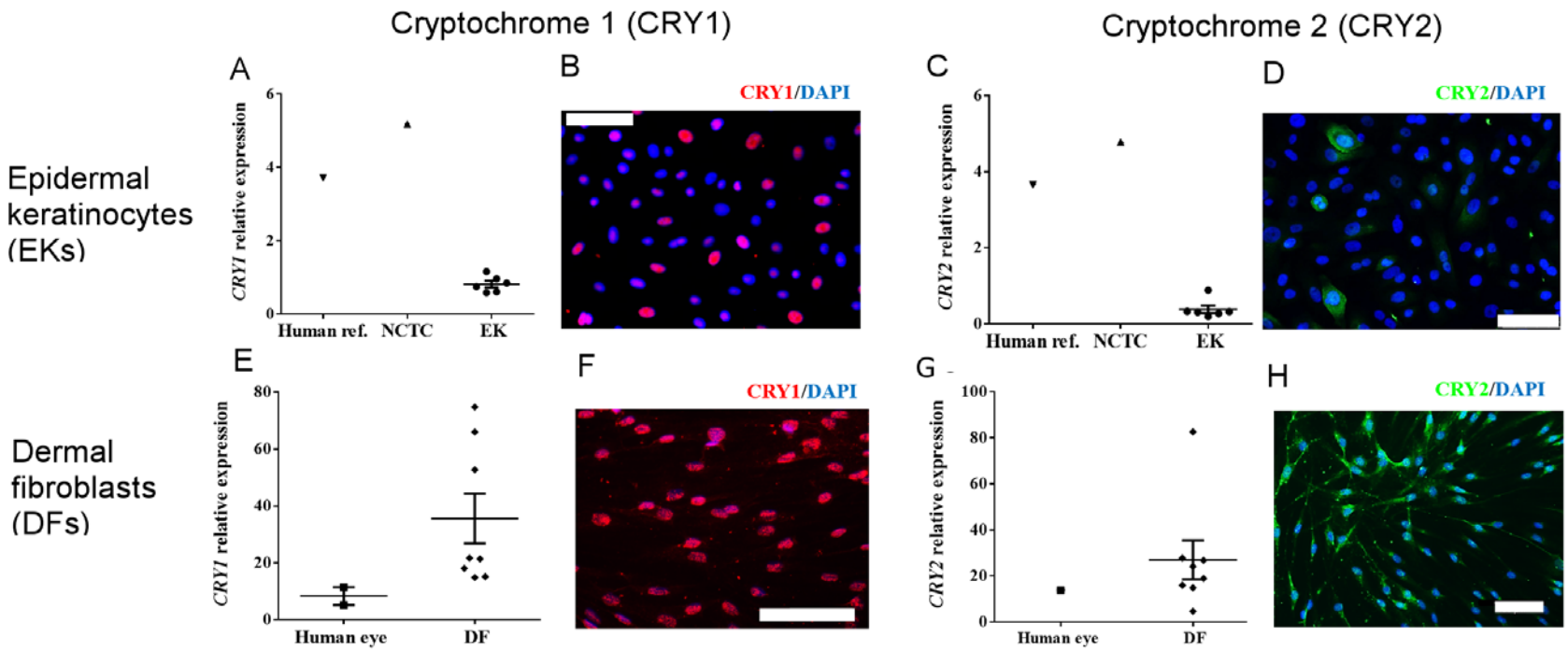

Figure 3-5: The expression of CRYs in primary cultures of human epidermal keratinocytes (EKs) and dermal fibroblasts (DFs).

Relative expression of mRNA in the NCTC cell line (indicated by a triangle) and EKs (indicated by a circle); for *CRY1* (n=6) (A) and *CRY2* (n=6) (C) and in DFs (indicated by a diamond) for *CRY1* (n=8) (E) and *CRY2* (n=8) (G) ±SEM quantitated by RT-qPCR; human eye RNA (indicated by a square) and human reference (ref.) RNA (indicated by an inverted triangle) were the positive controls. Representative images of CRY1 (red) and CRY2 (green) localisation in EKs (n=3) (B and D respectively) and DFs (n=3) (F and H respectively) by immunofluorescence; nuclei are counterstained with DAPi (blue). Scale bar is 75 µm.

mRNA	EK cell line	Primary keratinocytes				Primary fibroblasts									
		Face				Face				Scalp		Breast			Abdomen
Age	NCTC	61	53	53	49	61	53	53	57	56	51	48	44	34	55
Passage	-	4	3	3	5	4	4	3	4	4	4	7	4	5	6
Sample	NCTC	EK-F61*	EK-F53•	EK-F53▲	EK-F49	DF-F61*	EK-F53•	EK-F53▲	DF-F57	DF-S56	DF-S51	DF-B48	DF-B44	DF-B34	DF-A55
CRY1	✓	✓	✓	✓	✓	✓	NA	NA	✓	✓	✓	✓	✓	✓	✓
CRY2	✓	✓	✓	✓	✓	✓	NA	NA	✓	✓	✓	✓	✓	✓	✓
OPN1-SW	✓	✓	✓	✓	✓	✓	✓	NA	✓	✓	✓	✓	✓	✓	✓
OPN2	✓	ND	NA	NA	ND	ND	NA	NA	✓	ND	✓	✓	✓	✓	✓
OPN3	✓	✓	✓	✓	✓	✓	✓	✓	✓	✓	✓	✓	✓	✓	✓
OPN5	✓	✓	✓	✓	✓	ND	ND	ND	ND	ND	ND	ND	ND	ND	ND

Table 3-1: Summary of the mRNA expression of different photoreceptors.

*, •, ▲ indicate cells derived from the same donor. ND denotes not detected. ✓ denotes detected. NA denotes not analysed.

Protein	Skin ¨in situ¨						Primary keratinocytes			Primary fibroblasts			
	Face	Abdomen					Face			Face	Scalp		Breast
Age	63	59	Unknown	51	44	55	64	61	53	57	53	51	48
Passage	-						3	4	4	4	4	4	7
CRY1	✓	ND	✓	✓	NA		✓	✓	✓	✓	✓	✓	NA
CRY2	✓	✓	✓	✓	NA		✓	✓	✓	✓	✓	✓	NA
OPN1-SW	✓		✓	✓	NA	✓	✓	✓	✓	✓	✓	✓	NA
OPN2	NA						NA			✓	✓	✓	✓
OPN3	✓	NA	✓	✓	✓	NA	✓	✓	✓	✓	✓	✓	NA
OPN5	✓	✓	✓	✓	✓	NA	✓	✓	✓	✓	NA	NA	NA

Table 3-2: Summary of the protein expression of different photoreceptors in human skin ¨in situ¨ and in cells in culture.

ND denotes not detected. ✓ denotes detected. NA denotes not analysed.

3.2 The effect of visible to infrared (IR) light on the metabolic activity of cultured epidermal keratinocytes: a screening of parameters

The metabolic activity of primary cultures of epidermal keratinocytes in response to a range of different light parameters after 24h was assessed with the Alamar Blue assay.

3.2.1 Short wavelength- and dose- dependent effect of light on the metabolic activity of primary human epidermal keratinocytes

Two different radiant exposures were used for each short-wavelength light tested (blue, cyan and green light). Low doses of blue and cyan light (2 J/cm^2) increased metabolic activity of keratinocytes while high doses (30 J/cm^2) did not have any significant effect (n=4 donors) (Figure 3-6).

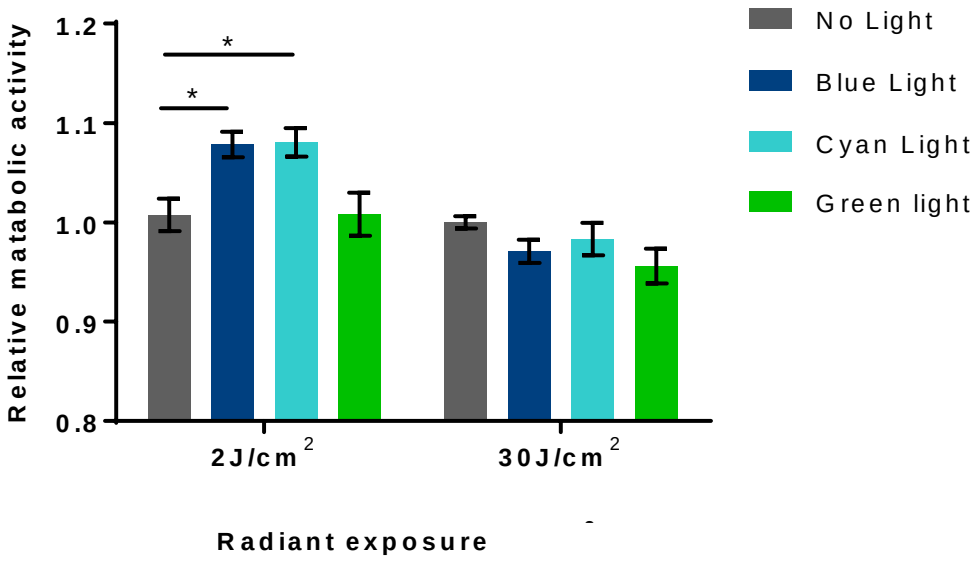

Figure 3-6: Blue and cyan, but not green light modulates the metabolic activity of cultured keratinocytes after 24h.

The relative metabolic activity of epidermal keratinocytes to metabolic activity of non-irradiated keratinocytes (no light, grey bar) 24h after exposure to blue (blue bar), cyan (turquoise bar) or

green (green bar) light at either 2 J/cm^2 or 30 J/cm^2. Data is presented as the mean of the relative metabolic activity ± SEM (n=4 donors, 6 replicates). * Denotes $p<0.05$ using a one-way ANOVA test.

3.2.2 Long wavelength- and dose- dependent effect of light on the metabolic activity of primary human epidermal keratinocytes

Two different radiant exposures were used for each long wavelength light tested (red and near infrared (NIR)). Low doses of red light (3.2 J/cm^2 and 30 J/cm^2) increased the metabolic activity of primary epidermal keratinocytes, while higher doses (200 J/cm^2) had no effect (Figure 3-7, A). Similarly, low doses of NIR light (60 J/cm^2) stimulated the metabolic activity of keratinocytes, but in contrast higher doses (250J/cm^2) supressed it (Figure 3-7, B).

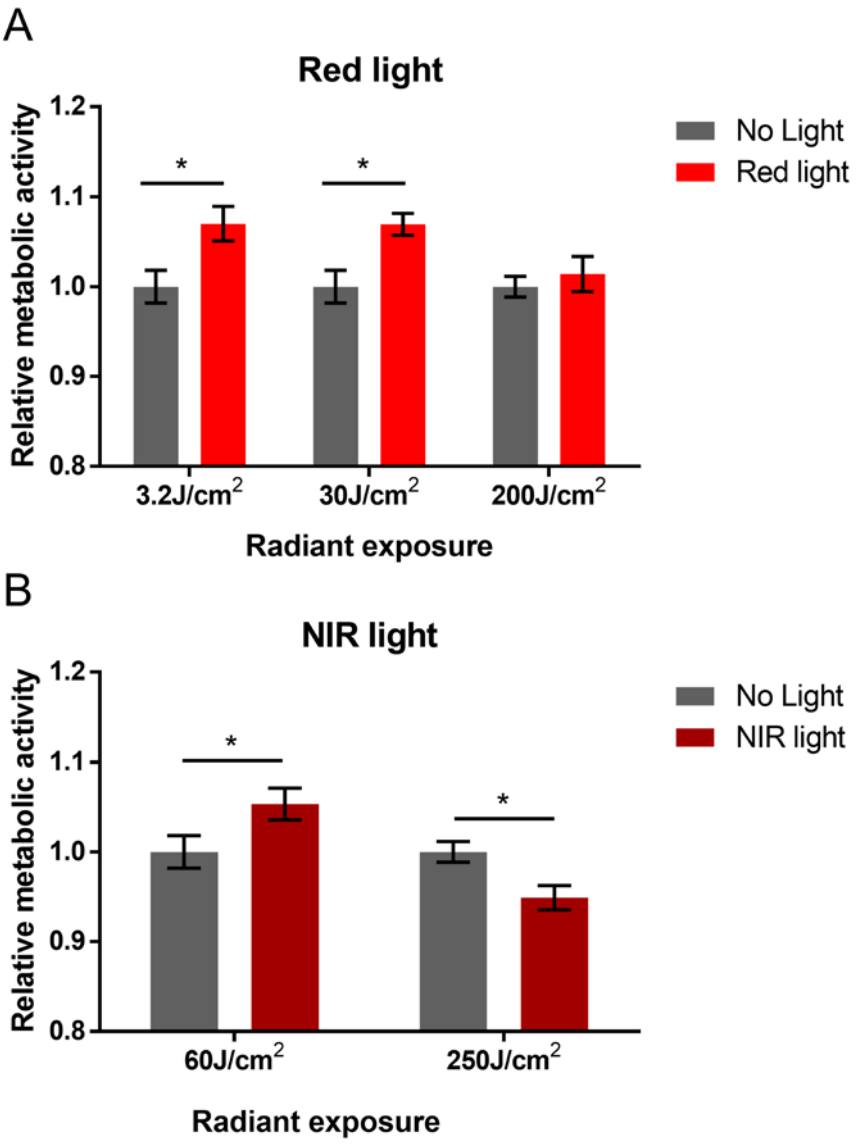

Figure 3-7: The effect of long wavelength (red and NIR) light on the metabolic activity of cultured keratinocytes.

(A) Relative metabolic activity of cultured epidermal keratinocytes 24h after exposure to no light (grey bar), or one exposure to red light at 3.2 J/cm^2, 30 J/cm^2 and 200 J/cm^2 (red bars). (B) Relative metabolic activity of cultured keratinocytes 24h after exposure to no light (grey bar), or one exposure to NIR light (dark red bars) at 60 J/cm^2 or 250 J/cm^2. Data is presented as the mean of the relative metabolic activity ± SEM (n=4 donors, 6 replicates). * Denotes $p<0.05$ using a one-way ANOVA test; NIR denotes near infrared.

3.3 Blue light modulates migration of human primary epidermal keratinocytes

The blue and red light parameters shown to modulate the metabolic activity of cultured keratinocytes (section 3.2) were selected to determine whether they could also modulate keratinocyte migration in a scratch-wound assay.

3.3.1 High doses of blue *light* modulate epidermal keratinocyte migration, but lower doses of blue light or red light had no effect

The speed of closure of epidermal keratinocytes was measured at 12h and 21h after scratching by analysing the area of the scratch-wound in comparison with the same scratch-wound at time 0h (Figure 3-8, A). No changes in keratinocyte migration were seen following exposure to lower doses of blue light (2J/cm^2). Only higher doses of blue light (30J/cm^2) modulated keratinocyte migration by reducing the speed of closure of the scratch wound by 20% when compared to the no light control (Figure 3-8, B). Furthermore, 30 J/cm^2 of red light did not have any significant effect on the rate of migration of epidermal keratinocytes (Figure 3-8, B).

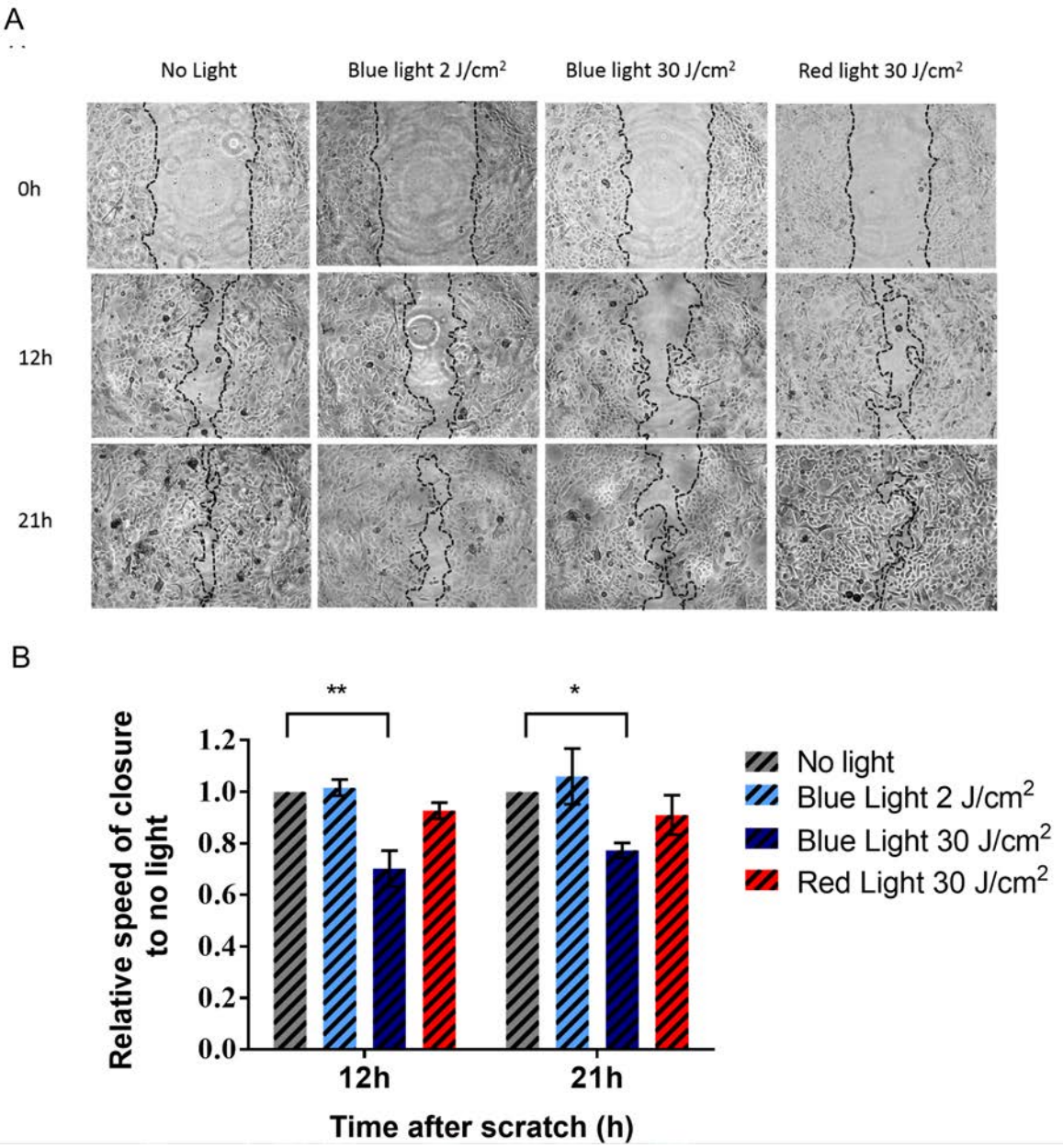

Figure 3-8: Low level blue light has no effect on epidermal keratinocyte speed of closure, higher doses delay migration, but higher doses of red light have no effect.

(A) Representative images of epidermal keratinocytes exposed to no light, 2 J/cm^2 of blue light, 30 J/cm^2 of blue light and 30 J/cm^2 of red light at 0h, 12h and 21h after scratch-wound. (B) Normalised speed of closure of epidermal kerationcytes after 2 J/cm^2 and 30 J/cm^2 of blue light exposure and 30 J/cm^2 of red light with respect to no light control. Analysis was done after 12 and 21 hours after scratch-wound/light treatment were performed. Data is presented as the

mean of the normalised speed of closure (n=3 donors, 4 replicates) ± SEM. ** denotes $p<0.01$ and *** denotes $p<0.001$ using two-way ANOVA test.

3.4 Blue light at low doses modulates DNA synthesis and KRT10 expression of human primary epidermal keratinocytes

Since OPNs have an absorption peak in the blue light wavelength, to further understand their potential role on epidermal keratinocytes, the effect of 2 J/cm^2 of 453nm (blue) light on DNA synthesis and cell differentiation was investigated. DNA synthesis of keratinocytes was reduced following exposure to low levels of blue light, as it was shown by the EdU incorporation assay in green (Figure 3-9). However, differentiation, as shown by expression of KRT10, a marker of early differentiation, was induced (Figure 3-9).

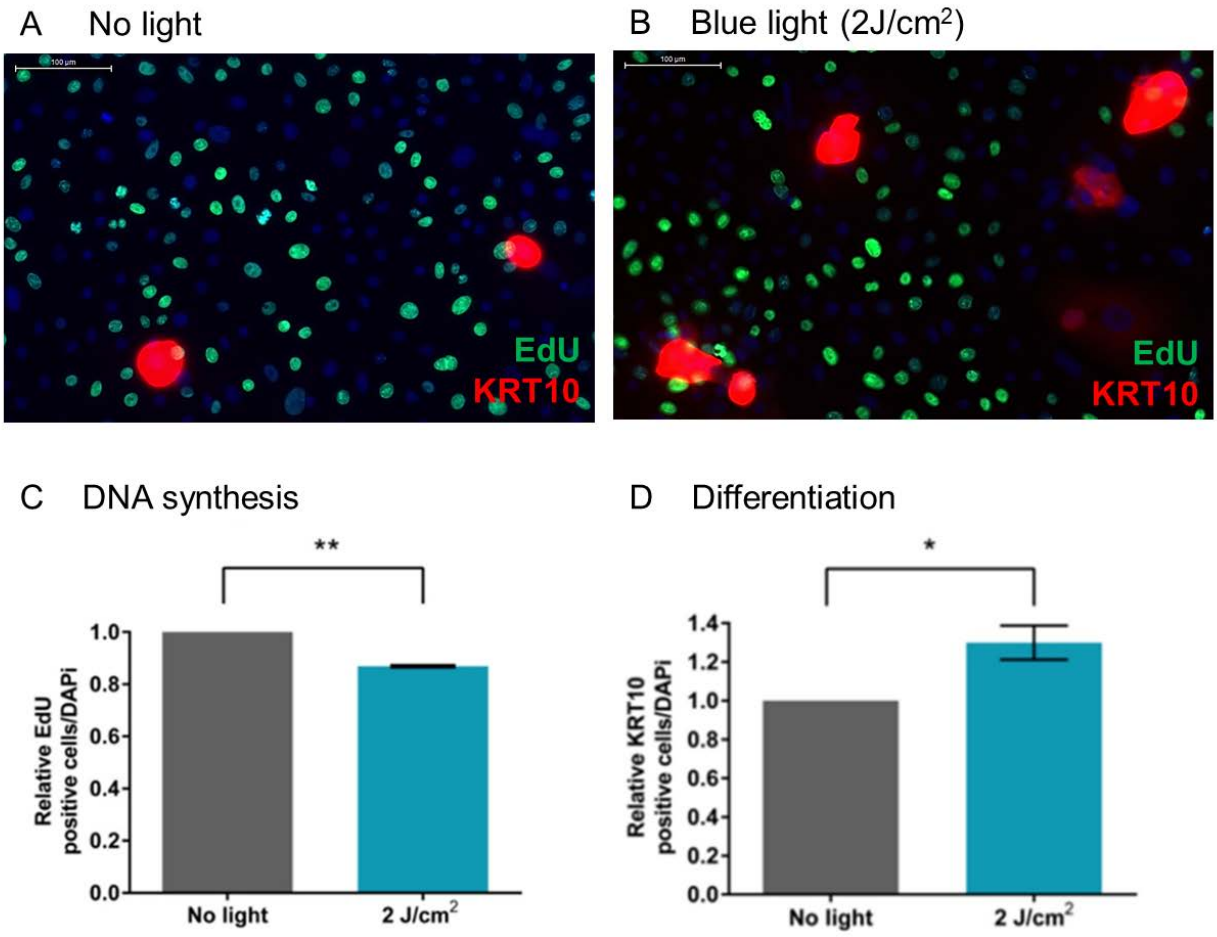

Figure 3-9: Low level blue light reduced DNA synthesis while induced differentiation of epidermal keratinocytes.

(A-B) Representative image of non-irradiated (A) and blue light (2 J/cm^2) irradiated epidermal keratinocytes, where DNA synthesis is indicated by incorporated EdU (green) and differentiation is indicated by KRT10 positive cells (red). Nuclei are counterstained with DAPI (blue). Scale bar Is 100 µm. (C) Quantification of DNA synthesis by EdU incorporation of epidermal keratinocytes after irradiation with 453 nm (blue) light at 2 J/cm^2. Data presented as relative mean of EdU positive cells/DAPI (n=2 donors) ± SEM. ** indicates $p > 0.01$ using unpaired t-test. (D) Quantification of differentiation by KRT10 expression after irradiation with 453 nm (blue) light at 2 J/cm^2. Data presented as relative mean of KRT10 positive cells/DAPI (n=3 donors) ± SEM. * indicates $p > 0.05$ using unpaired t-test.

3.5 Physiological significance of OPN3 and CRY1 in primary epidermal keratinocytes and dermal fibroblasts

OPN3 and CRY1 were highly expressed in both primary epidermal keratinocytes and dermal fibroblasts cultures (Figure 3-3). A more in depth study of OPN3 and CRY1 function in both epidermal keratinocytes and dermal fibroblasts is addressed in this section.

3.5.1 The synchronisation and transfection conditions of cultured cells

Circadian clock synchronisation is controlled by the suprachiasmatic nucleus (SCN) pacemaker *in vivo*, but since this synchrony can be lost *in vitro*, cell cultures require synchronisation when studying CRYs and other proteins involved in the molecular clock.

Silencing using siRNA is an efficient way to stop the production of target proteins. Transfection of the siRNA is a critical point in primary cell cultures. Therefore, both the optimisation of synchronisation, and the successful transfection of primary cell cultures are crucial steps in studying the role of OPNs and CRYs in primary epidermal keratinocytes and dermal fibroblasts *in vitro*.

3.5.1.1 Synchronisation of cultured human primary dermal fibroblasts

In culture, cells may lose the synchrony normally maintained *in vivo* and may cycle in a cell-autonomous manner. The circadian rhythm can be

synchronised in cultured cells by either serum starvation/serum shock or dexamethasone treatment (Balsalobre *et al.*, 2000).

Primary fibroblasts from facial skin were preincubated under different culture conditions and mRNA was analysed to determine changes in expression of circadian clock genes. Circadian clock gene expression was analysed at 4 h and 24 h after synchronisation following different culture conditions for 24h; i.e. normal fibroblast growth media (2.2.1.2) with 10% FBS (S+), serum starvation (SS) or 250 nM of dexamethasone (Dex). Expression of *CRY1*, *CRY2* and *PER1* was induced after SS and Dex incubation in comparison to non-synchronised cells (S+) indicating an induction of the circadian clock machinery at 4h after synchronisation (Figure 3-10). Furthermore, mRNA expression of *CRY1, PER1* and *BMAL1* was downregulated between 4 and 24h under all three culture conditions (Figure 3-10). In contrast, downregulation of *CRY2* was seen only after serum starvation (SS) (Figure 3-10).

.

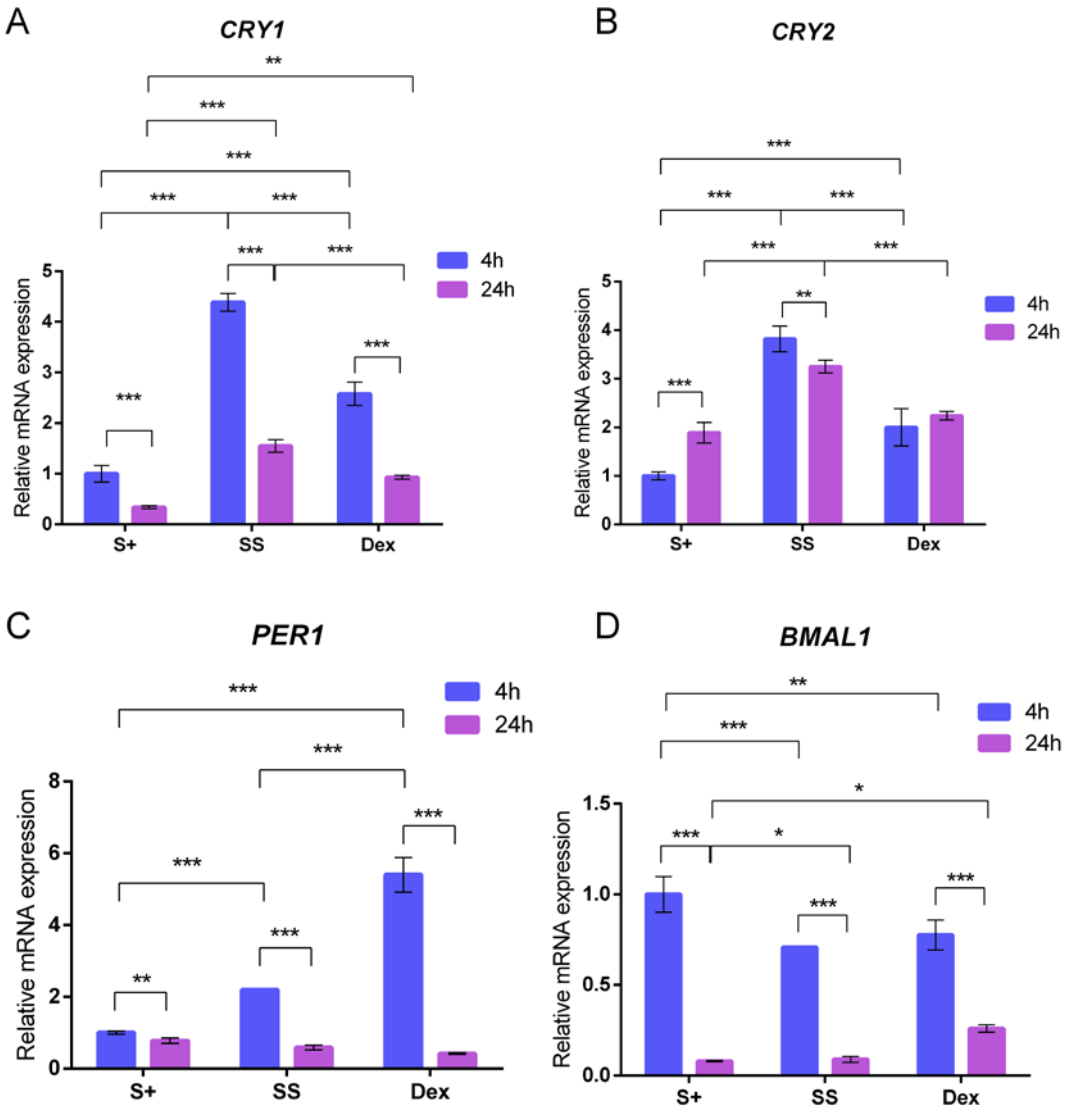

Figure 3-10: Dermal fibroblasts maintain circadian oscillations in culture.

(A) *CRY1* expression, (B) *CRY2* expression, (C) *PER1* expression and (D) *BMAL1* expression quantitated by RT-qPCR in cultured dermal fibroblasts after 4h and 24h following incubation with 10%FBS (S+), after synchronisation with serum starvation (SS) or synchronisation with 250 nM dexamethasone (Dex). Data presented as the mean relative expression to GAPDH of three technical replicates ± SD; ** denotes p<0.001 and *** denotes p<0.0001 in a two-way ANOVA.

3.5.1.2 KL001 and longdaysin modulate the circadian clock in cultured dermal fibroblasts: changes in expression of circadian clock genes

Dermal fibroblasts were synchronised by serum-starving and then scratching to study differences in circadian clock gene expression during fibroblasts migration. Interestingly, both *CRY2* and *PER2* were upregulated in scratch-wounded monolayers 36h after scratching while no changes were seen for the rest of clock genes, including the core circadian clock *BMAL1* and *CLOCK* (Figure 11-A).

Furthermore, the synchronised serum-starving and then scratching scratched fibroblasts were incubated with 8 µM of KL001 or longdaysin (LD) for 36h. Both molecules modulated the mRNA expression of most of the investigated circadian clock genes in cultured dermal fibroblasts; *CRY1, CRY2, PER1, PER2, PER3, BMAL1* and *CLOCK* (Figure 3-11, B). The same concentration of KL001 and LD modulated circadian clock gene expression in a differential manner; on one hand, 8 µM of KL001 significantly down regulated *CRY1, CRY2, PER1, PER2, PER3* and *BMAL1* mRNA expression, but there was no change in the expression of *CLOCK* mRNA after 36h. In contrast, 8 µM of LD significantly upregulated mRNA expression of *CRY1, PER1, PER2* and *PER3,* but had no effect on *CLOCK* mRNA expression. *BMAL1* was the only gene down regulated after 36h following incubation with LD, however its expression remained higher than corresponding dermal fibroblasts that had been treated with KL001 (Figure 3-11).

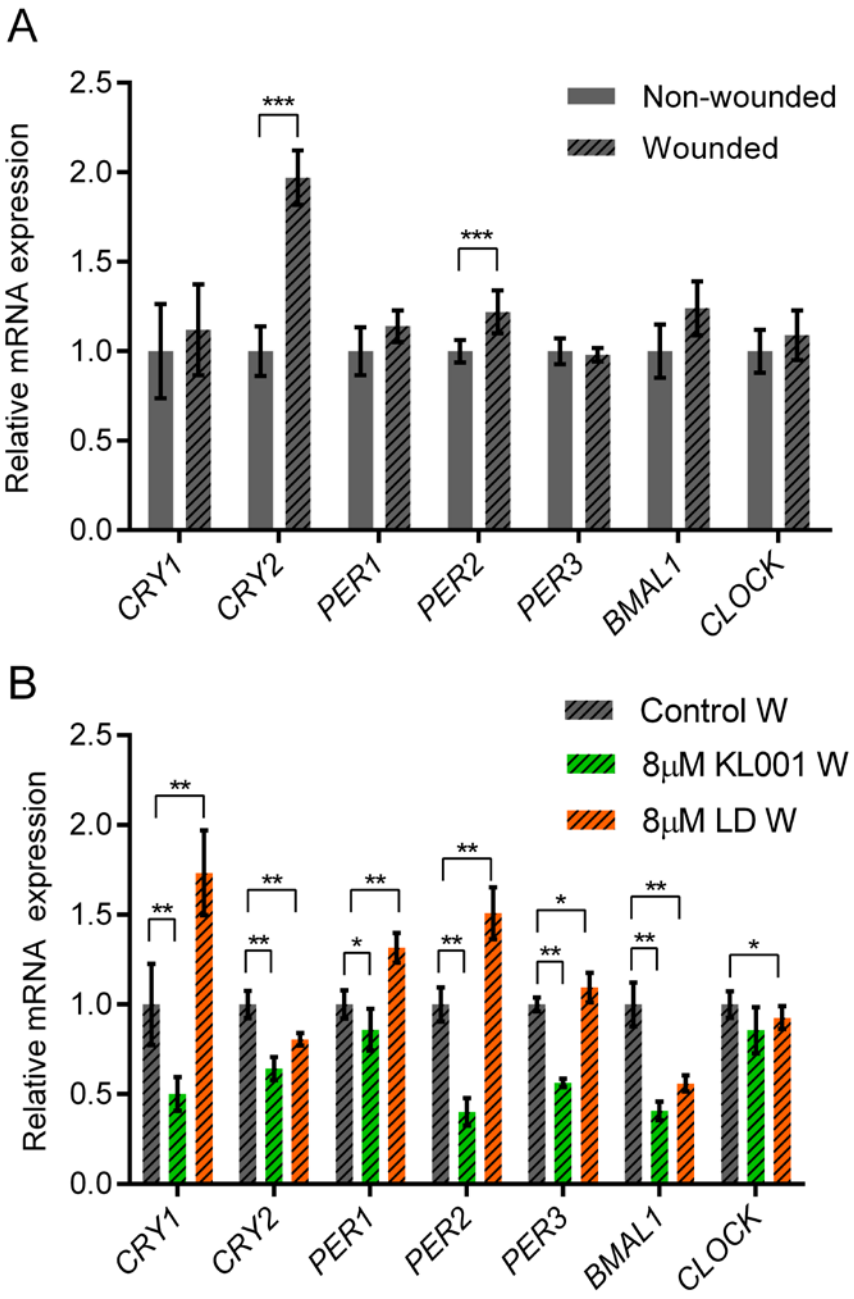

Figure 3-11: Expression and modulation with KL001 and longdaysin of clock genes in dermal fibroblasts.

(A) *CRY1, CRY2, PER1, PER2, PER3, BMAL1 and CLOCK* mRNA expression in non-wounded and wounded dermal fibroblasts quantitated by RT-qPCR in serum-starved synchronised cells at passage 5, 36h after scratching. Data presented as the mean relative to the expression of GAPDH of three technical replicates ± SD. *** Denotes $p<0.001$ in a multiple t-test using the

Holm-Sidak method. (B) *CRY1, CRY2, PER1, PER2, PER3, BMAL1 and CLOCK* mRNA expression quantitated by RT-qPCR in serum-starved synchronised dermal fibroblasts at passage 5, 36h after scratching and treatment with either 8 µM KL001 or 8 µM LD. Data presented as the mean relative to the expression of GAPDH of three technical replicates ± SD. * Denotes $p<0.05$, ** denotes $p<0.01$ in a two-way ANOVA. LD indicates longdaysin; W denotes wounded.

3.5.1.3 Viability of transfected epidermal keratinoctyes with lipofectamine-siRNA complexes

In order to optimise the conditions for silencing experiments, the viability of epidermal keratinocytes after treatment with 3µL/mL of lipofectamine alone, or as a complex with non-target siRNA (NTR), or OPN3 siRNA was assessed with trypan blue staining. All three conditions downregulated viability in comparison to the negative control, but viability always remained above 60% (Figure 3-12). There was no difference in cell viability between the three different treatment conditions tested.

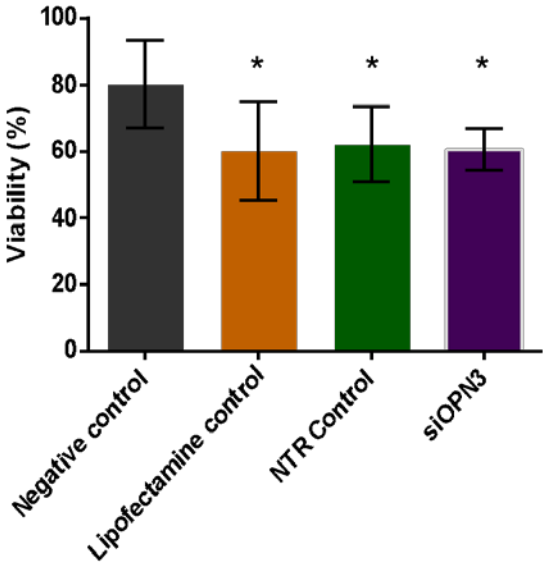

Figure 3-12: Lipofectamine (3uL/mL) reduced viability of epidermal keratinocytes by 20%.

The lipofectamine control (3uL/mL), lipofectamine with the non-target siRNA (NTR) control and lipofectamine with the siRNA targeting OPN3, all similarly reduced epidermal keratinocyte viability in comparison to the negative control. Data presented as the mean % of viable cells (n=1 donor, 6 replicates) ± SD. * Denotes $p<0.05$ using Mann Whitney non parametric t-test.

3.5.2 OPN3 and CRYs regulation in synchronised epidermal keratinocytes

It was previously shown that KL001 modulates circadian clock gene expression in dermal fibroblasts (Figure 3-8) previously by stabilising CRYs protein (Hirota et al. 2012), which was reflected in the downregulation of *CRY1* and *CRY2* mRNA expression (Figure 3-8). Furthermore, use of lipofectamine for siRNA transfection in epidermal keratinocytes maintained cell viability above 60% (Figure 3-9).

Synchronisation of epidermal keratinocytes was performed with 12% FBS for 2h as described by Janich *et al.,* (2015) and transfection with either 50 nM of siRNA against OPN3 (siOPN3), or CRY1 (siCRY1), or incubation with 8 µM of KL001 for 24h. A scratch-wound assay in epidermal keratinocytes was done after silencing or KL001 incubation to study the function of OPN3 and CRY1 in keratinocyte migration. Images of the scratch-wound were taken immediately after scratching and after 12 h and 21 h. The mRNA was collected 24h after scratching and the efficiency of silencing and effect of KL001 treatment was assessed.

3.5.2.1 Silencing efficiency of *OPN3* and *CRY1* was above 65% while KL001 downregulated both *CRYs*

Firstly, modulation of *OPN3, CRY1* and *CRY2* by either silencing or the CRY stabiliser molecule, KL001 was confirmed by RT-qPCR. Silencing OPN3 (siOPN3) reduced *OPN3* expression by 87% (n=3 donors) (Figure 3-13, A), while silencing CRY1 (siCRY1) reduced *CRY1* expression by 66% (Figure 3-13, B). In addition, pharmacological treatment with 8 µM of KL001 reduced the expression of both *CRY1* and *CRY2* by 71% and 41% respectively (Figure 3-13, C).

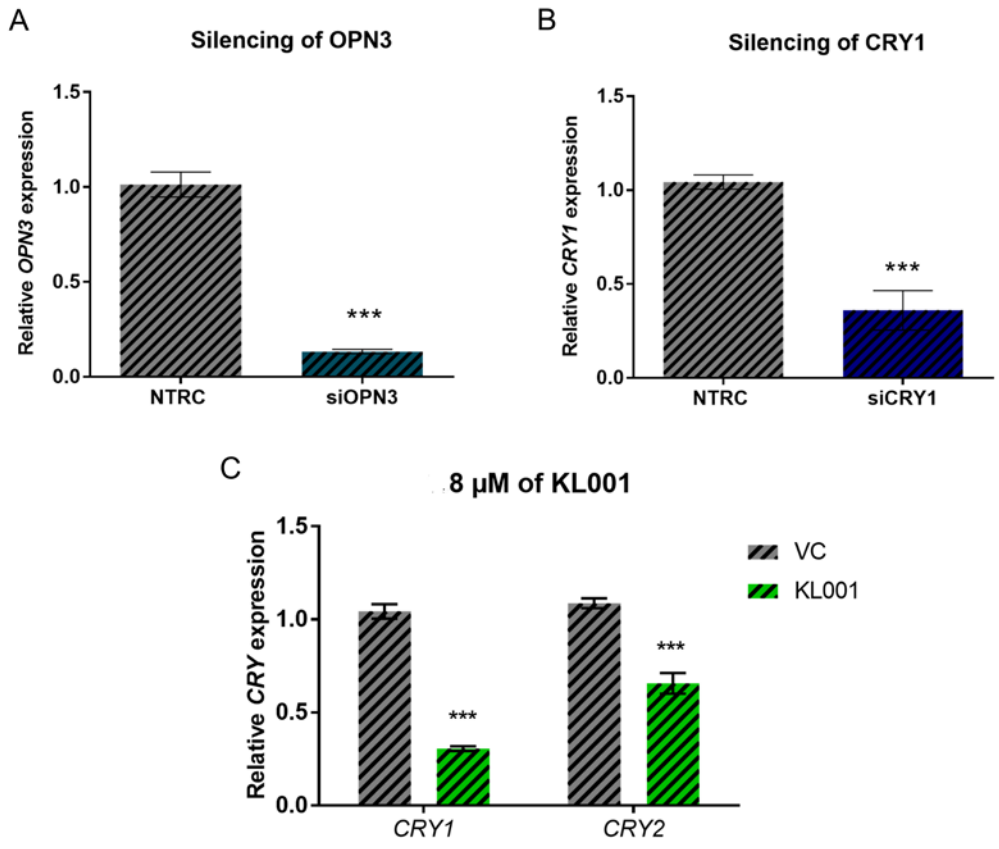

Figure 3-13: Transfection efficiency of OPN3 and CRY1 was above 65% while KL001 reduced mRNA of both CRYs in synchronised and scratched epidermal keratinocyte cultures.

(A) Silencing OPN3 with 50 nM of siRNA against OPN3 (siOPN3) reduced *OPN3* mRNA expression by 87% in comparison to 50 nM of non-target siRNA control (NTRC). (B) Silencing CRY1 with 50nM of siRNA against CRY1 (siCRY1) reduced *CRY1* mRNA expression by 66% in comparison to 50 nM of non-target siRNA control (NTRC). (C) 8 µM of KL001 treatment for 48 h reduced CRY1 and CRY2 mRNA expression by 71% and 40% respectively in comparison to vehicle control (VC). Data is presented as the mean relative expression to control (n=3 donors, triplicates) ± SEM. GAPDH was used as a housekeeping gene. Unpaired t-test was used to test silencing of OPN3 (A) and silencing of CRY1 (B) reduction while two-way ANOVA for KL001 treatment (C). *** denotes $p<0.001$.

3.5.2.2 Knockdown of *OPN3* upregulated *CRY1* expression while KL001 upregulated *OPN3*

In order to investigate the molecular mechanisms where OPN3 and circadian clock play a role and whether there is any relationship between them, changes in mRNA expression of different photoreceptors was analysed after silencing OPN3 and KL001 treatment.

Silencing of OPN3 downregulated *OPN3* expression in synchronised and scratched epidermal keratinocytes, both in the presence and absence of KL001 (Figure 3-13, A). However when epidermal keratinocytes were incubated with KL001 only, which stabilised CRY1 and CRY2 proteins (Hirota et al. 2012), there was a significant upregulation of *OPN3* mRNA (Figure 3-13, A). On the other hand, knockdown of CRY1 had no effect on *OPN3* mRNA expression (Figure 3-13, A).

In contrast, KL001 downregulated both *CRY1* and *CRY2* (Figure 3-14, B and C). Interestingly, knockdown of OPN3 significantly upregulated *CRY1* (Figure 3-14, B), but incubation of OPN3 knockdown cells with KL001

downregulated CRY1 expression to similar levels seen with KL001 incubation only. However, knockdown of OPN3 did not modulate expression of *CRY2* but knockdown *of* CRY1 upregulated *CRY2* expression (Figure 3-14, C). Incubation with KL001 downregulated *CRY2* expression and the combination of knockdown of OPN3 with KL001 did not attenuate the downregulation in response to KL001 (Figure 3.14, C) similar to the effects seen on the expression of *CRY1*.

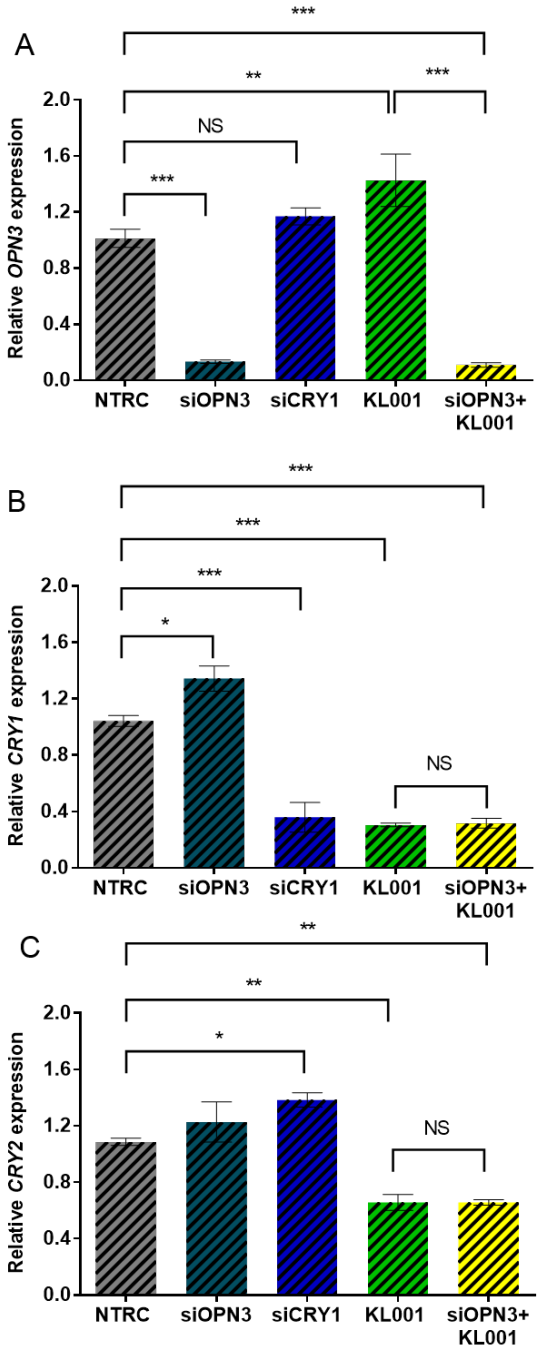

Figure 3-14: Silencing of OPN3, CRY1 or KL001 treatment of synchronised, scratched epidermal keratinocytes modulates *OPN3, CRY1* and *CRY2* mRNA expression. *OPN3* (A) *CRY1* (B) and *CRY2* (C) mRNA expression after treatment with 50 nM of non-target siRNA control (NTRC), 50 nM of siOPN3, 50 nM of siCRY1, 8 µM of KL001, or 50 nM of siOPN3 in combination with 8 µM of KL001. Data is presented as relative expression to control

(n=3 donors) mean ± SEM. GAPDH was used as a housekeeping gene. NS Denotes not significant, * denotes p<0.05, ** denotes p<0.01 and *** denotes p<0.001 (two-way ANOVA).

3.5.2.3 Effect of siOPN3, siCRY1 and KL001 treatment on the migration of epidermal keratinocytes

After confirmation of the successful downregulation of *OPN3* and *CRY1* in transfected epidermal keratinocytes and modulation of *CRY1* and *CRY2* with KL001 in scratched cultures of epidermal keratinocytes (Figure 3-13), scratch-wound images were analysed to determine whether OPN3 or CRYs have any role in the regulation of epidermal keratinocyte migration. A scratch assay was done 24h after silencing as previously described (section 3.4.2) and images were taken at 12h and 21h following the scratch-wound. Silencing OPN3 or CRY1 did not influence epidermal keratinocyte migration (Figure 3-15). However a delay in migration was seen after 21 h when epidermal keratinocytes were incubated with 8 µM of KL001 (n=3 donors). Silencing OPN3 in KL001 treated epidermal keratinocytes abrogated the delay in migration seen in cells treated with KL001 only (Figure 3-15). However, the combination of siOPN3 and siCRY1 had no effect on cell migration.

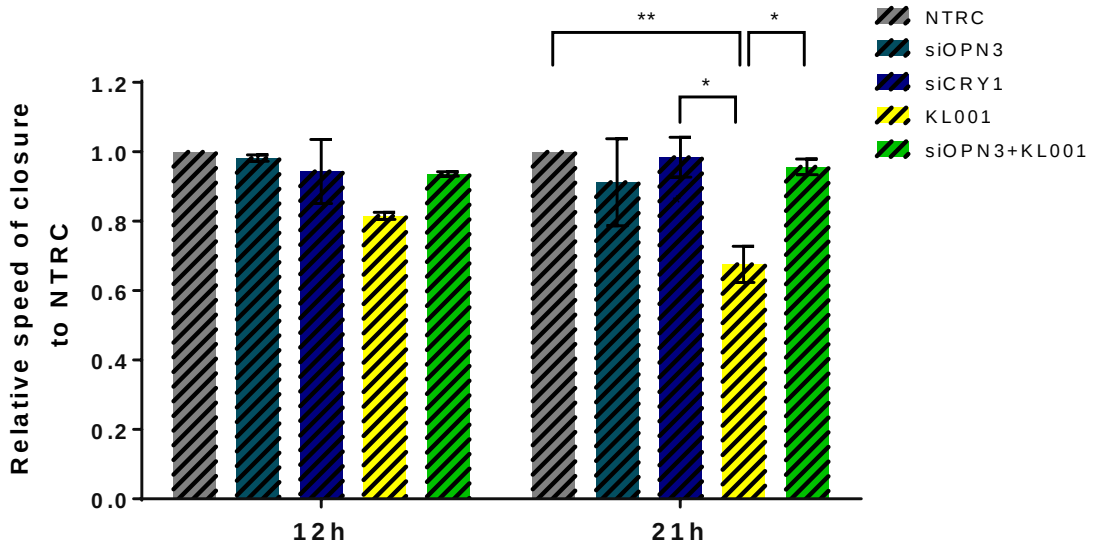

Figure 3-15: KL001 inhibits epidermal keratinocyte migration at 21h, which is attenuated by knockdown of OPN3.

Normalised speed of closure of synchronised epidermal keratinocytes to non-target siRNA control non treated cells (NTRC). Epidermal keratinocytes were treated with 50 nM of non-target siRNA control (NTRC), 50 nM of siOPN3, 50 nM of siCRY1, 8 µM of KL001 and 50 nM of siOPN3 in combination with 8 µM of KL001. Data presented as the speed of closure relative to NTRC (n=3 donors, passages 2-3) mean ± SEM. * Denotes $p<0.05$, ** denotes $p<0.01$ and *** denotes $p<0.001$ (two-way ANOVA).

3.5.2.1 Effect of siOPN3 and KL001 treatment on DNA synthesis of epidermal keratinocytes

The effect of silencing OPN3 and KL001 treatment on DNA synthesis of synchronised epidermal keratinocytes was investigated by the EdU incorporation assay. Silencing of OPN3 in non-irradiated cultures had no effect on DNA synthesis; however, KL001 downregulated DNA synthesis by approximately 50% as measured by EdU uptake (Figure 3-16). Knockdown of OPN3 in combination with KL001 treatment partially reversed this effect (Figure 3-16).

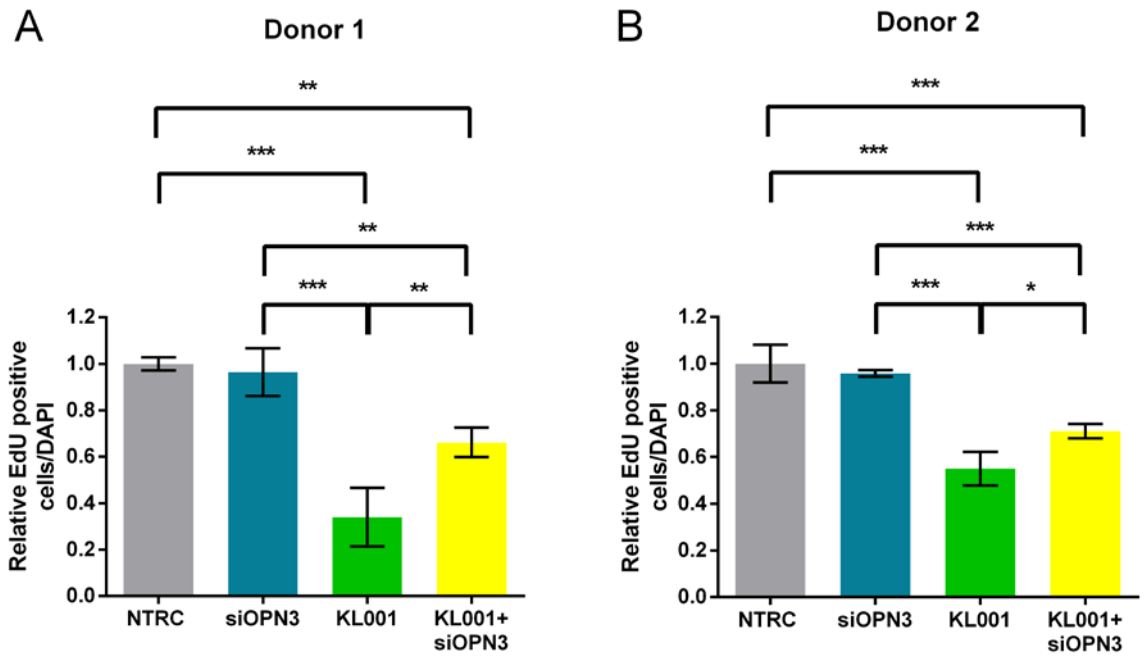

Figure 3-16: Effect of siOPN3 and KL001 on epidermal keratinocyte DNA synthesis.

EdU positive cells / DAPI for siOPN3, KL001 treatment and siOPN3+KL001 relative to non-target siRNA control (NTRC) control. Data was presented as the mean of relative EdU positive cells/DAPI ± SD (n=4) in donor 1 (A) and 2 (B). * Denotes $p<0.05$, ** denotes $p<0.01$ and *** denotes $p<1x10^{-3}$ in a one-way ANOVA.

3.5.2.2 Effect of siOPN3, siCRY1 and KL001 treatment on the early differentiation of epidermal keratinocytes

To understand further the role of OPN3 and CRY1 in epidermal keratinocyte differentiation, *KRT1* and *KRT10* expression was analysed by RT-qPCR as an indication of early differentiation in scratched cultures of epidermal keratinocytes. Silencing of OPN3 did not have any significant effect on either *KRT1* or *KRT10* mRNA expression. On the other hand, silencing of CRY1 stimulated early differentiation of keratinocytes by inducing a statistically significant increase in the expression of *KRT10*. Treatment with KL001 induced a two-fold significant upregulation in both *KRT1* and *KRT10* (Figure 3-17, A and

B respectively). Interestingly, knockdown of OPN3 in combination with KL001 abrogated the upregulation of differentiation induced by KL001.

Furthermore, the protein expression of KRT10 was also investigated by immunocytochemistry after silencing of OPN3 and KL001 treatment. Non-light irradiated keratinocytes showed a similar pattern of KRT10 protein expression to the mRNA expression demonstrated by RT-qPCR in the three donors studied (Figure 3-17). Incubation of epidermal keratinocytes with KL001 increased the number of KRT10 positive cells (Figure 3-17, C-E), and this effect which was supressed when combined with knockdown of OPN3 in two out of the three donors investigated (Figure 3-17, D and E).

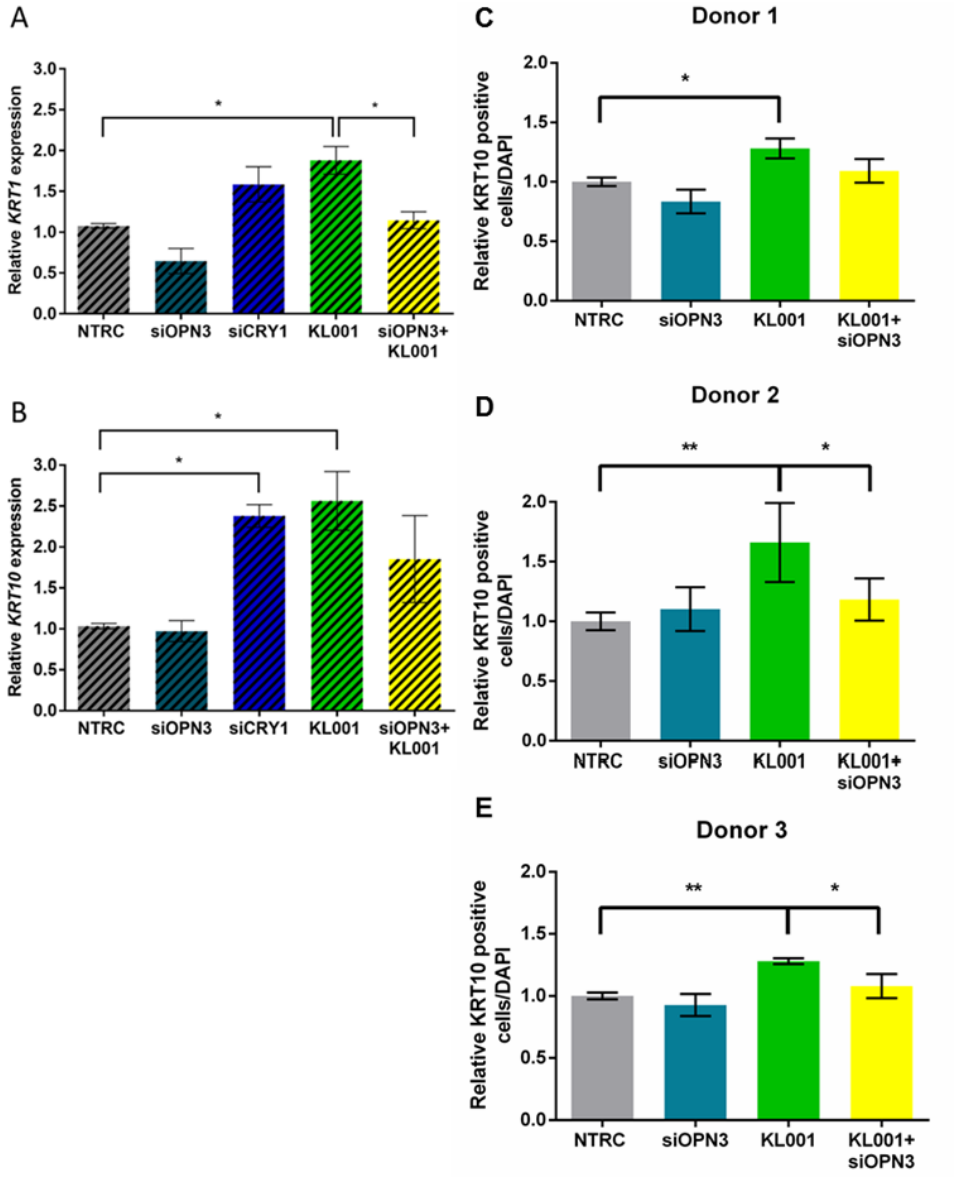

Figure 3-17: Silencing of CRY1 or incubation with KL001 upregulates differentiation in synchronised and scratched epidermal keratinocytes.

KRT1 (A) and *KRT10* (B) mRNA expression after incubation of epidermal keratinocytes with 50nM of non-target siRNA control (NTRC), 50nM of siRNA against OPN3 (siOPN3), 50nM of siRNA against CRY1 (siCRY1), 8µM of KL001, or a combination of 8µM of KL001 and 50nM of siRNA against OPN3 (KL001 + siOPN3) was normalised against GAPDH. Data is presented as relative expression to control (n=3 donors) mean ± SEM. * denotes $p<0.05$, ** denotes $p<0.01$ and *** denotes $p<0.001$ (one-way ANOVA). (C-E) KRT10 positive cells / DAPI for siOPN3, KL001 treatment or siOPN3+KL001 relative to non-target siRNA control (NTRC) in donor 1 (C), 2 (D) and 3 (E).

3.5.3 The role of OPN3, CRY1 and CRY2 in the blue light response of epidermal keratinocytes

It has previously been shown that KL001 downregulates *CRY1* and *CRY2* and upregulates *OPN3* (Figure 3-14). In terms of functionality it inhibits migration (Figure 3-15), proliferation (Figure3-16) while stimulated early differentiation of keratinocytes (Figure 3-17) both of which were abrogated by OPN3 knockdown. Non-scratched and synchronised cultures of epidermal keratinocytes were treated with non-target siRNA control (NTRC), siOPN3, incubation with 8 µM of KL001 or siOPN3 in combination with 8 µM of KL001. Parallel cultures of keratinocytes were irradiated with low level blue light (2 J/cm^2) to investigate if modulation of differentiation could be mediated by OPN3 or the circadian clock at 10 h after irradiation by ICC for KRT10. Changes in DNA synthesis was analysed in response to knockdown of OPN3 or KL001 treatment the presence or absence of 2 J/cm^2 of blue light irradiation, which was studied by EdU uptake.

3.5.3.1 Effect of siOPN3, siCRY1 and KL001 treatment on DNA synthesis in epidermal keratinocytes in the absence or presence of blue light irradiation

Low levels of blue light (2 J/cm^2) reduced DNA synthesis but induced differentiation of primary epidermal keratinocytes (Figure 3-9). In order to investigate the role of OPN3 and circadian clock to mediate this effect, the combination of siOPN3 and KL001 treatment was performed in non-irradiated and blue light irradiated cultures of epidermal keratinocytes in parallel.

When keratinocytes were irradiated with low level blue light, a decrease in DNA synthesis was seen in non-target siRNA control (NTRC) keratinocytes. This effect was also seen following OPN3 knockdown (Figure 3-18). However, in the presence of KL001 either alone or in combination with OPN3 knockdown, blue light did not modulate DNA synthesis (Figure 3-18).

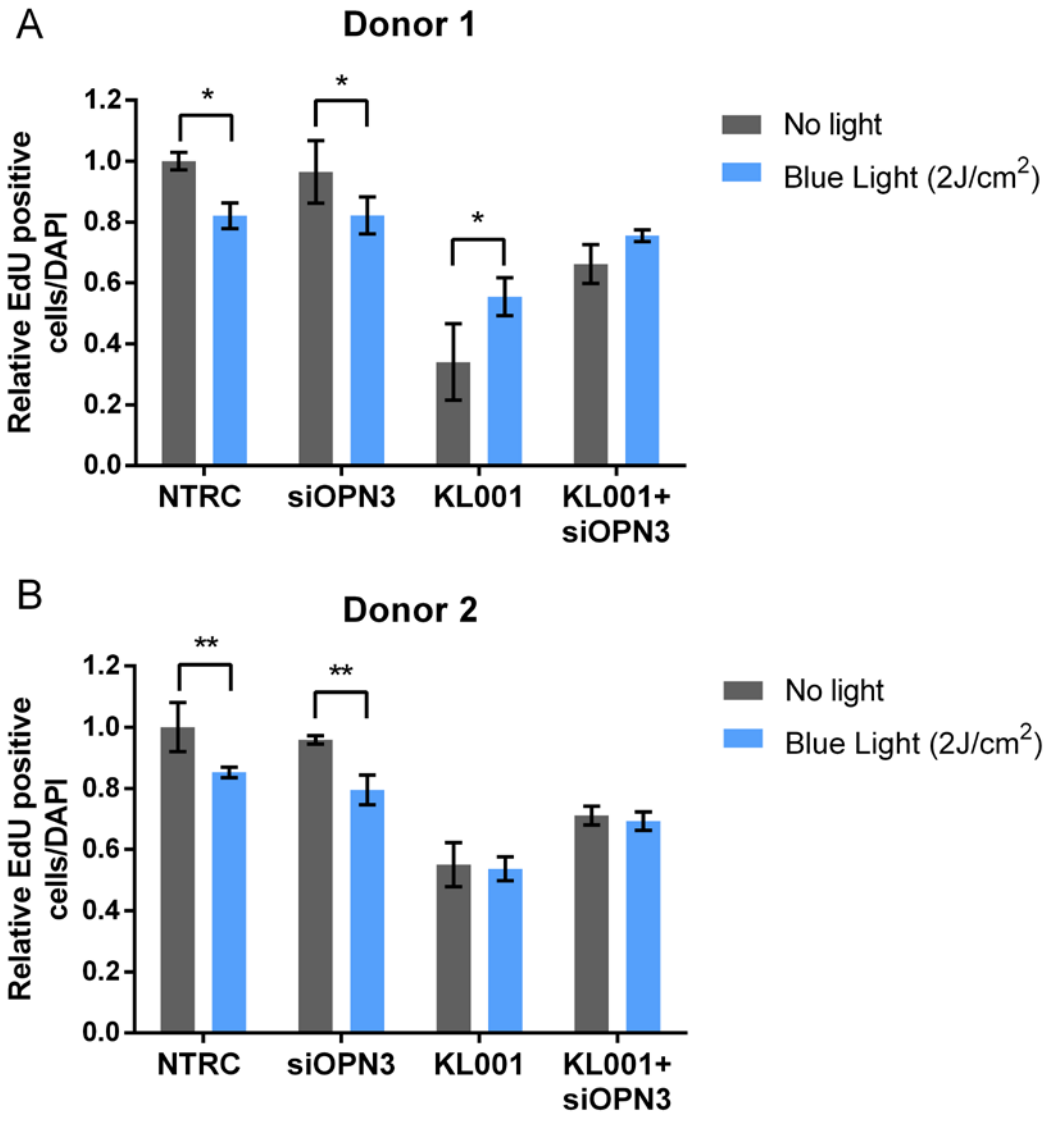

Figure 3-18: Effect of siOPN3 and KL001 on epidermal keratinocyte DNA synthesis after low level blue light irradiation.

EdU positive cells / DAPI for siOPN3, KL001 treatment and siOPN3+KL001 non irradiated and irradiated with 2 J/cm^2 of blue light relative to NTRC no light in donor 1 (A), donor 2 (B) and

donor 3 (C). Data was presented as the mean of relative EdU positive cells/DAPI ± SD (n=4 replicates). * Denotes p<0.05, ** denotes p<0.01 and *** denotes p<0.001 (two-way ANOVA).

3.5.3.2 Effect of siOPN3, siCRY1 and KL001 treatment on epidermal keratinocyte differentiation in response to blue light irradiation

When analysing the effect of blue light in silenced and/or KL001 treated cells, there was an increase in the number of differentiating keratinocytes treated with the non-target siRNA (NTRC) in response to low level blue light (Figure 3-19). However, blue light had no effect on KRT10 expression after OPN3 silencing, KL001 treatment or KL001 treatment in combination with siOPN3 (Figure 3-19).

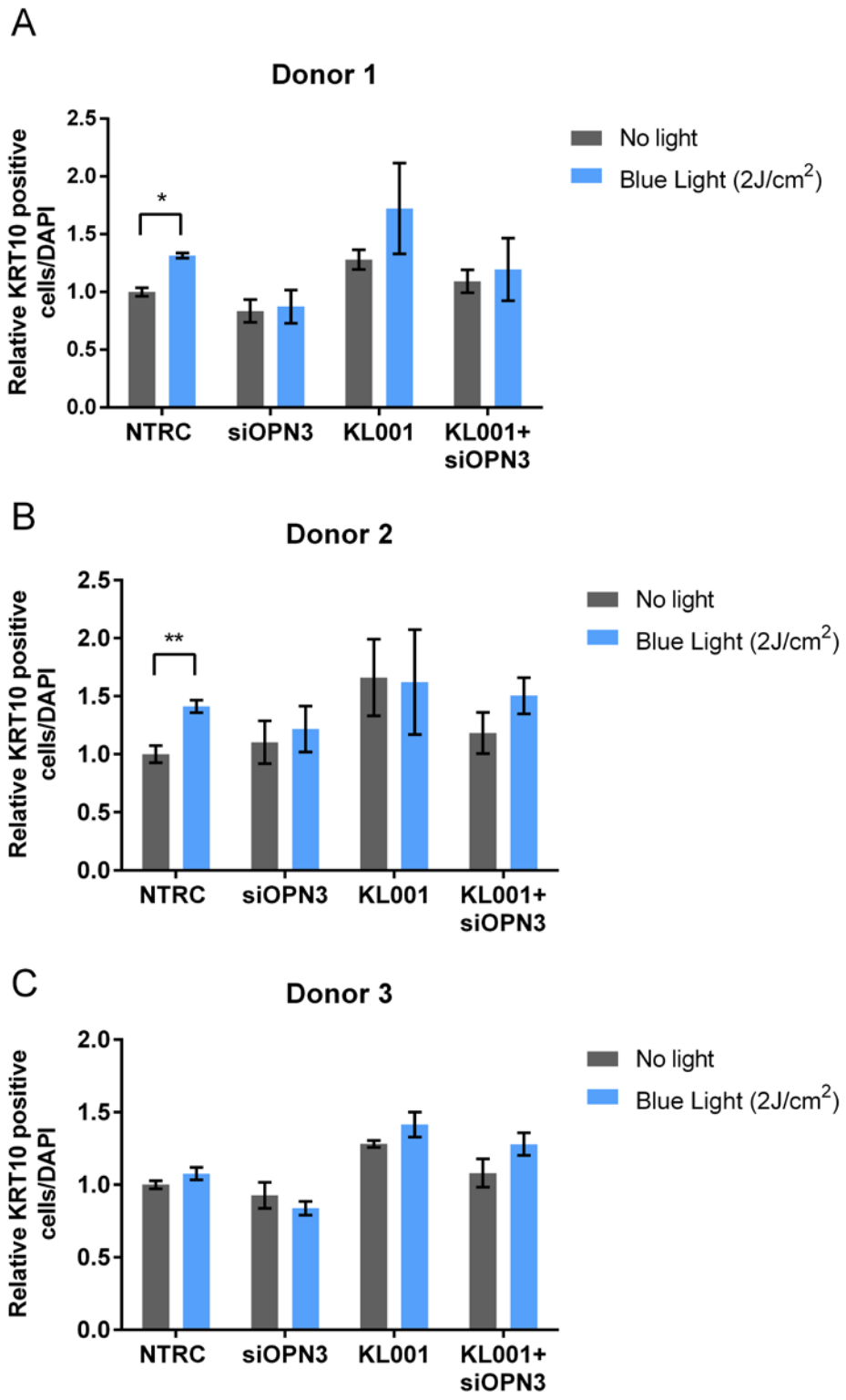

Figure 3-19: Effect of siOPN3 and KL001 on epidermal keratinocytes differentiation after low levels of blue light irradiation.

(A) Representative experiment of KRT10 positive cells / DAPI for siOPN3, KL001 treatment and siOPN3+KL001 non irradiated and irradiated with 2 J/cm^2 of blue light relative to NTRC no light.

Data was presented as the mean of relative KRT10 positive cells/DAPI ± SD (n=4 replicates). * Denotes p<0.05, ** denotes p<0.01 and *** denotes p0.001 (two-way ANOVA). Experiment was repeated in two extra donors.

3.6 Effect of blue and red light on an *ex vivo* human skin wound healing model

While published data has confirmed the effect of red light in wound healing (Posten et al. 2005), there is no data on the effect of blue light. Therefore, the development of efficient and knowledge-based light devices to improve wound healing is required. In order to test the effect of red light and blue light on wound healing, an *ex vivo* human skin wound healing model was developed to investigate the response to light in conditions that resemble human skin wound healing *in vivo*.

3.6.1 Expression of KRT17 in *ex vivo* wounds after two days in culture

Ex vivo wounds from female abdominal skin were frozen in OCT immediately after wounding (day 0) or after two days in culture (day 2). KRT17 and 14 were detected by immunofluorescence on day 0 and day 2 (Figure 3-20, shown in green and red respectively). While at day zero wounds showed expression of these two proteins in the basal layer of the epidermis (Figure 3-20, A and B), they both were also expressed throughout the epidermis and epithelial tongue of *ex vivo* wounds after 2 days in culture, showing an increase in the level of expression (Figure 3-20, C and D).

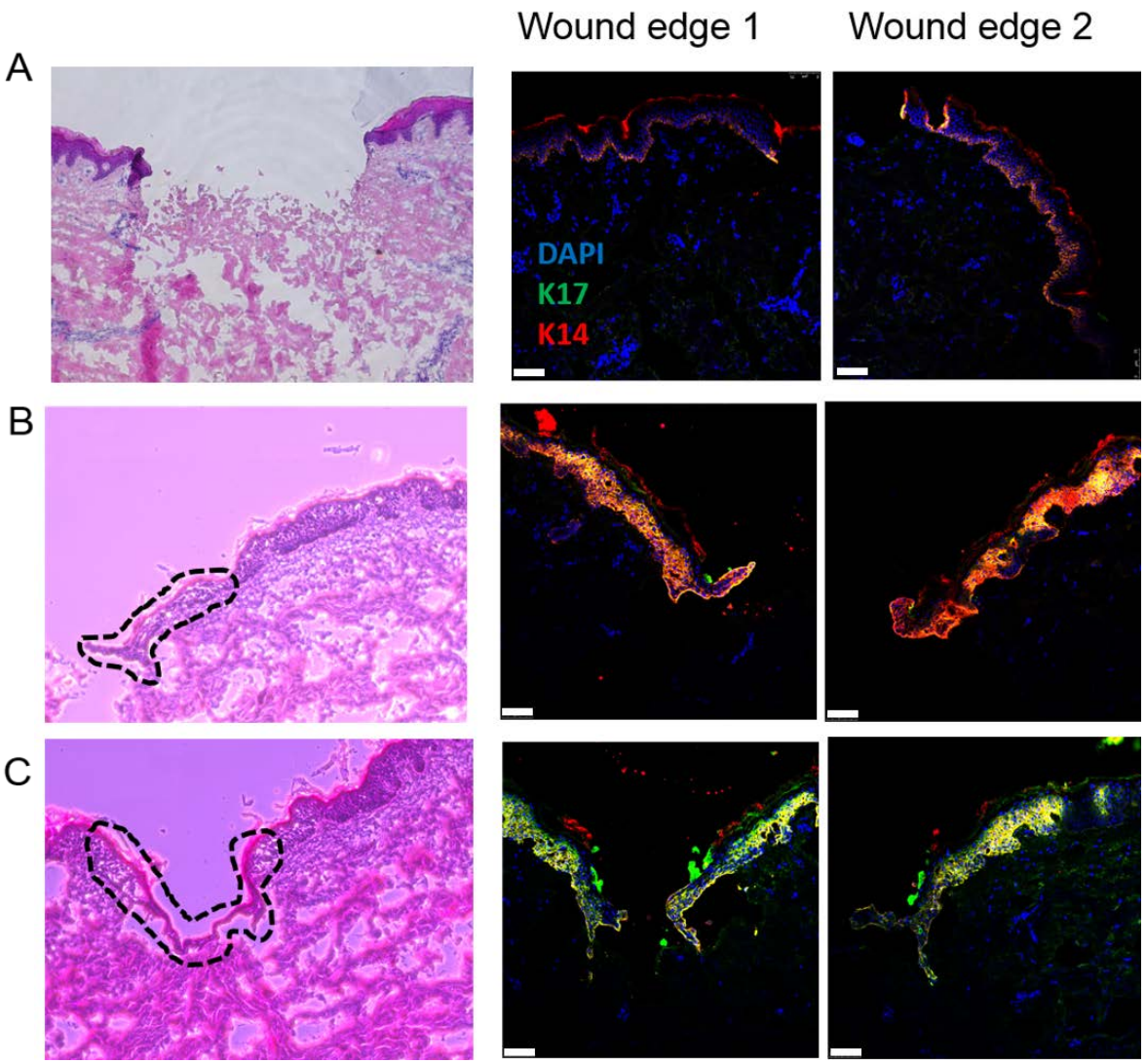

Figure 3-20: KRT14 and KRT17 upregulation during human wound healing.

First panel shows H&E staining, second panel shows merged KRT17 (green) and KRT14 (red) immunofluorescence in one of the wound edges, third panel shows merged KRT17 (green) and KRT14 (red) immunofluorescence in the opposite wound edge. (A) H&E staining of *ex vivo* wound, KRT17 (green) and KRT14 (red) are expressed in the basal layer of human *ex vivo* wounds at day 0. (B and C) An epithelial tongue (within dashes) was formed after two days in culture (H&E staining); KRT17 (green) and KRT14 (red) are upregulated in the epithelial tongue and surrounding epidermis of day 2 wounds. Scale bar = 75 µm.

3.6.2 Expression of photoreceptors in the epithelial tongue of human *ex vivo* wounds

The protein expression of photoreceptors has already been demonstrated in facial and abdominal skin (Figure 3-1 and 3-2) as well as in cultures of primary keratinocytes and fibroblasts (Figure 3-3, 3-4 and 3-5) in this study. Re-epithelialisation is one of the most important phases of wound healing in order to close the wound and avoid infection, and epidermal keratinocytes are main players in this phase. In order to understand the role of photoreceptors in this process, the expression at both mRNA and protein levels in the epithelial tongue of the *ex vivo* wounds was investigated.

Wound cryosections were stained with haematoxylin and the desired area selected and cut by the laser microdissection technique. Images were taken before and after the cut (Figure 3-21). The collected material was used for RNA extraction and amplification.

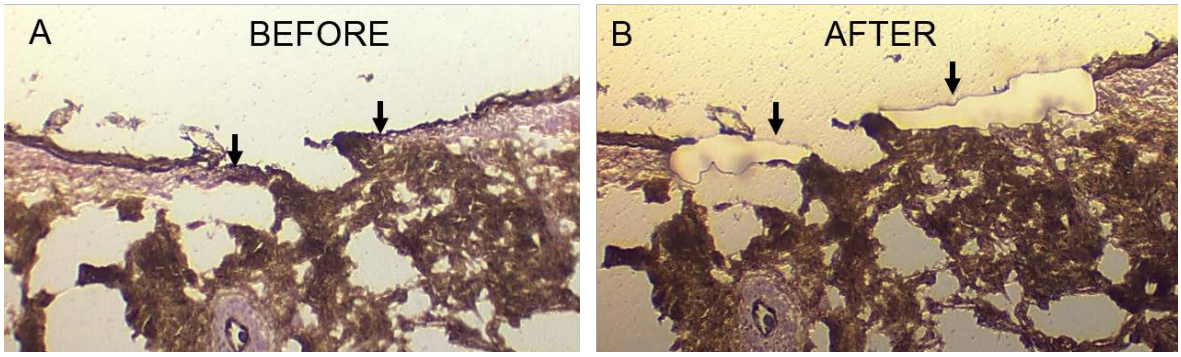

Figure 3-21: Laser microdissection of epithelial tongue as part of *ex vivo* human wounds after two days in culture.

(A) Haematoxylin staining of an *ex vivo* wound before performance of laser microdissection. (B) Haematoxylin staining of an *ex vivo* wound after performance of laser microdissection. Abdominal skin from a 55-year-old female. Arrows indicate epithelial tongue.

Samples with good RNA quality were selected for analysis of photoreceptors by RT-qPCR. Human reference RNA was used as a positive control. There was no amplification of *OPN1-SW*, *OPN5* and *CRY2* during the RT-qPCR process (Figure 3-22, A, C and E respectively). However, *OPN3* and *CRY1* showed very similar melt curve peaks to the positive control (Figure 3-22, B and D). This indicates positive expression of *OPN3* and *CRY1* in the epithelial tongue of human wounds *ex vivo*.

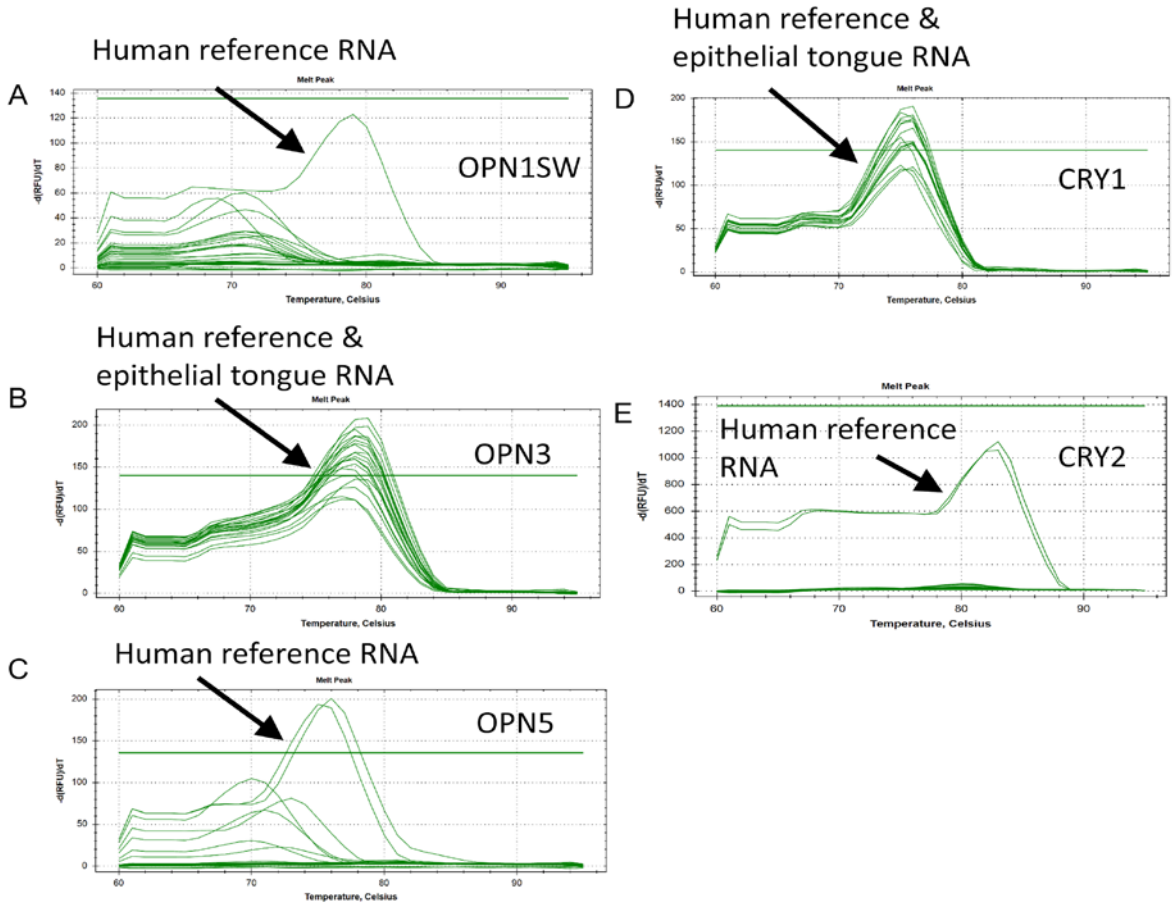

Figure 3-22: *OPN3* and *CRY1* mRNA expression in the epithelial tongue of human wounds *ex vivo*.

Melt curves obtained after qPCR amplification of epithelial tongue RNA (n=9 wounds from 55-year-old female abdominal skin) and human reference RNA for OPN1-SW (A), OPN3 (B), OPN5 (C), CRY1 (D) and CRY2 (E).

In order to verify the mRNA expression data of newly formed epithelium during re-epithelialisation, protein expression was also investigated using immunofluorescence staining for OPN1-SW, OPN3 and OPN5.

Although, *OPN1SW* mRNA was not detected in the RT-qPCR analysis (Figure 3-22), positive staining for the protein was seen in the new epithelium formed. This expression was more prominent in the more differentiated keratinocytes of the epithelial tongue (Figure 3-23, A).

OPN3 protein expression was in agreement with mRNA expression. OPN3 was highly expressed in the most basal layer of the new epithelium formed during wound healing showing co-localisation with KRT14 (Figure 3-23, B).

Finally, OPN5 was expressed in the edges of epithelial tongue of the wound only (Figure 3-23, C). This expression was less prominent than in the normal, intact epidermis, where a clear signal was seen in the basal layer of the epidermis (Figure 3-1). This low expression could be one reason why *OPN5* was not detectable by RT-qRT (Figure 3-23, C).

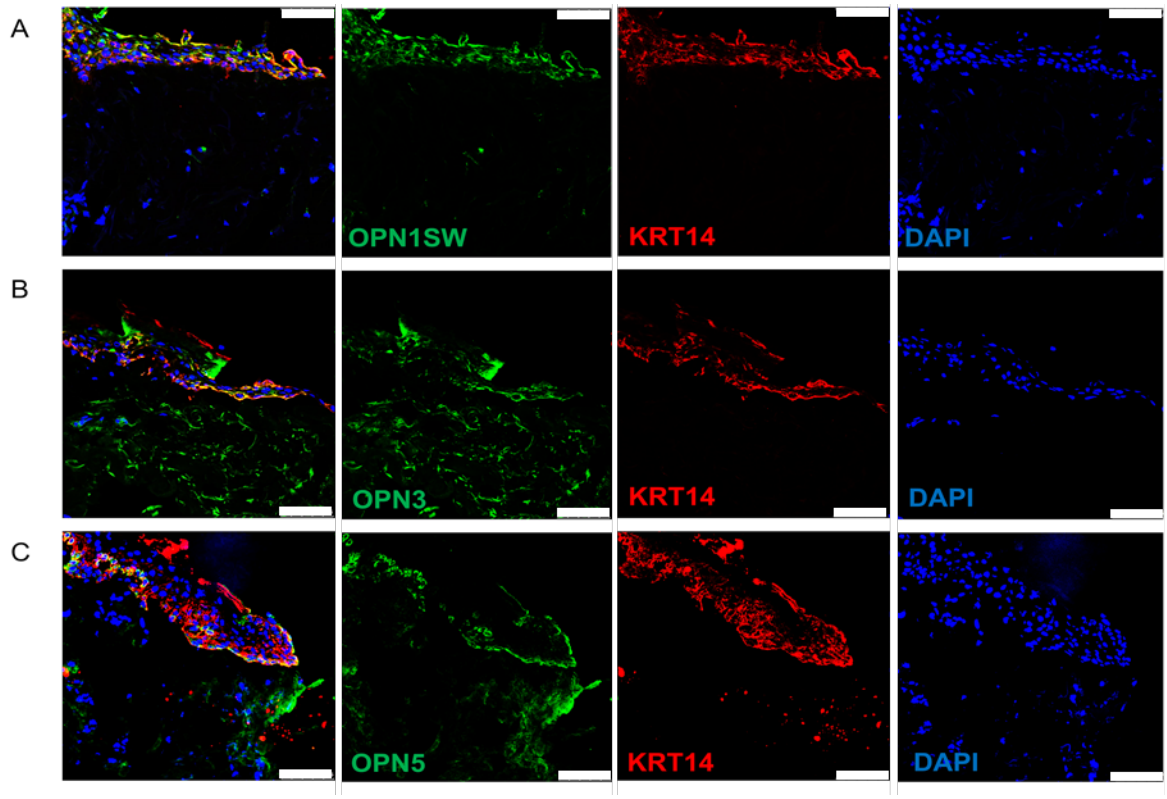

Figure 3-23: Localisation of OPNs in *ex vivo* wounds.

Co-localisation of OPN1SW (A), OPN3 (B) and OPN5 (C) (green) with KRT14 (red) in *ex vivo* wounds. Nuclei are counterstained with DAPi (blue). First panel indicates merged, second panel indicates photoreceptors staining (green), third panel indicates KRT14 staining (red) and fourth paned indicates DAPi (blue) .Representative images of wounds from two different donors.

3.6.3 Blue and red light modulate wound healing *ex vivo*

Reproducible *ex vivo* wounds were performed as previously explained (section 2.10). Speed of closure was highly variable between donors. Donor 1 had the highest speed of closure followed by donor 3 and finally donor 2 (Table 3-3).

	Donor 1	Donor 2	Donor 3
Age	51	44	55
Area	4 - 12 mm^2		
Speed of closure at day 2 (mm^2/h)	0.132 ± 0.017	0.048 ± 0.016	0.071 ± 0.016
Speed of closure at day 5 (mm^2/h)	0.065 ± 0.016	0.032 ± 0.010	0.053 ± 0.003

Table 3-3: Rate of closure in an *ex vivo* human skin wound healing model in three different donors.

Information about age of donors, the wound area at day 0 of all each donor and the mean speed of closure ± SD of control wounds at day 2 and 5 for each donor.

The speed of closure for each wound was analysed at 2 days and 5 days after wounding. Two different doses of blue light 2 J/cm^2 (n=3 donors) and 30J/cm^2 (n=2 donors) were used, while 30J/cm^2 (n=3 donors) was used for red light. Wounds were exposed to the relevant doses of light once a day.

Low doses of blue light (2J/cm^2) increased the rate of re-epithelialisation after two days in culture in both donor 2 and 3 (Figure 3-24, A) following a similar trend at day 5 (Figure 3-24, B). Donor 1 did not show a statistically significant response in wound closure after treatment with light. In contrast, high doses of blue light (30 J/cm^2) inhibited wound closure in donor 1 at day 2 (Figure 3-24, A) and day 5 (Figure 3-24, B), while donor 3 did not respond to

this level of blue light. Red light (30 J/cm^2) increased wound closure only in donor 2 at day 2 (Figure 3-24, A) and in donor 1 at day 5 (Figure 3-24, B).

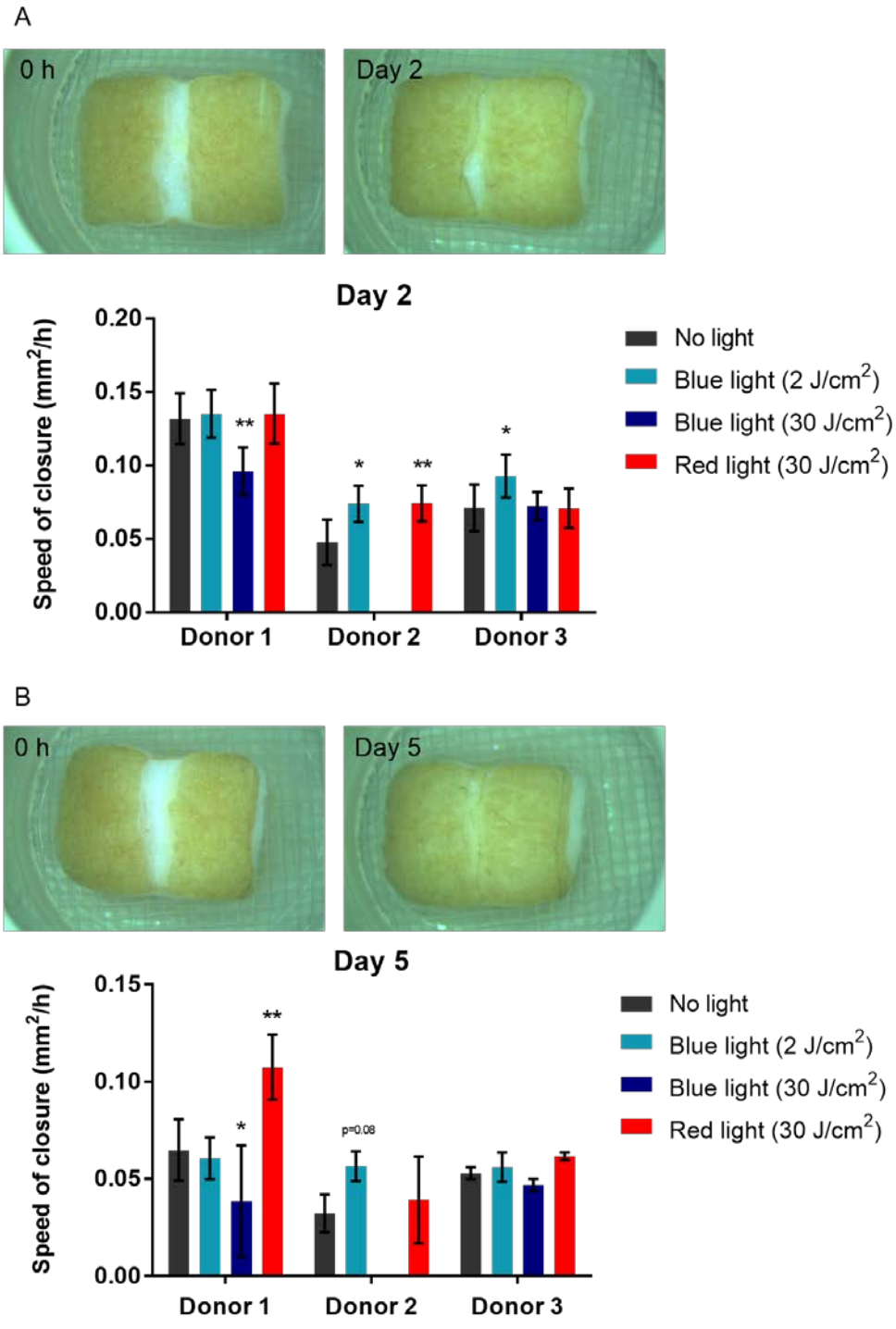

Figure 3-24: Effect of blue and red light on wound closure in an *ex vivo* human skin wound healing model.

(A) Representative pictures of wounds at 0 h and 2 days in culture and the mean of speed of closure after light exposures ±SD (n=5-7 wounds per donor). (B) Representative pictures of wounds at 0 h and 5 days in culture and the mean of speed of closure after light exposures ±SD (n=3-5 wounds per donor). Wounds were treated with light every 24h starting at 0h. * Denotes $p<0.05$, ** denotes $p<0.01$ in a two-way ANOVA.

3.6.4 *KRT17*, *OPN3* and *CRY1* expression after light treatment of *ex vivo* wounds

In order to further understand the effect of blue and red light on wound closure, *KRT17* mRNA expression in the isolated epithelial tongue was analysed. There was no significant difference (Figure 3-25), probably as a result of the low number of wounds analysed (n=2 or 3 wounds per group), and the high variability between them.

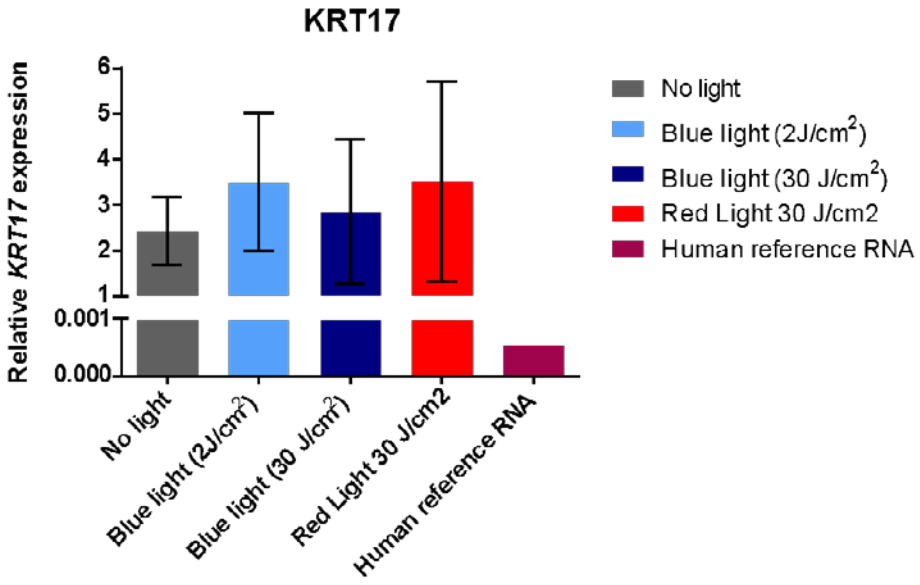

Figure 3-25: Effect of blue and red light on the expression of *KRT17*.

Effect of blue (2 J/cm^2 or 30 J/cm^2) and red (30 J/cm^2) light on *KRT17* expression. Data was calculated relative to GAPDH and presented as the mean of the normalised (no light) relative expression of n=2-3 wounds ± SD. NS indicates not significant (one-way ANOVA).

The expression of *OPN3* and *CRY1* in the RNA isolated from the epithelial tongue was also analysed. Again, no significant differences were found, although low doses of blue light upregulated mRNA expression of these two photoreceptors in most of the wounds analysed (Figure 3-26).

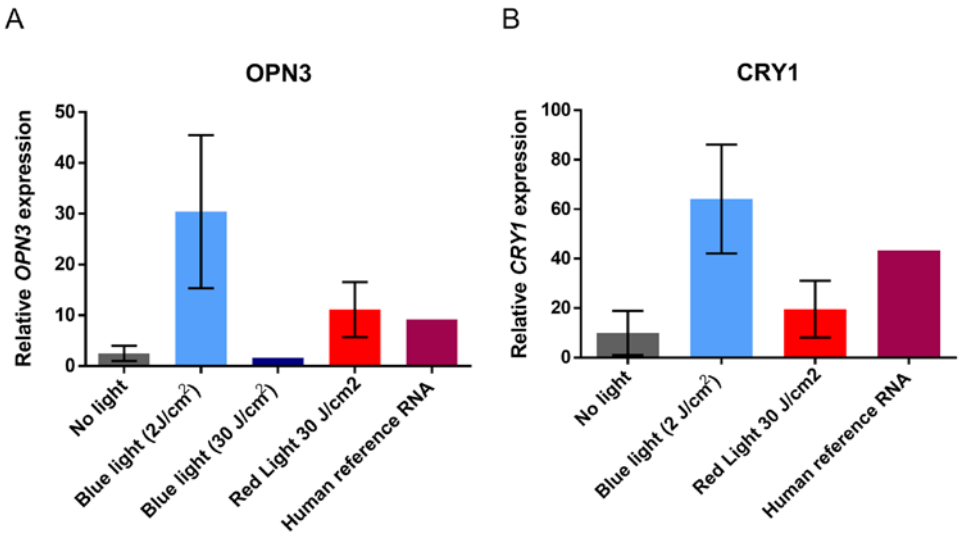

Figure 3-26: Expression of *OPN3* and *CRY1* in the epithelial tongue of *ex vivo* wounds treated with blue and red light.

Relative mRNA expression of *OPN3* (A) and CRY1 (B) after irradiation with blue light (2 or 30 J/cm^2) or red light (30 J/cm^2). Human reference RNA was used as a positive control. Data was calculated relative to GAPDH and presented as the mean of the normalised (no light) relative expression of n=2-3 wounds ± SD. There were not significant differences (one-way ANOVA).

4 Discussion

There is growing evidence that light may have an important role in different processes within human skin. For example, melanin production is a skin defence response to UV light (Slominski et al. 2004), while vitamin D synthesis, an essential hormone is synthesised in keratinocytes following exposure to UV light (Webb 2006). However, there is a growing amount of literature reporting a considerable range of effects in different types of skin cells, including cultured human keratinocytes and fibroblasts, as well as in *in vivo* mouse models after exposure to different light parameters (Hawkins et al. 2005). Light-based devices for skin disorders are already commercially available and claim to produce beneficial effects in conditions such as psoriasis (Kleinpenning et al. 2012; Pfaff et al. 2015), and hair loss (Jimenez et al. 2014). However, it is not clear which molecular mechanisms are involved in these responses to light, yet this knowledge is required for the development of reliable light-based therapeutic devices.

4.1 Photoreceptors are expressed in human skin

The OPN family are GPCRs involved in functions related to vision within the eye of humans and other animals, and the molecular mechanisms are well established in this organ (Ebrey and Koutalos 2001). Recently, the visual opsins OPN1-SW, OPN1-MLW and OPN2 have been identified in human epidermis (Tsutsumi et al. 2009). In addition, expression of the non-visual OPN, OPN3 has been reported in human scalp skin and the terminal hair follicles (Buscone et al. 2017).

In agreement with Tsutsumi *et al.,* (2009), OPN1-SW was highly expressed in the stratum granulosum of the epidermis of facial skin (Figure 3-1). The OPN1-SW receptor is activated by violet light (420-440 nm) (Terakita 2005), and violet light is a powerful wavelength but it does not penetrate very deep into the skin (Lister et al. 2012). This phenomenon may be the reason for OPN1-SW to be highly expressed in the more superficial layers of the epidermis (Figure 3-1).

In contrast, the expression of OPN3 in facial skin was mainly confined to the stratum basal of the epidermis, although a low expression was also seen in the suprabasal layer (Figure 3-1). This is partially in agreement with the localization of OPN3 in human scalp epidermis (Buscone et al. 2017), although human scalp shows a higher expression of OPN3 in differentiated layers of the epidermis compared to facial skin (Figure 3-1). One explanation could be the different antibody used against OPN3; while Buscone *et al.,* (2017) did not specify to which part of the OPN3 receptor their antibody binds to, this study used an antibody specifically directed against the C terminus of OPN3 (Table 2-3), which is the part of the GPCR in charge of transmitting the signal intracellularly. Therefore, while Buscone *et al.,* (2017) reported expression of OPN3 throughout all the epidermal layers of the scalp, an OPN3 capable of activating intracellular signalling pathways is mainly expressed in the basal layer of facial skin (Figure 3-1). Further studies of OPN3 expression in both facial and scalp skin using both antibodies will help to determine whether these differences between anatomical sites are only due to the different functionality of the face in comparison to the scalp, or whether it is related to the functionality

of the OPN3 receptor itself. Focusing on facial skin, OPN3 is expressed deeper in the skin than OPN1-SW. This could be related to the absorption spectra of this protein, which has its peak of absorption at a slightly longer wavelength (465 nm, blue spectrum) (Koyanagi et al. 2013) compared to OPN1-SW at 420-440 nm (Terakita 2005).

This is the first time that localization of OPN5, a UV-absorbing receptor (Yamashita et al. 2010), in human skin *in situ* has been described (Figure 3-1). In contrast to the other OPNs, OPN5 was restricted exclusively to the basal layer of the epidermis as illustrated by its perfect co-localization with KRT14, a specific marker of basal keratinocytes (Figure 3-1). This layer is composed of stem cells and highly proliferating keratinocytes, but also melanocytes which are responsible for the production of melanin required for protection of the skin from UV radiation (Singh et al. 2010). The peak of absorption for OPN5 is within the UV-A spectra (nm) (Yamashita et al. 2010). The penetration of UV light in the skin is more superficial than visible light, including violet light. However, OPN5 is expressed in the layer of the skin where protection against UV light is more critical, as it contains proliferative keratinocytes (Seery and Watt 2000; Blanpain and Fuchs 2009). Interestingly, OPN5 was also expressed in primary melanocytes from neonatal foreskin in culture (Haltaufderhyde et al. 2015). This could indicate a role of OPN5 in the UV response of basal keratinocytes, and there may be cross-talk with melanocytes to regulate skin protection against UV radiation which can induce DNA damage (Besaratinia et al. 2011).

Since it is possible that OPNs may be more predominately expressed in light-exposed areas of human skin such as facial skin, the localisation of OPNs in female abdominal skin from donors of a similar age was studied for comparison. The expression of OPN1SW, OPN3 and OPN5 was similar in facial and abdominal skin (Figure 3-1) suggesting there is no difference in expression with anatomical localisation. This could mean that abdominal skin may not the best anatomical region to study as a non-sun exposed area. Although normally covered, it may still be exposed to sun light during the summer period in many women. Alternatively, the biological function of OPNs may go beyond light reception in non-photoreceptive tissue, so that we still find these proteins in non-sun exposed areas. This is a relevant hypothesis especially for non-visual OPNs; for example, OPN3 has been found in a range of non-photoreceptive tissues such as brain, testis, liver, placenta, heart, lung, skeletal muscle, kidney and pancreas (Terakita 2005).

CRYs are transcription factors that form part of the human molecular circadian clock machinery (Bjarnason et al. 2001; Buhr and Takahashi 2013). Although CRY1 mRNA oscillations in human oral mucosa have been reported (Bjarnason et al. 2001), CRY1 and CRY2 localisation in human skin has never been addressed. Localisation of CRY1 was restricted to the nuclei of epidermal keratincoytes in facial skin (Figure 3-2). However, abdominal skin had very low expression of CRY1, and cellular localisation was cytoplasmic (Figure 3-2). The localisation of CRY1 in non-skin cells has previously been reported to be confined mainly to the cell nucleus, but expression has also been reported to be localised in the cytoplasm of some of the human kidney cell line 293A (Yoo et

al. 2013). Therefore, while expression of CRY can occur in both the nucleus and cytoplasm of cells, the fact that there were differences between facial and abdominal skin could have different explanations. First of all, the abdominal skin was obtained from patients going through abdominoplastia surgery where circadian clock might be disrupted (Shi et al. 2013). This could also explain the low expression of CRY1 in the abdominal skin of some of the donors. Secondly, CRYs are transcription factors which are able to travel from the cytoplasm to the nucleus in a circadian-dependent manner, and it is known that different tissues have their own rhythmicity (Hughey and Butte 2016). Therefore, it could also be the case that because the skin is the largest organ in the human body, different anatomical regions may keep their own circadian rhythmicity.

On the other hand, CRY2 was mainly located in the cytoplasm, although positive staining was also seen in the nucleus. Unlike CRY1, the expression of CRY2 in facial and abdominal skin was similar, indicating a more consistent role and therefore, probably function of CRY2.

The important role of both keratinocytes and fibroblasts in wound healing and the ability of light to go through the epidermis and reach the dermis, makes them both important targets for the action of light on the skin during tissue repair. In order to confirm the relevance of primary cell cultures for studies of responses to light, expression of photoreceptors was also analysed in primary epidermal keratinocytes (n=4) and primary dermal fibroblasts (n=8-9) from different anatomical regions, all at early passage numbers. A keratinocyte human epidermal cell line (NCTC) was also included for comparison (Table 3-

1). The mRNA expression of *OPN1SW, OPN2, OPN3* and *OPN5* in cultured normal human epidermal keratinocytes purchased from Lifeline Cell Technology has previously been reported (Haltaufderhyde et al. 2015), who did not specify the anatomical site that these keratinocytes were isolated from but whether this expression is retained at the protein level has only been reported for OPN2 (Kim et al. 2013). Furthermore, the expression of OPNs in primary cultures of human dermal fibroblasts has not yet been explored.

Primary human epidermal keratinocytes derived from female facial skin express *OPN1-SW*, *OPN3* and *OPN5* at the mRNA level (Figure 3-3 and Table 3-1), confirming the results of a previous study by Haltaufderhyde and colleagues (2015). However, this study has also confirmed that *OPN1-SW*, *OPN3* and *OPN5* are expressed at the protein level (Figure 3-3). Interestingly, *OPN2* was not detectable in the primary cultures of keratinocytes analysed, while an immortalized keratinocyte cell line NCTC 2544, did express mRNA for *OPN2* (Table 3-1). These results are not in line with published data, as *OPN2* mRNA has been found in primary keratinocytes from neonatal foreskin (Kim et al. 2013) as well as in primary adult keratinocytes from an unknown anatomical site (Haltaufderhyde et al. 2015). It is not surprising to find differences between primary keratinocytes in culture and cell lines due to their different characteristics. Specifically, NCTC 2544 cells were derived from human skin after continuous growth in culture by spontaneous transformation (Bakken et al. 1961). This process requires the overexpression of cell cycle genes and downregulation of cell differentiation genes (Katayama et al. 2015). OPN2 has been shown to reduce differentiation after activation with violet light in neonatal

foreskin keratinocytes (Kim et al. 2013), therefore, its positive expression in the NCTC 2544 cell line (Table 3-1) as well as in the highly proliferative neonatal foreskin keratinocytes (Kim et al. 2013) may be related to the maintenance of a reduced differentiation status in these two models. More information regarding the isolation of the keratinocytes used by Haltaufderhyde and co-workers (2015) would be required in order to further understand differences in *OPN2* expression in primary keratinocytes.

In cultured keratinocytes, the protein expression of OPN1-SW was confined to the peri-nuclear region (Figure 3-4). This suggests localization to the Golgi apparatus, since GPCRs are present in the Golgi following protein synthesis, when they undergo post-translational modifications before locating to the plasma membrane. However, this would imply that OPN1SW is not a completely functional protein in keratinocytes. An alternative is that this compartment may be an endosome or a lysosome, since GPCRs are subjected to receptor trafficking (Drake et al. 2006). Co-localization of OPN1SW with specific organelle markers such as GM130, a Golgi apparatus marker, will help to define their role in human keratinocytes. In contrast, OPN3 and OPN5 were both localized to the plasma membrane and cytoplasm in cultured keratinocytes in a similar manner to the expression of OPN2 in neonatal foreskin keratinocytes reported by Kim and co-workers (2014). Furthermore, this is the most common localisation for GPCRs, which are transmembrane receptors (Magalhaes et al. 2012).

Regarding dermal fibroblasts, this is the first report that shows the expression of *OPN1SW*, *OPN2* and *OPN3* mRNA in cultured human dermal fibroblasts. They were studied from fibroblasts isolated from different anatomical regions (breast, face, abdomen and scalp) (Table 3-1). However, *OPN5* was not detected in any of the primary dermal fibroblast cultures (Table 3-1), in agreement with data previously shown in skin immunohistochemistry *in situ,* where the dermis of both facial and abdominal skin did not show expression of OPN5 (Figure 3-4). Although OPN2 was expressed in some dermal fibroblast cultures, it was absent in two out of the eight donors analysed (Table 3-1). Interestingly, the matching keratinocytes for one of these donors also did not express OPN2. This could mean that expression of OPN2 is donor-dependent; however, there were no more donor-matched keratinocytes and fibroblasts to be able to confirm this (Table 3-1). Another possible explanation is that cells in culture tend to loose OPN2 expression as differentiation of epidermal keratinocytes increases with passaging. In contrast, papillary fibroblasts only start to differentiate at later passages in culture, where expression of markers for fibroblast differentiation, such as α-SMA, only increased after at least 16 passages in culture, reaching the levels found in reticular fibroblast (Janson et al. 2013). Since the cultures of primary fibroblasts used to determine OPN2 expression were less than passage 10 (Table 3-1), any loss of OPN2 expression due to differentiation in these fibroblasts is less likely.

The protein expression for OPN1-SW was localised to the perinuclear region of primary dermal fibroblasts in culture, while OPN3 was found in both the cytoplasm and cell membrane. This expression was similar to that seen in

keratinocyte cultures, suggesting a similar function of these two proteins in both cells types.

Non-synchronised primary human keratinocytes and fibroblasts derived from neonatal foreskin demonstrate oscillations in the expression of *CLOCK* and *PER1* mRNA with protein localised to the cell nucleus of both cell types (Zanello et al. 2000). Furthermore, PER1 was also found in the cytoplasm of those cells (Zanello et al. 2000). A more extensive study of circadian clock cycling of the main circadian clock genes was reported by Sandu *et al.,* (2012). They showed cycling of both *CRY1* and *CRY2* mRNAs in human primary abdominal keratinocytes and fibroblasts synchronised with dexamethasone (Sandu et al. 2012). Cycling of *CRY1* and *CRY2* in epidermal keratinocytes has also been reported after synchronisation with 12% serum shock (Janich et al. 2013). However, localisation of CRY1 and CRY2 proteins in primary keratinocytes and fibroblasts in culture has never been reported. This study has confirmed the gene expression of both *CRYs* in non-synchronised primary keratinocytes from facial skin and fibroblasts from different anatomical regions (Figure 3-3 and Table 3-1). Furthermore, protein localisation of CRY1 was mainly confined to the cell nucleus, although cytoplasmic localisation was also seen in one of the three primary epidermal keratinocyte cultures. On the other hand, CRY2 was consistently localised to the cytoplasm (Figure 3-5). CRYs are transcription factors of the circadian clock, and they translocate from the nucleus to the cytoplasm in order to maintain circadian rhythmicity (Matsui et al. 2016). The inconsistency shown by CRY localisation in primary keratinocytes

could be due to the lack of synchronisation, as rhythmicity has been shown to be lost in culture in rat-1 fibroblasts (Balsalobre et al. 2000).

Since primary keratinocytes and fibroblasts retain the same expression of OPN1-SW, OPN3 and OPN5, as well as CRY1 and CRY2 *in vitro* as they do *in vivo* at both the mRNA and protein levels, they provide a physiologically relevant culture model to explore the effect of light on the function the two main human skin cells, keratinocytes and fibroblasts and to understand the role of these photoreceptors in cell migration and wound healing.

4.2 The effect of visible to infrared (IR) light on the metabolic activity of cultured epidermal keratinocytes: a screening of parameters

Photobiomodulation is known to follow a dose-dependent response for long-wavelengths (Huang et al. 2009; Chung et al. 2012), which has been reported to be beneficial in the treatment of pressure ulcers *in vivo* (Lanzafame et al. 2007) and the stimulation of human dermal fibroblast metabolism in culture (Mignon et al. 2017). In contrast, short wavelength light has been mainly reported to supress metabolism of primary human keratinocytes in culture in a dose-dependent manner (Liebmann et al. 2010), although blue light also stimulates the metabolic activity of cultured human dermal fibroblasts (Mignon et al. 2017) and outer root sheath keratinocytes (Buscone et al. 2017), following one exposure at 2 J/cm^2 or 3.2 J/cm^2 respectively. Since the expression of the photoreceptors OPN2 and OPN5 was seen to be cell type specific (Figure 3-1 and 3-3), this could have an impact on the response of epidermal keratinocytes

and dermal fibroblasts to the same light parameters. A comprehensive screening of the effect of light of different wavelengths and radiant exposures on metabolic activity has been reported recently for dermal fibroblasts by Mignon and co-workers (2017), however, it has never been studied in primary human epidermal keratinocyte cultures.

Since the metabolic activity of human dermal fibroblasts has already shown to be impacted by photobiomodulation (Mignon et al. 2017), this was the first response chosen to assess the effect of different wavelengths and radiant exposure on primary human epidermal keratinocytes.

Interestingly, a dose-dependent response in terms of metabolic activity of keratinocytes following exposure to different wavelengths of light was seen (Figure 3-6 and 3-7). For blue (447nm) and cyan (505nm) light similar results were found; 2 J/cm^2 induced metabolic activity of epidermal keratinocytes while 30 J/cm^2 had no effect (Figure 3-6). This effect would be due to different molecular mechanisms, since there are a large number of photoreceptors which absorb short-wavelength light. For example, CCO has different peaks of absorption throughout the visible spectrum, one of them is at 400 nm in the blue light region (Karu 1999). However, this starts decreasing at longer wavelengths, so that its ability to absorb green light is less than blue and cyan light. CCO is part of the respiratory chain of mammalian cells and blue light can increase its activity leading to an increase in ATP synthesis (Hamblin and Demidova 2006), ROS production and NO bioavailability (Poyton and Ball 2011), leading eventually to the increase in metabolic activity at low doses of blue and cyan

light seen in this study (Figure 3-6). However, CCO is not the only photoreceptor present in primary human epidermal keratinocytes. The current study has demonstrated that the expression of OPN1-SW, OPN3 and OPN5 is retained in cultured epidermal keratinocytes in culture (Figure 3-3 and 3-4). Since an increase in metabolic activity was stimulated with light at 447 nm, 505 nm, but not at 530 nm, this may be mediated partially by OPN1-SW or OPN3 as they have their peaks of absorption at 430 and 465 nm respectively, which is close to the wavelength of light which stimulated the metabolic activity of keratinocytes (Figure 3-6). Furthermore, OPN5 may also be involved since it has been shown to be capable of absorbing light at 447 nm after photoconversion following UV stimulation (Kojima et al. 2011). OPNs have been shown to respond to short wavelength light in different skin cells including melanocytes (Wicks et al. 2011; Regazzetti et al. 2017), epidermal keratinocytes (Kim et al. 2013) and outer hair follicle root sheath keratinocytes (Buscone et al. 2017). They induce Ca^{2+} signalling (Wicks et al. 2011) and regulate circadian clock photoentrainment (Do and Yau 2010). Circadian clock is a central regulator of metabolic activity in all different type of cells including keratinocytes (Spörl et al. 2011) which could explain the changes in metabolic activity of keratinocytes seen in this study (Table 3-6). Furthermore, short wavelength light can induce ROS production, for example by the FAD group of CRYs (Hoang et al. 2008) which could therefore, affect expression of circadian clock genes (CCGs) (Gauger and Sancar 2005). Finally, the activation of ion channels were found to be mediated by both blue and green light (Wang et al. 2016) in human adipose-derived stem cells. However, since green light did not

modulate the metabolic activity of keratinocytes (Figure 3-6), activation of ion channels is not likely to be involved in this effect.

With exposure to long wavelength light, a biphasic dose-dependent response in metabolic activity was also found. However, in this case, the stimulation of metabolic activity was also seen at the higher doses. For red (655nm) light, stimulation of metabolic activity was found at doses of both 3.2 and 30J/cm^2, while there was no effect with the higher dose of 200 J/cm^2 (Figure 3-7). NIR (850nm) light stimulated epidermal keratinocyte metabolism at 60J/cm^2, but suppression of metabolism was seen at extremely high doses, 250 J/cm^2 (Figure 3-7). This effect can probably be explained by the already established mechanism suggested by Karu and co-workers (2005), CCO which can also absorb red and NIR light. This protein is part of the respiratory chain of mammalian cells, which can increase its activity leading to an increase in ATP synthesis (Hamblin and Demidova 2006), ROS production and NO bioavailability (Poyton and Ball 2011), which eventually, will induce gene expression through the NF-κB and AP-1 transcription factors, which leads to production of growth factors, extracellular matrix deposition, cell motility and cell metabolism and the reduction of cell apoptosis (Hamblin and Demidova 2006). All these beneficial effect of red and NIR light are able to improve wound healing; for example, red light has been shown to induce interleukin-1 (IL-1) and 8 (IL-8) production by adult foreskin keratinocytes, two essential interleukins during the initiation of the inflammatory phase of wound healing (Yu et al. 1996), while clinical studies have proposed the use of red and NIR light as an

adjunctive therapy for split-thickness skin grafting in burn patients with diabetic ulcers (Dahmardehei et al. 2016).

However, increasing radiant exposure to higher levels, ATP and ROS increase above the necessary levels (Huang et al. 2009; Chen et al. 2011), producing a negative effect on metabolic activity of epidermal keratinocytes.

4.3 Effect of blue and red light on migration of human primary epidermal keratinocytes

Since OPNs have their absorption peak at wavelengths between 360-465 nm (UV and blue light) and blue light increased the metabolic activity of primary keratinocytes (Figure 3-6), this makes blue light a promising wavelength at low and high doses to further investigate the effect of light on keratinocyte migration. While OPNs are not able to absorb red light, since red light also stimulated metabolic activity (Figure 3-7), and there is a large amount of literature supporting the use of red light to improve wound healing (Mignon et al. 2016; Yadav and Gupta 2017), its effect on migration was also studied.

Previous studies have reported that low doses of blue light (up to 10 J/cm^2) does not modulate migration of primary human dermal fibroblasts in culture (Masson-Meyers et al. 2016; Oh et al. 2017), or the human fibrosarcoma cell line HT10-80 (Oh et al. 2017). However, higher doses of blue light between 30 to 80 J/cm^2 have a negative effect on migration of dermal fibroblasts (Masson-Meyers et al. 2016), while migration of the human fibrosarcoma cell line HT10-80 is inhibited at even lower doses, 11 J/cm^2 (Oh et al. 2017). This current study is the first report the effect of blue light on primary human

epidermal keratinocyte migration. Since the response was similar to published studies on primary dermal fibroblasts (Mamalis et al. 2015a; Masson-Meyers et al. 2016; Oh et al. 2017) this suggests similar molecular mechanism in both cell types may be involved in this response. Low doses (2 J/cm^2) of blue light did not modulate epidermal keratinocyte migration, while higher doses (30 J/cm^2) reduced the speed of epidermal keratinocyte migration by approximately 20% after 12h and 21h in a scratch-wound assay (Figure 3-8). Although OPN1-SW and OPN3 are both present in primary epidermal keratinocytes, as well as in dermal fibroblasts, so that they could be mediating the decrease in migration of these cell types, the doses of light producing this effect are high. This suggests that a chemical, rather than a biological effect might be involved, such as the increase in ROS production after blue light irradiation seen in primary dermal fibroblasts (Mamalis et al. 2015a). While ROS was increased by blue light as low as 5 J/cm^2, the effect was dose-dependent, reaching levels that could impact on migration following exposure to 30 J/cm^2 of blue light (Mamalis et al. 2015a). An increase in ROS production has been demostrated in the keratinocyte HaCaT cell line after high irradiation with 41 J/cm^2 of blue light (Becker et al. 2016). No positive effect of blue light in migration has been shown with any of the doses used in this study, similarly to what was found in primary dermal fibroblasts (Figure 3-8). Although blue ligh is not the right wavelength to induce migration and re-epithelialisation during wound healing, the absence of inhibition of migration with low doses of blue light (2 J/cm^2) (Figure 3-8) makes blue light an interesting wavelength for treatment during other stages of the wound healing process; for example, blue light has been shown to prevent

infection during the inflammatory phase of wound healing (Lipovsky et al. 2010; Dai et al. 2013), as well as prevent scarring during the long and last remmodelling phase of wound helaing through the effect of blue light in the fibroblasts residing in the dermis (Mamalis et al. 2015a). Other type of skin conditions could also be improved by blue light treatment by directly targeting the epidermal keratincytes such as psoriasis (Weinstabl et al. 2011). Athopic dermititis can also improve with blue light treatment although exact machanism of action has not been uncovered yet (Becker et al. 2011).

The effect of red light on keratinocytes has previously been studied; a helium neon laser (632.8 nm) increased migration of primary human keratinocytes after three treatments of 0.8 J/cm^2 each (Haas et al. 1990). A more recent study on the HaCaT keratinocyte cell line showed an increase in migration after exposure to 0.6 J/cm^2 of red light (638 nm) after 24h in a scratch-wound assay (Fushimi et al. 2012). On the other hand, very high doses of red light have been shown to decrease the migration of primary human dermal fibroblasts at 320 to 640 J/cm^2 (Mamalis et al. 2015b). However, impact of doses between 2 to 200 J/cm^2 of red light in keratinocyte migration has never been established. Although metabolic activity increased after red light treatment at 30 J/cm^2 (Figure 3-7), no significant effect was observed on cell migration (Figure 3-8) at either 12 or 21h after light treatment. While red light is known to be absorbed by CCO (Karu and Kolyakov 2005), and has been shown to induce wound healing *in vivo* (Minatel et al. 2009; Kajagar et al. 2012) through the activation of NF-κB and AP-1 transcription factors, 30 J/cm^2 of 656 nm light did not modulate migration of primary human epidermal keratinocytes in culture

(Figure 3-7). As response to light normally follows a biphasic dose response (Huang et al. 2009), it is possible that this dose is too high to have a beneficial effect on keratinocyte migration, but not enough to produce a negative effect. A wider range of doses of red light on the migration of epidermal keratinocytes need to be studied in order to better understand the biphasic dose response of this effect and identify whether there is a stimulatory dosage-range as it has been suggested (Haas et al. 1990; Fushimi et al. 2012). It is possible that since photobiomodulation effects are normally small, differences are difficult to establish in a scratch-wound assay and more sensitive assays, such as the Boyden chamber assay is required. Furthermore, photobiomoduluation has shown to improve the inflammatory phase of wound healing due to its anti-inflammatory effects *in vivo* (Hamblin 2017). Therefore, more relevant models, such as co-cultures with dermal fibroblasts or macrophages and lymphocytes, or a human *ex vivo* wound healing model would be required to further test the effect of red light in re-epithelialisation. Cell communication in the skin, an organ with a high amount of different cell types, is essential for a proper wound healing response (Werner et al. 2007).

Finally, blue light (453 nm) at low doses (2 J/cm^2) increased the percentage of KRT10 positive cells (Figure 3-9), while the percentage of EdU positive cells was decreased (Figure 3-9), a dye which is incorporated only by cells synthesising DNA during the S phase of the cell cycle. Interestingly, these light parameters were previously shown to increase the metabolic activity in terms of redox potential of epidermal keratinocytes (Figure 3-6), which would enable epidermal keratinocytes to leave the cell cycle and go into differentiation

(Wanet et al. 2015). Interestingly, Buscone and co-workers (2017), also reported an increase the metabolic activity of outer root sheath hair follicle keratinocytes in response to 3.2 J/cm^2 blue light, however, it induced proliferation in these cells as measure by EdU incorporation assay. This difference in response is possibly related to the different function of epidermal keratinocytes in comparison to outer root sheath hair follicle keratinocytes. While epidermal keratinocytes undergo continuous self-renewal, outer root sheath keratinocytes are more quiescent cells and have less proliferative potential (Tanaka et al. 1998). Other published studies using primary human epidermal keratinocytes reported an increase in early differentiation under low level blue light (5 J/cm^2), while only high doses (66 and 100 J/cm^2) induced late differentiation (Liebmann et al. 2010). Furthermore, blue light has also been reported to delay epidermal barrier recovery in mice *in vivo* (Denda and Fuziwara 2008), which support the anti-proliferative and pro-differentiation effect of blue light seen in this study. In general, the anti- proliferative effect of blue light as well as the blue light induced differentiation suggest the use of blue light to be more suitable for the treatment of psoriasis, and fibrotic skin conditions, as well as to prevent keloids or hypertrophic scar formation in the latter stages of wound healing.

4.4 Physiological significance of OPN3 and CRY1 in primary skin cells

A good understanding of the function of photoreceptors in skin is key to determine whether they have a role in photobiomodulation of human skin. This study has confirmed the expression of OPN3 in human facial and abdominal skin (Figure 3-1), but beyond the skin, OPN3 has been reported to be widely expressed in non-photoreceptive tissues such as brain, testis, liver, placenta, heart, lung, skeletal muscle, kidney and pancreas (Terakita 2005). However, the specific function of OPN3 in human cells, and specifically in the human epidermis is unclear.

CRY1 and CRY2 are two important transcription factors that are part of the molecular transcription loop of the circadian clock. They may also be involved in light reception, either directly as suggested by Hoang et al., (2008), or indirectly by regulating the circadian clock after photoentrainment by another photoreceptor such as one of the OPNs (Poletini et al. 2015).

4.4.1 The synchronisation and transfection conditions of cultured cells

4.4.1.1 Synchronisation of cultured human primary dermal fibroblasts

As a result of the involvement of CRYs in the peripheral clock of human skin (Plikus et al. 2015) and the inconsistency of localisation of CRY1 in non-synchronised epidermal keraitnocytes in culture (Table 3-2), synchronisation of

primary cell cultures is desirable to further study the mechanism of action of OPN3, CRY1 and CRY2.

Unlike other organisms such as drosophila and zebrafish, mammalian peripheral clocks are entrained by neuronal and hormonal signals, whose production is controlled by the SCN pacemaker (Balsalobre et al. 2000). In culture, primary cells maintain circadian oscillations but they lose their synchrony which is regulated by the SCN *in vivo*. Therefore, an input signal that synchronises circadian clock gene expression is needed. Previous studies have shown that clock gene expression was induced by serum shock and oscillations were maintained for three days in serum-free conditions in rat-1 fibroblasts and H35 hepatoma cell lines (Balsalobre et al. 1998). It has also been hypothesised that one or more blood-borne factors are responsible for clock gene stimulation, therefore another study has shown that glucocorticoid hormones, specifically dexamethasone can entrain the circadian clock in rat dermal fibroblasts in culture (Balsalobre et al. 2000).

To determine the best way of synchronisation of human skin cells, the effect of different methods of synchronisation on circadian clock gene expression in human dermal fibroblasts derived from facial skin was analysed by RT-qPCR. Cells were treated with either dexamethasone (dex), serum starvation (SS) or 10% FBS (S+) to establish whether the circadian clock is synchronised in culture. Ideally a number of time points should be analysed to determine a typical circadian curve of mRNA expression (Benegiamo et al. 2016). Although the total RNA expression of clock genes was only analysed

after 4h and 24h, the data shows different levels of expression at these two time points for *CRY1, PER1* and *BMAL1* following all three synchronisation conditions (Figure 3-10), indicating that the expression of clock gene are cycling *in vitro* after a successful synchronisation. In non-synchronised cells, the level of expression of clock genes varies from cell to cell, making it more difficult to establish differences in expression at different time points, as reported for rat-1 fibroblasts (Balsalobre et al. 2000). Synchronised cultures of dermal fibroblasts (Balsalobre et al. 2000) and epidermal keratinocytes (Janich et al. 2013) showed a drop in clock gene expression between 4 and 24h after synchronisation. Similarly, dermal fibroblasts in this study showed a dramatic drop in gene expression of *CRY1, PER1* and *BMAL1* between 4 and 24h after synchronisation with serum starvation or Dex (Figure 3-10), while cells incubated with 10% FBS (S+) only showed a similar drop in level of expression of *BMAL1*. Only small or non-significant differences in *CRY2* mRNA expression was seen between 4 and 24 h after synchronisation, which could be a consequence of similar oscillation levels of *CRY2* at the selected time points (Figure 3-10), illustrating the need of extra time points in order to study circadian clock oscillations.

These results demonstrate that synchronisation in similar in response to SS or Dex groups. However, glucocorticoids both natural and synthetic have a huge impact on skin physiology (Zouboulis 2004), while they have significant anti-inflammatory properties, they can also result in dermal atrophy because of their effect on dermal fibroblasts, producing less collagen and elastin (Kahari et al. 1995). Due to the possible indirect impact of dexamethasone in skin

physiology, serum starvation appears to be the best method of synchronisation of human primary dermal fibroblasts.

4.4.1.2 KL001 and longdaysin modulate the circadian clock in cultured dermal fibroblasts: changes in expression of circadian clock genes

In order to investigate whether the circadian clock of primary dermal fibroblasts in culture can be modulated pharmacologically, two different molecules were identified and used; longadaysin (LD) and KL001. Both are pharmacological tools developed to regulate the CRY/PER feedback loop of the molecular clock; LD is a casein kinase I (CKI) inhibitor, preventing PER protein degradation (Hirota et al. 2010), while KL001 prevents the degradation of both cryptochromes through FBXL3, stabilising the proteins (Hirota et al. 2012) (Figure 1-12). Previously, LD has been shown to modulate circadian clock mRNAs and protein oscillations at concentrations of 3 and 9 µM (Hirota et al. 2010), while KL001 has been reported to downregulate mRNA of *CRY1*, *CRY2*, *PER1* and *PER2* at concentrations between 0.9 to 8 µM in the human epithelial osteosarcoma cell line U2OS, although it had no effect on *CLOCK* and *BMAL* (Hirota et al. 2012).

Circadian clock mRNA expression was assessed in serum-starved synchronised and scratched cultures of dermal fibroblasts 36 h after synchronisation/scratching. KL001 at 8 µM strongly downregulated most of the clock genes except for *CLOCK* (Figure 3-11). This confirms that KL001 can modulate clock genes in cultured dermal fibroblasts. At the same time, it also reflects the robustness of this biological network, as no change was seen in the

expression of *CLOCK,* one of the core circadian clock genes. These data are consistent with the effect of KL001 in U-2 OS cells, with the exception of *BMAL1.* BMAL1 is the other circadian clock core protein of the molecular clock machinery, which was downregulated in primary dermal fibroblasts, while KL001 reputedly did not modulate changes in *BMAL1* expression in U-2 OS cells (Hirota et al. 2012), so that primary dermal fibroblasts seem to be more susceptible than U-2 OS cells to experience circadian clock changes. Contrary to KL001, LD upregulated most clock genes studied; *CRY1, PER1, PER2* and *PER3* with the exception of *BMAL1,* which was down regulated. All clock genes showed a higher level of expression in cells treated with LD in comparison to the ones treated with KL001 (Figure 3-11). While both compounds have been shown to lengthen the circadian clock (Hirota et al. 2012), this cannot be confirmed with the present data, however the effect of both compounds in modulating the circadian clock was verified in dermal fibroblasts reflecting their differential mechanisms of action on clock gene expression 36 h after scratch-wounding. This differential effect of KL001 and LD in dermal fibroblasts is in agreement with the effect seen in the human embryonic kidney cell line, HEK293 by St John and co-workers (2014). The HEK293 cell line constitutively expressed the PER1-LUC and CRY1-LUC reporters; levels of PER1-LUC were only increased by LD, while levels of CRY1-LUC were repressed by KL001 (St John et al. 2014). This data confirms that although both pharmacological tools can modulate the CRY-PER feedback loop of the circadian clock, the fact that KL001 inhibits FBXL3 while LD inhibits CKI (Figure 1-12), results in a different type of regulation of circadian clock oscillations, not only in cell lines such as

HEK293 or U-2 OS, but also in primary human dermal fibroblasts in culture (Figure 3-11). This will probably impact circadian clock functions of human dermal fibroblasts in a different way, showing a different therapeutic potential for treatment of circadian clock disorders. Interestingly, KL001 was proposed to be used for diabetes as a result of the KL001 control of fasting hormone-induced gluconeogenesis in U-2 OS cells (Hirota et al. 2012). However, more work has to be done in order to use these drugs pharmaceutically. In the meanwhile, they are an extremely good tool for the study of circadian oscillations in primary cells in culture.

4.4.1.3 Viability of transfected epidermal keratinoctyes with lipofectamine-siRNA complexes

Synchronisation of the circadian clock (Figure 3-10) and its modulation with KL001 and LD (Figure 3-11) has been confirmed in primary dermal fibroblasts. However, there is a high level of expression of OPNs and CRYs in epidermal keratinocytes and a lack of knowledge of the effect of light on primary keratinocytes in comparison with dermal fibroblasts; therefore, the effect of OPN3 and CRY1 knockout was studied in primary human epidermal keratinocytes.

The only way to specifically control OPN3 and CRY1 expression is with siRNA technology (Dana et al. 2017). siRNA technology can target OPN3 and CRY1 only by the design of specific siRNA sequences against the RNA of interest. Following the transfection protocol previous described (Section 2.9.3), the cell viability of non-transfected keratinocytes (negative control), keratinocytes transfected with no siRNA (lipofectamine control), transfected with

non-target siRNA (NTR) control and keratinocytes transfected with siRNA against OPN3 (siOPN3), were compared. The viability of primary human epidermal keratinocytes decreased as soon as lipofectamine® RNAiMAX was added (Figure 3-12), similar to what has been reported in other cell types, e.g. the MCF-7 cell line (Majid et al. 2002). However, no differences were found between the lipofectamine control, NTR control and siOPN3 treated keratinocytes (Figure 3-12), where viability remained above 60% in all cases (Figure 3-12). Therefore, transfection using siRNA technology is a useful approach to further study photoreceptors in primary human epidermal keratinocytes.

4.4.2 OPN3 and CRYs regulation in synchronised epidermal keratinocytes

4.4.2.1 Transfection efficiency and effect of KL001 in primary epidermal keratinocytes

While the effect of 8 µM of KL001 on the expression of clock genes in primary dermal fibroblasts has been confirmed (Figure 3-11), its effect on primary epidermal keratinocytes is unknown.

Knockdown of OPN3 was highly efficient (Figure 3-13, A) with keratinocytes treated with siOPN3 showing an 83% reduction of OPN3 mRNA expression in comparison to the non-target siRNA control (NTRC). Interestingly, efficiency of CRY1 silencing, although still significant was not as high at 66% (Figure 3-13, B). The same conditions were followed for silencing both proteins

so the different results may be due to different specificity of the siRNA sequences to the different proteins (Kurreck 2006).

Interestingly, KL001 treatment downregulated both CRYs in scratched epidermal keratinocytes 24 h after serum synchronisation (Figure 3-13, C), as was also demonstrated in primary fibroblasts (Figure 3-11). In response to KL001, there was a 71% reduction in *CRY1* mRNA expression, while *CRY2* mRNA was reduced by 40% (Figure 3-13, C). This difference implies a different molecular mechanism for both CRYs. Although both can be degraded through FBXL3, CRY2 is also able to go through a double phosphorylation in the Ser557/Ser553, which triggers an FBXL3-independent mechanism for proteasomal degradation in mice (Kurabayashi et al. 2010; Lowrey and Takahashi 2011). Therefore, under the action of KL001, CRY2 still may be able to go through proteosomal degradation unlike CRY1, which may explain the different level of downregulation of the two CRYs after KL001 treatment.

4.4.2.2 Knockdown of *OPN3* modulates *CRY1* expression, while KL001 upregulates *OPN3*

In order to have a better understanding of the molecular mechanisms behind the knockdown of OPN3 and KL001 treatment, the level of expression of the photoreceptors, *OPN3*, *CRY1* and *CRY2* was investigated after the scratch-wound assay was on silenced and KL001 treated epidermal keratinocytes (section 3.4.2.2).

Interestingly, silencing of OPN3 induced levels of expression of *CRY1,* while KL001 treatment induced expression of *OPN3* (Figure 3-14, A and B).

One possible mechanism which could connect OPN3 to circadian clock regulation is through the activation of the cAMP-responsive element (CRE), which has been found in the promoter region of PER1 and PER2 in the HuH-7 human hepatoma cell line (Motzkus et al. 2007), and in the SCN of mice (O'Neill et al. 2008) (Figure 4-1, A). Although CRE elements have not been found in the CRY promoter yet (Koyanagi et al. 2011), it may be possible they also exist in a similar way to the PER promoter. Alternatively, the changes produced by CREB proteins in *PER* mRNA expression are likely to affect *CRY*1 expression as a consequence. Furthermore, activation of CREB signalling pathway may happen through different mechanisms; e.g. cAMP signalling, Ca^{2+} signalling, and Ras signalling (Figure 4-1, A). Both cAMP and Ca^{2+} signalling are regulated by GPCRs (Figure 4-1, B) (Syrovatkina et al. 2016). Indeed, it has been reported that knockdown of OPN3 blocked the calcium flux and the phosphorylation of CREB and Ca^{2+}/calmodulin-dependent protein kinase II (CAMKII) in human epidermal melanocytes in both non-irradiated and blue light-irradiated cultures (Regazzetti et al. 2017), which was probably mediated by Go protein (Table 4-1). Furthermore, OPN2 has been shown to contribute to the induction of UV-dependent Ca^{2+} mobilisation in epidermal melanocytes (Wicks et al. 2011). In human epidermal keratinocyte, a non-canonical OPN2 signalling pathway mediated through Gi protein has been reported (Kim et al. 2013) (Table 4-1). Therefore, CREB signalling may be involved in the upregulation of *CRY1* seen after silencing of OPN3 in primary epidermal keratinocytes (Figure 3-14), which makes OPN3 a target for the regulation of the peripheral circadian clock of the epidermis.

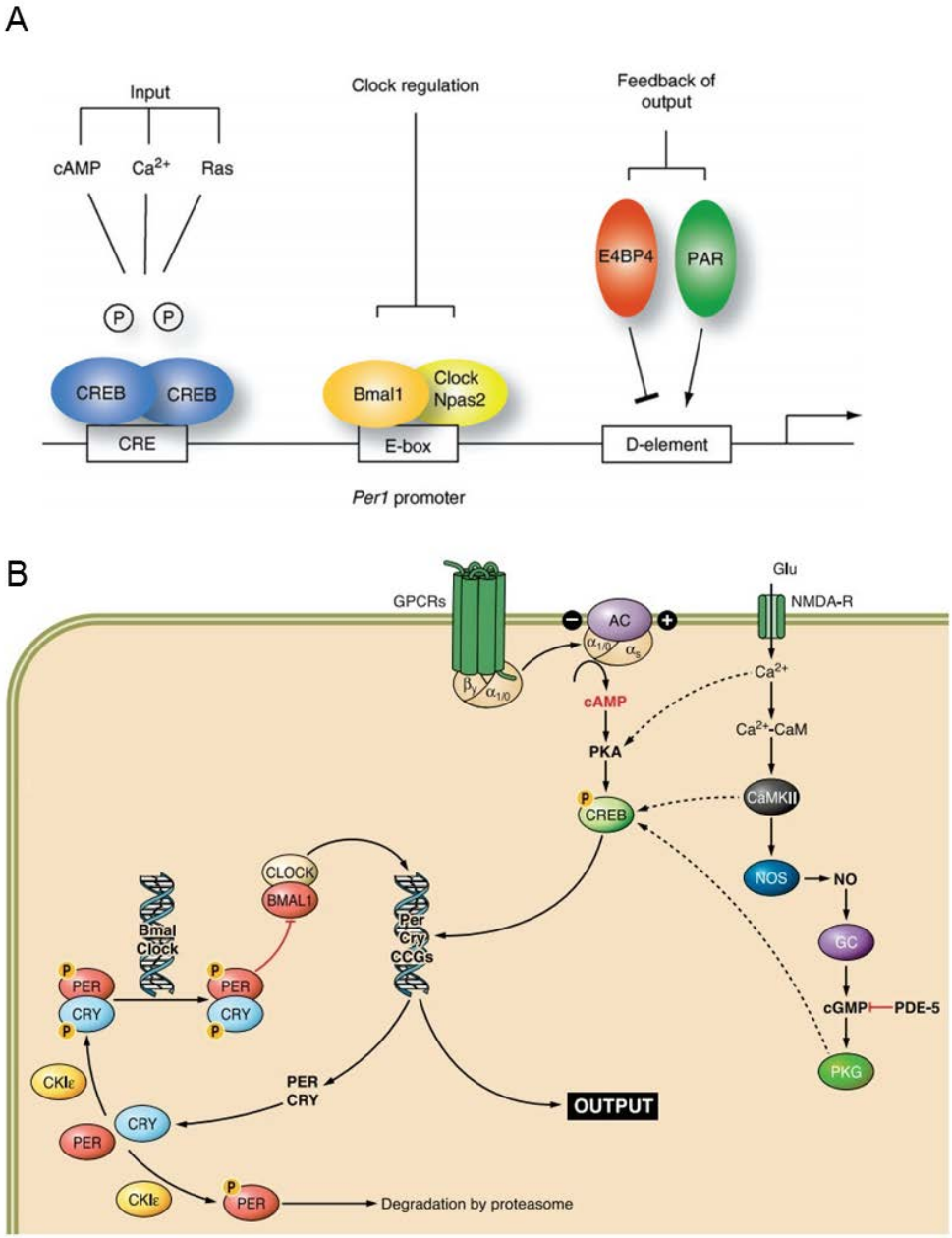

Figure 4-1: Signalling pathway regulating the molecular clock in mammals.

(A) Per1 promoter in mice includes three different regulatory elements; CRE element is regulated by phosphorylated CREB after cAMP, Ca^{2+} or Ras inputs. E-box is regulated by the clock transcription factors BMAL and CLOCK. The D element is regulated by the feedback of the clock output, through the proline and acidic amino acid– rich (PAR) and E4BP4 transcription factors. Adapted from Travnickova-Bendova et al., (2002). (B) GPCR through activation of adenylate cyclase and *N*-methyl-D-aspartate receptor (NMDAR) through activation of CAMKII

can induce phosphorylation of CREB to regulate *PER* and *CRY* expression in a CLOCK-independent manner. Adapted from Golombek and Rosenstein (2010).

Family	Gα protein	Pathway	Opsins (OPNs)
I	Gs	Activation of AC	NA
	Golf		
II	Gi	Inhibition of AC Independent kinases actions: activation of K^+ channels	OPN2 (Kim et al. 2013) OPN3 (Koyanagi et al. 2013) and OPN5 (Yamashita et al. 2010)
	Go	Activation of PLC and increase in Ca^{2+} Independent kinases actions: activation of K^+ channels&inhibition of Ca^{2+} channels	OPN3 (Koyanagi et al. 2013; Regazzetti et al. 2017)
	Gt	Activation of cGMP phosphodiesterase	OPN1 and OPN2 (Terakita 2005)
III	Gq	Activation of PLC and Ca^{2+} increase	OPN4 (Koyanagi and Terakita 2008)
IV	G12-13	Activation of GTPases of the Rho family	NA

Table 4-1: OPNs activate different type of Gα proteins which are in charge of different downstream signalling pathways.

The activation of adenylyl cyclase (AC) by Gs or Golf induces the intracellular cAMP levels and phosphorylates CREB. Go and Gq activate the inositol phospholipid signalling pathway through

phospholipase C (PLC), increasing the intracellular Ca^{2+} concentration and activating different protein kinases such as CAMKII, which can also phosphorylate CREB . The activation of cGMP phosphodiesterase by Gt closes Na^{+} channels creating an electrical signal. G12-13 activates a monomeric GTPase of the Rho family which alters the active cytoskeleton. Adapted from Alberts et al., (2007). NA indicates not applicable.

Knockdown of CRY1 did not induce a significant change in *OPN3* expression (Figure 3-14, A), suggesting there is no feedback in the regulation of OPN3 and CRY1. However, an upregulation of *CRY2* was seen in order to compensate for the lack of CRY1, in a similar manner to what was previously reported in the U-2 OS cell line (Baggs et al. 2009).

Finally, differences in expression of photoreceptors between KL001 treatment in non-silenced and silenced cells was only found for *OPN3* mRNA expression, presumably as a result of the knockout of OPN3. However, there were no differences in the expression of *CRY1* or *CRY2* (Figure 3-14, A, B and C). Although knockdown of OPN3 suggests a role for OPN3 in mediating, or even gating the circadian clock oscillations of epidermal keratinocytes, it was not enough to reverse the effect of KL001 in the regulation of the expression of *CRYs* (Figure 3-14, B and C). This observation highlights the strong effect of KL001 in regulating CRYs, but it also discards the hypothesis of CRYs mediating the abrogation of the decrease in migration and increase in differentiation shown after knockdown of OPN3 in KL001 treated keratinocytes. In order to further understand the molecular mechanism behind those, chromatin immunoprecipitation sequencing (ChIP-Seq) of CREB in normal and OPN3 knockdown epidermal keratinocytes is recommended. This experiment

will show which genes are regulated by OPN3-CREB signalling, and whether they are related to keratinocyte migration and differentiation.

4.4.2.3 Effect of OPN3 and CRY1 knockdown and treatment with KL001 on the migration of epidermal keratinocytes

In order to elucidate whether OPN3, CRY1 or CRY2 have any role in the migration of epidermal keratinocytes, two strategies have been investigated; modulation of CRYs with the chemical KL001, and selected silencing of the photoreceptors OPN3 and CRY1. However, in order to have a better idea about the interconnection of these proteins, if any, a combination of KL001 with gene silencing was also performed.

Knockdown of OPN3 or CRY1 did not have any effect on epidermal keratinocyte migration, suggesting that neither protein has a main role in the migration of keratinocytes. Although an impaired circadian clock has been previously shown to impair mouse wounds healing (Kowalska et al. 2013), silencing of only CRY1 would probably not be enough to affect oscillations of the core clock proteins BMAL1 and CLOCK, since the robustness of the circadian clock probably maintains some circadian oscillations, keeping the migratory ability of keratinocytes in place. Robustness of the circadian clock has previously been shown in the U-2 OS cell line, where BMAL1 oscillations were still present after knockdown of CRY1 (Baggs et al. 2009) but they were gone after knocking down both CRYs at the same time. However, this study shows how KL001 significantly inhibited migration of keratinocytes (Figure 3-15). Unlike direct silencing of CRY1, KL001 has been shown to stop PER2 oscillations almost completely, while it lengthened the period and reduced the

amplitude of BMAL1 oscillations until they were also lost 72h later in the U-2 OS cell line (Hirota et al. 2012). A similar effect may be occuring in primary epidermal keratinocytes, since the presence of KL001 but not the silencing of CRY1 inhibited keratinocyte migration (Figure 3-15). The molecular mechanisms by which disruption of circadian oscillations by KL001 could impact cell migration has not been identified, however a similar effect of KL001 was found in re-epithelialisation in mice retina (Xue et al. 2017). Interestingly, one of the propsed mechanisms was through the negative regulation of the mitotic rhythm of the corneal epithelium, which led to a decrease in both mitosis and re-epithelialisation after wounding. Furthermore, an effect of KL001 on inflammation after wounding was also hypothesised as a result of the rhythmicity of different inflammatory cytokines, such as *IL4RA* and *CXCL14* (Gibbs et al. 2012; Plikus et al. 2015).

Interestingly, silencing of OPN3 abrogated the effect of KL001 on keratinocyte migration (Figure 3-15). The molecular mechanism of this exciting observation will need further investigation. A direct effect of OPN3 in circadian clock could be behind this behaviour. OPN3 could activate downstream signalling pathways with the ability of regulating circadian clock genes such as the transcription factor cAMP response element-binding protein (CREB) (Motzkus et al. 2007). Another possibility is the indirect effect that knocking down OPN3 has on proliferation (Buscone et al. 2017) and inflammation (White et al. 2008) which could be responsible for reversing the delayed migration induced by KL001 (Figure 3-15). More specifically, silencing of OPN3 in the Jurkat cell line resulted in upregulation of interleukin 2 (IL-2) mRNA (White et al.

2008). Although IL-2 is mainly secreted by T helper cells and is required for survival of regulatory T cells (Barron et al. 2010; Sharma et al. 2011), so that, OPN3 might have a similar function in epidermal keratinocytes. Epidermal keraintocytes have not been shown to secreate IL-2, but OPN3 might induce the secreation of other interleukins with similar functions IL-7 or IL-15 (Gröne 2002). An enzyme-linked immunosorbent assay (ELISA) after OPN3 silencing in epidermal kerainocytes would be recommended in order to investigate this hypothesis.

4.4.2.4 Effect of siOPN3, siCRY1 and KL001 treatment on the early differentiation of epidermal keratinocytes

In order to understand the mechanism behind the inhibition of epidermal keratinocyte migration after KL001 treatment and how knock down of OPN3 can abrogate that effect, mRNA was extracted 21 h after the scratch-wound to investigate any changes in the expression of genes for differentiation. It has been previously described that there is an induction of involucrin (INV), a late differentiation marker, in primary epidermal keratinocytes after silencing of CRY1 and CRY2, in addition to a reduction in the number of small colonies and an increase in the number of large colonies (Janich et al. 2013). This demonstrates a role for CRYs in the regulation of differentiation in epidermal keratinocytes (Janich et al. 2013) which may be the reason for the inhibition of migration in primary kerainocytes following treatment with KL001. However, the role of CRYs in the early differentiation of epidermal keratinocytes has never been studied. Knockdown of OPN3 did not modulate the expression of the early differentiation markers *KRT1* or *KRT10*, however silencing of CRY1 upregulated

KRT10 (Figure 3-12, A and B respectively) in line with the increase of INV reported by Janich and co-workers (2013). KL001 upregulated both *KRT1* and *KRT10* expression suggesting a strong induction of early differentiation by this stabilisation of CRY. Since epidermal keratinocytes have to downregulate cytokeratins to enable motility (Haensel and Dai 2017), this may explain the delay in migration seen by KL001. Further evidence is provided by the observation that silencing of OPN3 in combination with KL001 also neutralised these effect on differentiation. On the other hand, since the knockdown of OPN3 did not have a significant effect on *KRT1* and *KRT10* expression (Figure 3-12, A and B), the neutralisation of the KL001 effect on differentiation may be an indirect consequence of the knock down of OPN3, possibly through the circadian clock.

4.4.3 The role of OPN3 and the circadian clock in the blue light response of epidermal keratinocytes

To establish whether the modulation of keratinocytes by blue light is modulated by OPN3 or the circadian clock, the effect of low doses of blue light (2 J/cm^2) on the differentiation and proliferation of OPN3-knockdown and KL001-treated keratinocytes was investigated.

Interestingly, the decrease in DNA synthesis induced by blue light (Figure 3-9) also occurred in OPN3 knockout keratinocytes, but not in KL001 treated cells, indicating that OPN3-independent circadian clock oscillations mediate the blue light inhibition of DNA synthesis in epidermal keratinocytes (Figure 3-18).

In contrast, the increase in keratinocyte differentiation after blue light irradiation already reported (Figure 3-9) was only seen in the non-target siRNA control cells, but not in OPN3 knockout keratinocytes, KL001 treated keratinocytes or OPN3 knockout in combination with KL001 (Figure 3-19). This indicates the role of OPN3 and circadian clock in mediating early differentiation of epidermal keratinocytes after blue light irradiation (Figure 4-2), in a similar manner OPN2 induces differentiation of epidermal keratinocytes following irradiation with violet-light (Kim et al. 2013).

Circadian clock has shown to regulate cell cycle at the G1/S, G2/M and mitosis checkpoints. Interestingly, one of the checkpoints which is highly affected by circadian oscillations is the restriction point G1/S through the regulation of CSK-homologous kinase1/2 (CHK1/2) proteins, *p21* and NONO (Kowalska et al. 2013). Furthermore, Per1/Per2 knockout mouse showed defects in wound healing mainly related to re-epithelialisation, dermal organisation and collagen deposition (Kowalska et al. 2013). In conclusion, the circadian clock and DNA synthesis downregulation by 2 J/cm^2 of blue light might probably happen through any of the G1/S checkpoints and could have a negative impact in re-epithelialisation and wound healing. The use of blue light seems to have a great potential to reduce proliferation and DNA synthesis for hiperproliferative chronic wound edges or psoriatic skin. However, the investigation of lower doses of blue light, and its translation *ex vivo* and *in vivo* would be useful to understand whether blue light could have a proliferative effect through circadian clock regulation of the skin in humans. For example,

DNA synthesis of outer root sheath keratinocytes was stimulated after blue light irradiation (Buscone et al. 2017) as previously discussed.

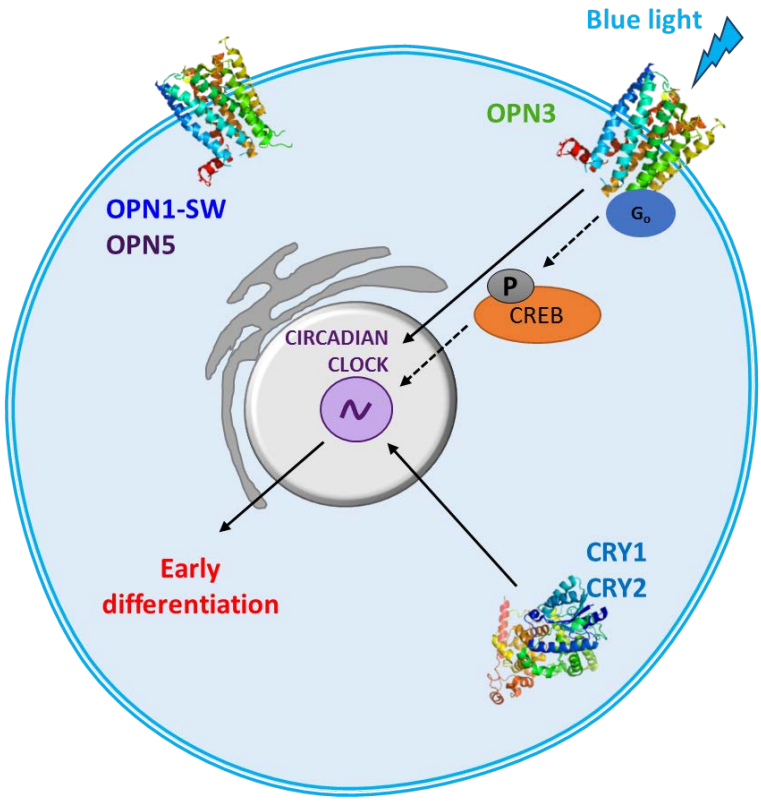

Figure 4-2: Blue light induction of early differentiation in human primary epidermal keratinocytes.

OPN1-SW, OPN3 and OPN5 expression in primary epidermal keratinocytes. OPN3 is able to respond to blue light and activate the Go signalling pathway which led to the phosphorylation of CREB and regulation of CRY1 and CRY2 circadian oscillations to finally induce early differentiation of primary human epidermal keratinocytes in culture. Dotted arrows indicate findings reported in literature, full arrows indicate findings reported in this study.

4.5 Effect of blue and red light in a human *ex vivo* wound healing model

Scratch assays have been shown to mimic cell migration during wound healing especially in terms of cell-matrix and cell-cell interactions in

epithelial/endothelial cells (Liang et al. 2007). However, they do not recapitulate the whole physiology of keratinocytes *in vivo* as a result of different gene expression profiles (Katayama et al. 2015), and lack of communication with other skin cells such as fibroblasts, melanocytes and immune cells. To overcome these issues, an *ex vivo* human skin wound healing model was modified from Stojadinovic and Tomic-Canic (2013). Expression of OPN1-SW, OPN3 and OPN5 in the migrating epithelial tongue and blue and red light effects were studied using this more representative model.

4.5.1 Epidermal KRT17 expression is increased in *ex vivo* wounds after two days in culture

Human *ex vivo* wound healing models are difficult to establish. The lack of blood flow makes it difficult for oxygen and nutrients to diffuse inside the tissue. Irregularities while making the wound will consequently have a significant impact in accessibility to all these important factors and influence the wound healing response. Because of this, confidence and reliability of the model is very important. In order to confirm the appearance of re-epithelialisation the epithelial tongue was identified after two days in culture by H&E staining (Figure 3-20). In addition, the expression of the re-epithelialisation markers KRT17 and KRT14 was also analysed. Induction of KRT17 normally occurs in activated keratinocytes thereby makes this an excellent marker for re-epithelialisation (Stojadinovic and Tomic-Canic 2013). Furthermore, while KRT14 is normally expressed in the basal layer of the epidermis it is also upregulated during re-epithelialisation of human skin *ex vivo* (Mendoza-Garcia et al. 2015). The expression of KRT17 in the epidermis of *ex vivo* wounded skin

was confirmed in this study (Figure 3-20). KRT17 was present in the basal layer in basal keratiocytes in epidermis of wounds at day 0, although expression was not as prominent as for KRT14 (Figure 3-20, A). After 2 days in culture, expression of both KRT17 and KRT14 was found in the new epithelial tongue as well as all thoguhout the sourranding epidermis (Figure 3-20, B and C). These results verified that the cell phenotype was comparable to migrating keratinocytes seen in wound repair (Pastar et al. 2014; Mendoza-Garcia et al. 2015) and therefore validating the use of this model to study re-epithelialisation in human wound healing.

4.5.2 Expression of photoreceptors in the epithelial tongue of human *ex vivo* wounds

Once the *ex vivo* wound healing model was successfully established, two techniques were used to identify photoreceptors in the newly formed epithelial tongue; mRNA expression after laser microdissection of the epithelial tongue (Figure 3-21) and immunohistochemistry of OPN1-SW, OPN3 and OPN5. The expression of mRNA for *OPN3* and *CRY1* was confirmed by the melt curves from the RT-qPCR reaction (Figure 3-22 B and D respectively). However, no amplification of mRNA was seen for *OPN1-SW, OPN5* and CRY2 (Figures 3-22 A, C and E respectively). These transcripts were the most difficult to amplify in primary keratinocytes in culture by RT-qPCR, where amplification only occurred during the last cycles. This may indicate the low abundance of the transcripts of interest, and why there was no amplification of mRNA in the epithelial tongue.

Photoreceptor protein expression was also confirmed by immunofluorescence. In agreement with the RT-qPCR data, OPN3 was present in the epithelial tongue. Interestingly, the OPN1-SW and OPN5 proteins were also expressed in the epithelial tongue. The presence of OPN3 mRNA and protein suggests a role for this receptor in re-epithelialisation. While OPN1-SW and OPN5 were not detected at the mRNA level, protein expression was confirmed by immunohistochemistry. The low abundance of the *OPN1-SW* and *OPN5* transcripts may explain why they were not identified by RT-qPCR, but were still detectable at the protein level. Further quantification of OPN1-SW and OPN5 expression could be done with another technique such as a Western Blot after detachment of the epidermis from the dermis of *ex vivo* wounds, with non-wounded *ex vivo* epidermis included as a negative control.

4.5.3 The effect of blue and red light on wound closure

In order to potentially translate light therapy to *in vivo* treatments, the same light parameters studied in human primary epidermal keratinocytes in culture were used for the *ex vivo* models; 2 and 30 J/cm^2 of blue light and 30 J/cm^2 of red light.

One of the main issues with *ex vivo* wounds was the reproducibility of the wounds. Even with standarised tools, the wound area varied from 3 to 15 mm^2 at day 0. Firstly, the rate of closure was analysed 2 and 5 days after wounding in non-irradiated controls to study differences in the speed of closure between donors under basal conditions. Donor 1 showed the highest speed of closure, 0.132 mm^2/h at day 2, while wounds generated from donor 2 showed closure

that was almost 3 times slower, 0.048 mm^2/h, although tissue was from the same anatomical site and from women of a similar age (Table 3-3). These big differences could be technical, such as the length of time passed since the tissue was outside the body until it was put in culture (between 6 to 12 h), but mainly biological, such as variability between different donor material. Donor variability has been previously reported in skin *ex vivo* cultures, which may be due to different inflammatory responses induced by tissue removal (D'Orazio and Wolf Horrell 2014). Variation in speed of closure within donors was not such a big issue as standard deviation was always below 0.017 (Table 3-3), which makes the model reproducible. In general, the speed of closure decreased at day 5 (Table 3-3). This observation could be due to two main factors; first of all, few wounds appeared closed before day 5, which makes speed of closure less informative so that they have to be discarded. Furthermore, the decline in viability of the skin explants has been previously shown after 7 days in culture, while it remained viable during the first three days (Park et al. 2015). Probably, the loss of viability in the papillary dermis, the one less exposed to the environmental oxygen, will have a negative impact on the keratinocytes immediately above, reducing re-epithelialisaion. This extensive variability makes it difficult to interprete data from all donors together, therefore the effect of light was studied independently in each donor.

Although different donors seemed to have a varied predisposition to the level of response to different light parameters, a similar trend was observed in the different donors. Furthermore, the results are in line with the scratch-wound assay; high doses of blue light slowed wound closure in Donor 1 after both 2

and 5 days in culture, however no significance was seen in Donor 3 (Figure 3-23). This downregulation of wound closure with 30J/cm^2 of blue light is less effective than in cells *in vitro*. This may be due to the fact that the *ex vivo* model presents a 3D organisation which includes all types of different skin cells (Lebonvallet et al. 2010) and therefore the induction of ROS by high doses of blue light, which has been reported in epithelial and dermal cells (Lockwood et al. 2005; Opländer et al. 2013; Becker et al. 2016) is less effective than in isolated cells in culture, since there may be other mechanisms in place to counteract it. The mechanism of high doses of blue light to induce ROS has been shown by the direct effect of short wavelength light on flavoproteins and nitrosated proteins (Oplander et al. 2013).

Although low doses of blue or red light did not influence keratinocyte migration *in vitro* (Figure 3-8), both light parameters induced wound closure in *ex vivo* wounds in Donor 2 after 2 days in culture (Figure 3-23). Red light also induced wound closure in Donor 1 at day 5 only, while low doses of blue light induced wound closure in donor 3 two days after wounding only (Figure 3-23). In contrast to the high doses of blue light, these two parameters seem to be more effective at stimulating re-epithelialisation in *ex vivo* wounds than in scratch wounds *in vitro.* However, molecular mechanism used by blue and red light are likely to be highly different.

4.5.4 Expression of the re-epithelialisation marker, *KRT17* and the photoreceptors *OPN3* and *CRY1* in the epithelial tongue of *ex vivo* wounds after light treatment

Expression of the re-epithelialisation marker *KRT17* as well as the photoreceptors *OPN3* and *CRY1* were analysed by RT-qPCR in epithelial tongue RNA isolated from non-irradiated and irradiated *ex vivo* wounds after two days in culture. Expression of *KRT17* was highly expressed in all samples analysed (Figure 3-24), indicating a normal re-epithelialisation process. Activation of KRT17 happens immediately after wounding and is required for re-epithelialisation (Patel et al. 2006), however no differences in expression were found in tissue exposed to the different light parameters, suggesting that light is not modulating *KRT17* to activate keratinocytes to migrate. Rather than studying a protein which is essential for re-epithelialisation, other markers might be more useful to study. Keratinocytes at the leading edge have to go through EMT to be able to migrate and create the epithelial tongue, therefore, markers such as vimentin which is needed for epidermal keratinocyte migration only, or E-cadherin, which is not downregulated during migration but it is essential in epidermal haemostasis (Haensel and Dai 2017). Furthermore, study of those markers *in situ* by immunohistochemistry is highly recommended to ensure results.

The delay in migration seen with high doses of blue light may be due to an increase in ROS production, so that changes in the expression of superoxide dismutase (SOD) may be a more relevant endpoint to measure. SODs are induced during wound healing in order to keep the level of ROS within a

beneficial range. However, when ROS production is excessive, there is induction of lipid peroxidation, protein modification and DNA damage, delaying the wound healing process (Schäfer and Werner 2008). In order to understand the beneficial effect of blue and red light, other mechanisms such as desmosome disruption, or integrin switch from α6β4 to α3β1 required for re-epithelialisation (Pastar et al. 2014) may also be worth investigating.

New molecular targets related to light reception are of particular interest for further study in the regulation of wound healing. Interestingly, expression of OPN3 and CRY1 were both upregulated following exposure to low levels of blue light. Since they both have their peak of absorption in the blue light part of the spectra (Hoang et al. 2008; Koyanagi et al. 2013), it makes sense that red light is not able to stimulate them. Furthermore, 30 J/cm^2 probably provides too much exposure to blue light and other phenomena such as bleaching (Morshedian and Fain 2017) might interfere with stimulation of the mRNA of the selected photoreceptors.

5 Conclusion

The photobiochemical effects driven by photobiomodulation, together with its non-invasive nature of light and the lack of systemic side effects make this treatment modality a very appealing therapy for skin disorders.

Photobiomodulation has been proposed for treatment of chronic wound healing, but most studies have focused on red light. On the other hand, blue light therapies have been proposed for the treatment of other skin conditions such as psoriasis. The different wound healing stages, the large variety of wounds, as well as the lack of knowledge in the molecular mechanisms involved in light reception in human skin, makes development of light-based therapies for this condition difficult to put forward.

The identification and localisation of different photoreceptors, OPN1-SW, OPN3, OPN5, CRY1 and CRY2 in human skin *in situ* and in primary cells *in vitro* is a step forward in understanding the potential role of these proteins in photobiomodulation of human skin.

Both a wavelength and dose dependent response to light was seen in cultures of primary epidermal keratinocytes. While low doses stimulated metabolism, higher doses suppressed metabolic activity. Light stimulation occurred within a larger dose range for long wavelengths such as NIR and red light, while stimulation with shorter wavelengths, such as blue and cyan light only occurred at extremely low doses. Migration of keratinocytes in culture was inhibited with high doses of blue light, while low doses of blue and red light had

no effect. Different molecular mechanisms are probably involved in the light responses seen in epidermal keratinocytes. While effects on cytochrome c oxidase could be mediated by any wavelength of visible light as a consequence of its different peaks of absorption throughout the spectra, ion channels are not likely to be involved since they also respond to green light. Interestingly, OPNs and CRYs are able to absorb short-wavelength light, so that they are potential candidates for mediating the increase in metabolic activity seen after exposure of low doses of blue and cyan light in cultures of human epidermal keratinocytes.

The lack of knowledge about the functionality of OPN3, CRY1 and CRY2 in primary human epidermal keratinocytes required the study of these photoreceptors under non-irradiated conditions. CRYs were important for maintaining circadian clock oscillations. Alteration of these circadian oscillations by stabilising CRY1 and CRY2 protein with KL001 disrupted migration and induced early differentiation of epidermal keratinocytes. These alterations were abrogated after knockdown of OPN3, which may be due to an effect of OPN3 in the regulation of the circadian clock. Although downstream signalling pathway still needs further investigation, the activation of the transcription factor CREB which can be phosphorylated by the OPN3 signalling pathway and it is able to bind to the PER1 promoter, might be a good candidate. The peripheral circadian clock of the skin is directly connected to the cell cycle, mainly through the G1/S checkpoint and can control re-epithelialisation and dermal organisation during wound healing.

The photoreceptors OPN3, CRY1 and CRY2 all have their absorption peak in the blue part of the light spectra; therefore, 453 nm of light was used to study the role of OPN3 and the circadian clock, including CRY1 and CRY2 in the blue light response of human epidermal keratinocytes in culture. Interestingly, the increase in metabolic activity previously seen with 2 J/cm^2 increased early differentiation of human epidermal keratinocytes, while DNA synthesis was decreased and epidermal differentiation increased. The effect of low doses of blue light on early differentiation was partially mediated by OPN3 signalling and the circadian clock, while downregulation of DNA synthesis may be affected by an OPN3-independent regulation of the circadian clock. These results are consistent with the reported anti-proliferative effect of blue light in the literature, which confirms the use of blue light for psoriasis and hyperproliferative edges of some type of chronic wounds. However, a new molecular mechanism of action of blue light through OPN3 and circadian clock is proposed in this report, which could have an impact on the photobiomodulation treatment regimes, such as time of the day to deliver light treatment as well as number of treatments recommended per day. A proper regulation of the peripheral skin clock is essential to maintain skin homeostasis and to produce a healthy granulation tissue and enable re-epithelialisation during wound healing.

Finally, in order to move forward in the translation of studied parameters *in vitro* to the *in vivo* situation, light exposure was studied in an *ex vivo* human skin wound healing model. Two J/cm^2 of blue light and 30 J/cm^2 of red light had a small, but beneficial effect in wound re-epithelialisation. However, the

expression of different photoreceptors, which absorb light of different wavelengths in human skin, suggests that different mechanisms of action may be involved in this effect. While red light probably mainly affects cytochrome c oxidase, the increase in mRNA expression of *OPN3* and *CRY1* after stimulation with 2 J/cm^2 blue light only in the epithelial tongue of the *ex vivo* wounds, strongly suggests a role for OPN3 signalling and circadian clock oscillations in the regulation of migration and differentiation of the epidermal keratinocytes at the wound edge. On the other hand, 30 J/cm^2 of blue light impaired wound healing *ex vivo* but had no effect on either *OPN3* or *CRY1* expression. It is possible that at this dose there is a high level of ROS production, which impairs the migratory capacity of wound edge keratinocytes. The present data suggests that 2 J/cm^2 blue light and 30 J/cm^2 red light show a beneficial potential for wound healing *ex vivo* but not *in vitro,* indicating a collaborative role of epidermal keratinocytes with other skin cell types such as dermal fibroblasts in mediating re-epithelialisation in response to light. As different OPNs were found in different cell types, it is likely that their response to different wavelengths of light would be needed to see a clear response during wound healing. Further work using more advance wound healing models and combination of the studied light parameters has to be done in order to achieve the most efficient photobiomodulation treatments for different type of chronic wound healing.

In conclusion, this work unravels new molecular targets for photobiomodulation of the skin, especially during wound healing processes. Furthermore, the role of OPN3 and the circadian clock in epidermal migration and differentiation, as a novel molecular mechanism in response to blue light

has been established. Finally, a step forward in translating light parameters from *in vitro* to *ex vivo* human wound healing models suggests the use of 2 J/cm^2 blue light or 30 J/cm^2 red light to improve re-epithelialisation. Further research deciphering underlying signalling pathways activated by OPNs and CRYs in response to photobiomodulation, as well as the translation of light parameters to *in vivo* will help to develop more reliable and scientific based-photobiomodulation therapies for human wound healing, as well as the establishment of treatment regimes and protocols in order to achieve its maximum efficacy.

6 PUBLICATIONS, ORAL PRESENTATIONS AND AWARDS

6.1 PUBLICATIONS

a) Castellano-Pellicena, N. E. Uzunbajakava, C. Mignon, B. Raafs, VA Botchkarev and MJ Thornton, **2018** "Does blue light restore human epidermal barrier function via activation of Opsin during cutaneous wound healing", *LMS, Submitted*

b) C. Mignon, N. E. Uzunbajakava, I. Castellano-Pellicena, N. V. Botchkareva and D. J. Tobin, **2018**. "Differential response of human dermal fibroblast subpopulations to visible and near-infrared light: potential of photobiomodulation for addressing cutaneous conditions", Lasers in Surgery and Medicine *,* doi: 10.1002/lsm.22823

c) C. Faniku, I. Castellano-Pellicena, T. Hoppenbrouwers and H. I. Korkmaz, **2017**. "Report on the 1st European Tissue Repair Society Summer School, London 29th June - 1st July 2016", *Wound repair and regeneration,* doi: 10.1111/wrr.12543

6.2 ORAL PRESENTATIONS

a) Irene Castellano-Pellicena, Natallia E. Uzunbajakava, Vladimir A. Botchkarev, M. Julie Thornton, *Understanding photobiomodulation for human wound healing,* 37th American Society for Laser Medicine and Surgery Annual Conference, **2017,** San Diego, USA

b) I. C. Pellicena, N.E. Uzunbajakava, M. Moolenaar, B. Raafs, C. Mignon, V. E. Botchkarev and M. J. Thornton, "Molecular mechanisms of photobiomodulation in wound healing". British Society of Investigative Dermatology Annual Meeting **2016**, Dundee, United Kingdom

c) (Short oral presentation) I. Castellano , N. E. Uzunbajakava, O. Kamala, B. Raafs, G. Westgate, V. A. Botchkarev and M. J. Thornton, 2015. *Expression of visual and non-visual photoacceptors in human dermal fibroblasts: implications for light-based wound healing therapies*. 7th Joint

Meeting of the European Tissue Repair Society and the Wound Healing Society, **2015**, Copenhagen, Denmark

6.3 POSTER PRESENTATIONS

a) I Castellano-Pellicena, NE Uzunbajakava , C de la Torre, V. A. Botchkarev, M. J. Thornton, *Opsins and cryptochromes in human epidermal keratinocytes: A perspective for blue light therapies*. 47th Annual European Society of Dermatological Research Meeting **2017**, Salzburg, Austria

b) I. C. Pellicena, C. Mignon, S. Buscone, B. Raafs, D.J. Tobin, M.J. Thornton, N.V. Botchkareva, N.E. Uzunbajakava, *Impact of visible light on multiple components of human skin brings new understanding to the therapeutic role of light for skin health*. British Society of Investigative Dermatology Annual Meeting **2016**, Dundee, The United Kingdom

c) Irene Castellano, Natallia E. Uzunbajakava, Ola Kamala, Gillian Westgate, Vladimir Botchkarev, M. Julie Thornton. *Dermal fibroblasts from different anatomical regions of human skin express visual and non-visual photoreceptors in culture; potential targets for modulation of the circadian clock genes?* Biological rhythms: mechanisms, functions, implications for health. Chronobiology Gordon Research Conference, **2015**, Girona, Spain

6.4 AWARDS AND TRAVEL GRANTS

a) **Best of Photobiomodulation Session Award.** 37th American Society for Laser Medicine and Surgery Annual Conference, **2017,** San Diego, USA

d) **Travel grant.** 47th Annual European Society of Dermatological Rresearch Meeting **2017**, Salzburg, Austria

d) **Travel grant.** British Society of Investigative Dermatology Annual Meeting **2016**, Dundee, United Kingdom

7 REFERENCES

Abe, M., Kurosawa, M., Ishikawa, O. and Miyachi, Y. (2000) Effect of mast cell–derived mediators and mast cell–related neutral proteases on human dermal fibroblast proliferation and type I collagen production. *Journal of Allergy and Clinical Immunology* 106 (1, Part 2), S78-S84.

Ahmad, M. and Cashmore, A. R. (1993) HY4 gene of A. thaliana encodes a protein with characteristics of a blue-light photoreceptor. *Nature* 366 (6451), 162-166.

Alberts, B., Johnson, A., Lewis, J., Raff, M., Roberts, K. and Walter, P. (2007) *Molecular biology of the cell.* 5th edition*.* New York: Garland science.

Alcolea, M. P. and Jones, P. H. (2014) Lineage analysis of epidermal stem cells. *Cold Spring Harb Perspect Med* 4 (1), a015206.

Alonso, L. and Fuchs, E. (2006) The hair cycle. *J Cell Sci* 119 (Pt 3), 391-3.

Altshuler, G. B. and Tuchin, V. V. (2009) *Cosmetic applications of laser and light-based systems. Physics Behind Light-Based Systems: Skin and Hair Follicle Interactions with Light.* New York, USA: William Andrew Inc.

André-Lévigne, D., Modarressi, A., Pepper, S. M. and Pittet-Cuénod, B. (2017). Reactive Oxygen Species and NOX Enzymes Are Emerging as Key Players in Cutaneous Wound Repair. *International Journal of Molecular Sciences* 18 (10).

Baggs, J. E., Price, T. S., DiTacchio, L., Panda, S., FitzGerald, G. A. and Hogenesch, J. B. (2009) Network features of the mammalian circadian clock. *PLoS biology* 7 (3), e1000052.

Bakken, P. C., Evans, V. J., Earle, W. R. and Stevenson, R. E. (1961) Establishment of a strain of human skin cells on chemically defined medium NCTC 109. *American Journal of Hygiene* 73, 96-104.

Balsalobre, A., Brown, S. A., Marcacci, L., Tronche, F., Kellendonk, C., Reichardt, H. M., Schütz, G. and Schibler, U. (2000) Resetting of circadian time in peripheral tissues by glucocorticoid signaling. *Science* 289 (5488), 2344-7.

Balsalobre, A., Damiola, F. and Schibler, U. (1998) A serum shock induces circadian gene expression in mammalian tissue culture cells. *Cell* 93 (6), 929-37.

Barron, L., Dooms, H., Hoyer, K. K., Kuswanto, W., Hofmann, J., O'Gorman, W. E. and Abbas, A. K. (2010) Cutting edge: mechanisms of IL-2-dependent maintenance of functional regulatory T cells. *Journal of Immunology* 185 (11), 6426-30.

Becker, A., Klapczynski, A., Kuch, N., Arpino, F., Simon-Keller, K., De La Torre, C., Sticht, C., van Abeelen, F. A., Oversluizen, G. and Gretz, N. (2016) Gene expression profiling reveals aryl hydrocarbon receptor as a possible target for photobiomodulation when using blue light. *Scientific Reports* 6, 33847.

Becker, D., Langer, E., Seemann, M., Seemann, G., Fell, I., Saloga, J., Grabbe, S. and von Stebut, E. (2011) Clinical Efficacy of Blue Light Full Body Irradiation as Treatment Option for Severe Atopic Dermatitis. *PLOS ONE* 6 (6), e20566.

Beckmann, K. H., Meyer-Hamme, G. and Schröder, S. (2014) Low level laser therapy for the treatment of diabetic foot ulcers: a critical survey. *Evid Based Complement Alternat Med* 2014, 626127.

Benegiamo, G., Brown, S. A. and Panda, S. (2016) RNA Dynamics in the Control of Circadian Rhythm. *Adv Exp Med Biol* 907, 107-22.

Besaratinia, A., Yoon, J.-i., Schroeder, C., Bradforth, S. E., Cockburn, M. and Pfeifer, G. P. (2011) Wavelength dependence of ultraviolet radiation-induced DNA damage as determined by laser irradiation suggests that cyclobutane pyrimidine dimers are the principal DNA lesions produced by terrestrial sunlight. *The FASEB Journal* 25 (9), 3079-3091.

Bjarnason, G. A., Jordan, R. C., Wood, P. A., Li, Q., Lincoln, D. W., Sothern, R. B., Hrushesky, W. J. and Ben-David, Y. (2001) Circadian expression of clock genes in human oral mucosa and skin: association with specific cell-cycle phases. *Am J Pathol* 158 (5), 1793-801.

Blanpain, C. and Fuchs, E. (2009) Epidermal homeostasis: a balancing act of stem cells in the skin. *Nat Rev Mol Cell Biol* 10 (3), 207-17.

Bolognia, J. L., Jorizzo, J. L. and Rapini, R. P. (2003) *Dermatology.* Edinburgh: Mosby Elviser.

Boulais, N. and Misery, L. (2008) The epidermis: a sensory tissue. *Eur J Dermatol* 18 (2), 119-127.

Boulnois, J.-L. (1986) Photophysical processes in recent medical laser developments: A review. *Lasers in Medical Science* 1 (1), 47-66.

Bourne, H. R. and Meng, E. C. (2000) Rhodopsin sees light. *Science* 289, 733-734.

Buhr, E. D. and Takahashi, J. S. (2013) Molecular components of the mammalian circadian clock. *Handbook of experimental pharmacology* (217), 3-27.

Burgeson, R. E. (1993) Type VII collagen, anchoring fibrils, and epidermolysis bullosa. *J Invest Dermatol* 101 (3), 252-5.

Burgess, L. P., Morin, G. V., Rand, M., Vossoughi, J. and Hollinger, J. O. (1990) Wound healing. Relationship of wound closing tension to scar width in rats. *Arch Otolaryngol Head Neck Surg* 116 (7), 798-802.

Buscone, S., Mardaryev, A. N., Raafs, B., Bikker, J. W., Sticht, C., Gretz, N., Farjo, N., Uzunbajakava, N. E. and Botchkareva, N. V. (2017) A new path in defining light parameters for hair growth: Discovery and modulation of photoreceptors in human hair follicle. *Lasers Surg Med*.

Chabert, R., Fouque, L., Pinacolo, S., Garcia-Gimenez, N., Bonnans, M., Cucumel, K. and Domloge, N. (2015) Evaluation of light-emitting diodes (LED) effect on skin biology (in vitro study). *Skin Res Technol*.

Chaves, I., Pokorny, R., Byrdin, M., Hoang, N., Ritz, T., Brettel, K., Essen, L.-O., van der Horst, G. T. J., Batschauer, A. and Ahmad, M. (2011) The Cryptochromes: Blue Light Photoreceptors in Plants and Animals. *Annual Review of Plant Biology* 62 (1), 335-364.

Chen, A. C., Arany, P. R., Huang, Y. Y., Tomkinson, E. M., Sharma, S. K., Kharkwal, G. B., Saleem, T., Mooney, D., Yull, F. E., Blackwell, T. S. and Hamblin, M. R. (2011) Low-level laser therapy activates NF-kB via generation of reactive oxygen species in mouse embryonic fibroblasts. *PLoS One* 6 (7), e22453.

Chung, H., Dai, T., Sharma, S. K., Huang, Y. Y., Carroll, J. D. and Hamblin, M. R. (2012) The nuts and bolts of low-level laser (light) therapy. *Ann Biomed Eng* 40 (2), 516-33.

Clayton, E., Doupe, D. P., Klein, A. M., Winton, D. J., Simons, B. D. and Jones, P. H. (2007) A single type of progenitor cell maintains normal epidermis. *Nature* 446 (7132), 185-189.

D'Orazio, J. and Wolf Horrell, E. (2014) UV-independent induction of beta defensin 3 in neonatal human skin explants. *F1000Research* 3.

Dahmardehei, M., Kazemikhoo, N., Vaghardoost, R., Mokmeli, S., Momeni, M., Nilforoushzadeh, M. A., Ansari, F. and Amirkhani, A. (2016) Effects of low level laser therapy on the prognosis of split-thickness skin graft in type 3 burn of diabetic patients: a case series. *Lasers in Medical Science* 31 (3), 497-502.

Dai, T., Gupta, A., Huang, Y.-Y., Yin, R., Murray, C. K., Vrahas, M. S., Sherwood, M. E., Tegos, G. P. and Hamblin, M. R. (2013) Blue light rescues mice from potentially fatal Pseudomonas aeruginosa burn infection: efficacy, safety, and mechanism of action. *Antimicrobial agents and chemotherapy* 57 (3), 1238-1245.

Dale, P. D., Sherratt, J. A. and Maini, P. K. (1996) A mathematical model for collagen fibre formation during foetal and adult dermal wound healing. *Proc Biol Sci* 263 (1370), 653-60.

Dana, H., Chalbatani, G. M., Mahmoodzadeh, H., Karimloo, R., Rezaiean, O., Moradzadeh, A., Mehmandoost, N., Moazzen, F., Mazraeh, A., Marmari, V., Ebrahimi, M., Rashno, M. M., Abadi, S. J. and Gharagouzlo, E. (2017) Molecular Mechanisms and Biological Functions of siRNA. *International Journal of Biomedical Science : IJBS* 13 (2), 48-57.

de Assis, L. V. M., Moraes, M. N., da Silveira Cruz-Machado, S. and Castrucci, A. M. L. (2016) The effect of white light on normal and malignant murine melanocytes: A link between opsins, clock genes, and melanogenesis. *Biochimica et Biophysica Acta (BBA) - Molecular Cell Research* 1863 (6, Part A), 1119-1133.

Dell'Orco, D. (2013) A physiological role for the supramolecular organization of rhodopsin and transducin in rod photoreceptors. *FEBS Lett* 587 (13), 2060-6.

Denda, M. and Fuziwara, S. (2008) Visible radiation affects epidermal permeability barrier recovery: selective effects of red and blue light. *J Invest Dermatol* 128 (5), 1335-6.

Diegelmann, R. F. and Evans, M. C. (2004) Wound healing: An overview of acute, fibrotic and delayed healing. *Frontiers in Bioscience* 9, 283-289.

Dignass, A. U., Becker, A., Spiegler, S. and Goebell, H. (1998) Adenine nucleotides modulate epithelial wound healing in vitro. *European journal of clinical investigation* 28, 554-561.

Do, M. T. H. and Yau, K.-W. (2010) Intrinsically Photosensitive Retinal Ganglion Cells. *Physiological Reviews* 90 (4), 1547.

Drake, M. T., Shenoy, S. K. and Lefkowitz, R. J. (2006) Trafficking of G protein-coupled receptors. *Circ Res* 99 (6), 570-82.

Ebrey, T. and Koutalos, Y. (2001) Vertebrate photoreceptors. *Prog Retin Eye Res* 20 (1), 49-94.

Eming, S. A., Krieg, T. and Davidson, J. M. (2007) Inflammation in wound repair: molecular and cellular mechanisms. *J Invest Dermatol* 127 (3), 514-25.

Foster, R. G. and Helfrich-Förster, C. (2001) The regulation of circadian clocks by light in fruitflies and mice. *Philos Trans R Soc Lond B Biol Sci* 356 (1415), 1779-89.

Fowler, J., Cohen, L. and Jarvis, P. (1998) *Practical statistics for field biology.* Second Edition edition*.* Chichester (United Kingdon): John Wiley & Sons.

Fuchs, E. and Raghavan, S. (2002) Getting under the skin of epidermal morphogenesis. *Nat Rev Genet* 3 (3), 199-209.

Fushimi, T., Inui, S., Nakajima, T., Ogasawara, M., Hosokawa, K. and Itami, S. (2012) Green light emitting diodes accelerate wound healing: characterization of the effect and its molecular basis in vitro and in vivo. *Wound Repair Regen* 20 (2), 226-35.

Garza, L. A., Yang, C.-C., Zhao, T., Blatt, H. B., Lee, M., He, H., Stanton, D. C., Carrasco, L., Spiegel, J. H., Tobias, J. W. and Cotsarelis, G. (2011) Bald scalp in men with androgenetic alopecia retains hair follicle stem cells but lacks CD200-rich and CD34-positive hair follicle progenitor cells. *The Journal of Clinical Investigation* 121 (2), 613-622.

Gauger, M. A. and Sancar, A. (2005) Cryptochrome, circadian cycle, cell cycle checkpoints, and cancer. *Cancer research* 65 (15), 6828-6834.

Geerligs, M. (2009) *Skin layer mechanics.* Eindhoven, The Netherlands: Philips Electronics N.V. .

Gelse, K., Poschl, E. and Aigner, T. (2003) Collagens--structure, function, and biosynthesis. *Adv Drug Deliv Rev* 55 (12), 1531-46.

GenScript (2002) *GenScript real-time PCR (TaqMan) primer design.* https://www.genscript.com/ssl-bin/app/primer. Accessed 8th September 2015.

Gether, U. (2000) Uncovering molecular mechanisms involved in activation of G protein-coupled receptors. *Endocr Rev* 21 (1), 90-113.

Geyfman, M. and Andersen, B. (2009) How the skin can tell time. *J Invest Dermatol* 129 (5), 1063-6.

Gibbs, J. E., Blaikley, J., Beesley, S., Matthews, L., Simpson, K. D., Boyce, S. H., Farrow, S. N., Else, K. J., Singh, D., Ray, D. W. and Loudon, A. S. (2012) The nuclear receptor REV-ERBalpha mediates circadian regulation of innate immunity through selective regulation of inflammatory cytokines. *Proc Natl Acad Sci U S A* 109 (2), 582-7.

Goto, M., Ikeyama, K., Tsutsumi, M., Denda, S. and Denda, M. (2011) Phosphodiesterase inhibitors block the acceleration of skin permeability barrier repair by red light. *Exp Dermatol* 20 (7), 568-71.

Griffiths, H. R., Gao, D. and Pararasa, C. (2017) Redox regulation in metabolic programming and inflammation. *Redox Biology* 12, 50-57.

Gröne, A. (2002) Keratinocytes and cytokines. *Veterinary Immunology and Immunopathology* 88 (1), 1-12.

Guest, J. F., Ayoub, N., McIlwraith, T., Uchegbu, I., Gerrish, A., Weidlich, D., Vowden, K. and Vowden, P. (2017) Health economic burden that different wound types impose on the UK's National Health Service. *Int Wound J* 14 (2), 322-330.

Haas, A. F., Isseroff, R. R., Wheeland, R. G., Rood, P. A. and Graves, P. J. (1990) Low-energy helium-neon laser irradiation increases the motility of cultured human keratinocytes. *J Invest Dermatol* 94 (6), 822-6.

Haensel, D. and Dai, X. (2017) Epithelial-to-mesenchymal transition in cutaneous wound healing: Where we are and where we are heading. *Dev Dyn*.

Haltaufderhyde, K., Ozdeslik, R. N., Wicks, N. L., Najera, J. A. and Oancea, E. (2015) Opsin expression in human epidermal skin. *Photochem Photobiol* 91 (1), 117-23.

Hamblin, M. R. (2017) Mechanisms and applications of the anti-inflammatory effects of photobiomodulation. *AIMS Biophysics* 4 (3), 337-361.

Hamblin, M. R. and Demidova, T. N. (2006) Mechanisms of low level light therapy. Vol. 6140.

Hamblin, M. R., Hamblin, M. R., Demidova, T. N., Waynant, R. W. and Anders, J. (2006) Mechanisms of low level light therapy. Vol. 6140.

Hankins, M. W., Peirson, S. N. and Foster, R. G. (2008) Melanopsin: an exciting photopigment. *Trends Neurosci* 31 (1), 27-36.

Hawkins, D., Houreld, N. and Abrahamse, H. (2005) Low level laser therapy (LLLT) as an effective therapeutic modality for delayed wound healing. *Ann N Y Acad Sci* 1056, 486-93.

Hirota, T., Lee, J. W., Lewis, W. G., Zhang, E. E., Breton, G., Liu, X., Garcia, M., Peters, E. C., Etchegaray, J. P., Traver, D., Schultz, P. G. and Kay, S. A. (2010) High-throughput chemical screen identifies a novel potent modulator of cellular circadian rhythms and reveals CKIα as a clock regulatory kinase. *PLoS Biol* 8 (12), e1000559.

Hirota, T., Lee, J. W., St John, P. C., Sawa, M., Iwaisako, K., Noguchi, T., Pongsawakul, P. Y., Sonntag, T., Welsh, D. K., Brenner, D. A., Doyle, F. J., 3rd, Schultz, P. G. and Kay, S. A. (2012) Identification of small molecule activators of cryptochrome. *Science* 337 (6098), 1094-7.

Hoang, N., Schleicher, E., Kacprzak, S., Bouly, J. P., Picot, M., Wu, W., Berndt, A., Wolf, E., Bittl, R. and Ahmad, M. (2008) Human and Drosophila cryptochromes are light activated by flavin photoreduction in living cells. *PLoS Biol* 6 (7), e160.

Houreld, N. and Abrahamse, H. (2010) Low-intensity laser irradiation stimulates wound healing in diabetic wounded fibroblast cells (WS1). *Diabetes Technol Ther* 12 (12), 971-8.

Hsu, D. S., Zhao, X., Zhao, S., Kazantsev, A., Wang, R.-P., Todo, T., Wei, Y.-F. and Sancar, A. (1996) Putative Human Blue-Light Photoreceptors hCRY1 and hCRY2 Are Flavoproteins†. *Biochemistry* 35 (44), 13871-13877.

Hsu, Y. C., Li, L. and Fuchs, E. (2014) Emerging interactions between skin stem cells and their niches. *Nat Med* 20 (8), 847-56.

Huang, Y. Y., Chen, A. C., Carroll, J. D. and Hamblin, M. R. (2009) Biphasic dose response in low level light therapy. *Dose Response* 7 (4), 358-83.

Hughey, J. J. and Butte, A. J. (2016) Differential Phasing between Circadian Clocks in the Brain and Peripheral Organs in Humans. *Journal of Biological Rhythms* 31 (6), 588-597.

Jahoda, C. A. B. and Reynolds, A. J. Hair follicle dermal sheath cells: unsung participants in wound healing. *The Lancet* 358 (9291), 1445-1448.

Jahoda, C. A. B. and Reynolds, A. J. (2001) Hair follicle dermal sheath cells: unsung participants in wound healing. *The Lancet* 358 (9291), 1445-1448.

Janich, P., Toufighi, K., Solanas, G., Luis, N. M., Minkwitz, S., Serrano, L., Lehner, B. and Benitah, S. A. (2013) Human epidermal stem cell function is regulated by circadian oscillations. *Cell Stem Cell* 13 (6), 745-53.

Janson, D., Saintigny, G., Mahe, C. and El Ghalbzouri, A. (2013) Papillary fibroblasts differentiate into reticular fibroblasts after prolonged in vitro culture. *Exp Dermatol* 22 (1), 48-53.

Janson, D. G., Saintigny, G., van Adrichem, A., Mahé, C. and El Ghalbzouri, A. (2012) Different gene expression patterns in human papillary and reticular fibroblasts. *J Invest Dermatol* 132 (11), 2565-72.

Jimenez, J. J., Wikramanayake, T. C., Bergfeld, W., Hordinsky, M., Hickman, J. G., Hamblin, M. R. and Schachner, L. A. (2014) Efficacy and safety of a low-level laser device in the treatment of male and female pattern hair loss: a multicenter, randomized, sham device-controlled, double-blind study. *Am J Clin Dermatol* 15 (2), 115-27.

Jones, P. H. and Watt, F. M. (1993) Separation of human epidermal stem cells from transit amplifying cells on the basis of differences in integrin function and expression. *Cell* 73 (4), 713-724.

Kahari, V. M., Hakkinen, L., Westermarck, J. and Larjava, H. (1995) Differential regulation of decorin and biglycan gene expression by dexamethasone and retinoic acid in cultured human skin fibroblasts. *J Invest Dermatol* 104 (4), 503-8.

Kajagar, B. M., Godhi, A. S., Pandit, A. and Khatri, S. (2012) Efficacy of low level laser therapy on wound healing in patients with chronic diabetic foot ulcers-a randomised control trial. *Indian J Surg* 74 (5), 359-63.

Kalluri, R. and Neilson, E. G. (2003) Epithelial-mesenchymal transition and its implications for fibrosis. *Journal of Clinical Investigation* 112 (12), 1776-1784.

Kalluri, R. and Weinberg, R. A. (2009) The basics of epithelial-mesenchymal transition. *J Clin Invest* 119 (6), 1420-8.

Karu, T. (1999) Primary and secondary mechanisms of action of visible to near-IR radiation on cells. *J Photochem Photobiol B.* Vol. 49. Switzerland: 1-17.

Karu, T. I. and Kolyakov, S. F. (2005) Exact action spectra for cellular responsesrelevant to phototherapy. *Photomedicine and Laser Surgery* 23 (4), 355-361.

Katayama, S., Skoog, T., Jouhilahti, E. M., Siitonen, H. A., Nuutila, K., Tervaniemi, M. H., Vuola, J., Johnsson, A., Lonnerberg, P., Linnarsson, S., Elomaa, O., Kankuri, E. and Kere, J. (2015) Gene expression analysis of skin grafts and cultured keratinocytes using synthetic RNA normalization reveals insights into differentiation and growth control. *BMC Genomics* 16, 476.

Kendall, A. C. and Nicolaou, A. (2013) Bioactive lipid mediators in skin inflammation and immunity. *Progress in Lipid Research* 52 (1), 141-164.
Khan, I. and Arany, P. (2015) Biophysical Approaches for Oral Wound Healing: Emphasis on Photobiomodulation. *Adv Wound Care (New Rochelle)* 4 (12), 724-737.
Kibbe, W. A. (2007) OligoCalc: an online oligonucleotide properties calculator. *Nucleic Acids Research* 35 (suppl 2), W43-W46.
Kim, H. J., Son, E. D., Jung, J. Y., Choi, H., Lee, T. R. and Shin, D. W. (2013) Violet light down-regulates the expression of specific differentiation markers through Rhodopsin in normal human epidermal keratinocytes. *PLoS One* 8 (9).
Kishimoto, J., Burgeson, R. E. and Morgan, B. A. (2000) Wnt signaling maintains the hair-inducing activity of the dermal papilla. *Genes Dev* 14 (10), 1181-5.
Kleinpenning, M. M., Otero, M. E., van Erp, P. E., Gerritsen, M. J. and van de Kerkhof, P. C. (2012) Efficacy of blue light vs. red light in the treatment of psoriasis: a double-blind, randomized comparative study. *J Eur Acad Dermatol Venereol* 26 (2), 219-25.
Kleinpenning, M. M., Smits, T., Frunt, M. H. A., Van Erp, P. E. J., Van De Kerkhof, P. C. M. and Gerritsen, R. M. J. P. (2010) Clinical and histological effects of blue light on normal skin. *Photodermatology, Photoimmunology & Photomedicine* 26 (1), 16-21.
Koh, T. J. and DiPietro, L. A. (2011) Inflammation and wound healing: the role of the macrophage. *Expert Rev Mol Med* 13, e23.
Koivisto, L., Heino, J., Häkkinen, L. and Larjava, H. (2014) Integrins in Wound Healing. *Advances in wound care* 3 (12), 762-783.
Kojima, D., Mori, S., Torii, M., Wada, A., Morishita, R. and Fukada, Y. (2011) UV-Sensitive Photoreceptor Protein OPN5 in Humans and Mice. *PLoS ONE* 6 (10), e26388.
Kowalska, E., Ripperger, J. A., Hoegger, D. C., Bruegger, P., Buch, T., Birchler, T., Mueller, A., Albrecht, U., Contaldo, C. and Brown, S. A. (2013) NONO couples the circadian clock to the cell cycle. *Proc Natl Acad Sci U S A* 110 (5), 1592-9.
Koyanagi, M., Takada, E., Nagata, T., Tsukamoto, H. and Terakita, A. (2013) Homologs of vertebrate Opn3 potentially serve as a light sensor in nonphotoreceptive tissue. *Proc Natl Acad Sci U S A* 110 (13), 4998-5003.
Koyanagi, M. and Terakita, A. (2008) Gq-coupled rhodopsin subfamily composed of invertebrate visual pigment and melanopsin. *Photochem Photobiol* 84 (4), 1024-30.
Koyanagi, S., Hamdan, A. M., Horiguchi, M., Kusunose, N., Okamoto, A., Matsunaga, N. and Ohdo, S. (2011) cAMP-response element (CRE)-mediated transcription by activating transcription factor-4 (ATF4) is essential for circadian expression of the Period2 gene. *J Biol Chem* 286 (37), 32416-23.
Kurabayashi, N., Hirota, T., Sakai, M., Sanada, K. and Fukada, Y. (2010) DYRK1A and Glycogen Synthase Kinase 3β, a Dual-Kinase Mechanism

Directing Proteasomal Degradation of CRY2 for Circadian Timekeeping. *Molecular and Cellular Biology* 30 (7), 1757-1768.
Kurreck, J. (2006) siRNA efficiency: structure or sequence—that is the question. *BioMed Research International* 2006.
Landen, N. X., Li, D. and Stahle, M. (2016) Transition from inflammation to proliferation: a critical step during wound healing. *Cell Mol Life Sci* 73 (20), 3861-85.
Lanzafame, R. J., Stadler, I., Kurtz, A. F., Connelly, R., Peter, T. A., Sr., Brondon, P. and Olson, D. (2007) Reciprocity of exposure time and irradiance on energy density during photoradiation on wound healing in a murine pressure ulcer model. *Lasers Surg Med* 39 (6), 534-42.
Lavker, R. M. and Sun, T. (1982) Heterogeneity in epidermal basal keratinocytes: morphoogical and functional correlations. *Science* 215, 1239-1241.
Lebonvallet, N., Jeanmaire, C., Danoux, L., Sibille, P., Pauly, G. and Misery, L. (2010) The evolution and use of skin explants: potential and limitations for dermatological research. *Eur J Dermatol* 20 (6), 671-84.
Levy, V., Lindon, C., Zheng, Y., Harfe, B. D. and Morgan, B. A. (2007) Epidermal stem cells arise from the hair follicle after wounding. *FASEB J* 21 (7), 1358-66.
Liang, C. C., Park, A. Y. and Guan, J. L. (2007) In vitro scratch assay: a convenient and inexpensive method for analysis of cell migration in vitro. *Nat Protoc* 2 (2), 329-33.
Liebmann, J., Born, M. and Kolb-Bachofen, V. (2010) Blue-light irradiation regulates proliferation and differentiation in human skin cells. *J Invest Dermatol* 130 (1), 259-69.
Lipovsky, A., Nitzan, Y., Gedanken, A. and Lubart, R. (2010) Visible light-induced killing of bacteria as a function of wavelength: Implication for wound healing. *Lasers in surgery and medicine* 42 (6), 467-472.
Lippert, J., Halfter, H., Heidbreder, A., Röhr, D., Gess, B., Boentert, M., Osada, N. and Young, P. (2014) Altered dynamics in the circadian oscillation of clock genes in dermal fibroblasts of patients suffering from idiopathic hypersomnia. *PLoS One* 9 (1), e85255.
Lister, T., Wright, P. A. and Chappell, P. H. (2012) Optical properties of human skin. *J Biomed Opt* 17 (9), 90901-1.
Lockwood, D. B., Wataha, J. C., Lewis, J. B., Tseng, W. Y., Messer, R. L. W. and Hsu, S. D. (2005) Blue light generates reactive oxygen species (ROS) differentially in tumor vs. normal epithelial cells. *Dental Materials* 21 (7), 683-688.
Lowrey, P. L. and Takahashi, J. S. (2011) Genetics of Circadian Rhythms in Mammalian Model Organisms. *Advances in genetics* 74, 175-230.
Lucas, R. J. and Foster, R. G. (1999) Photoentrainment in mammals: a role for cryptochrome? *J Biol Rhythms* 14 (1), 4-10.
Mackenzie, I. C. (1970) Relationship between mitosis and the ordered structure of the stratum corneum in mouse epidermis. *Nature* 226, 653-655.
Magalhaes, A. C., Dunn, H. and Ferguson, S. S. G. (2012) Regulation of GPCR activity, trafficking and localization by GPCR-interacting proteins. *British Journal of Pharmacology* 165 (6), 1717-1736.

Mahmoud, B. H., Hexsel, C. L., Hamzavi, I. H. and Lim, H. W. (2008) Effect of visible light on the skin. *Photochemistry and Photobiology* 84, 450–462.

Majid, M. A., Smith, V. A., Easty, D. L., Baker, A. H. and Newby, A. C. (2002) Sorsby's fundus dystrophy mutant tissue inhibitors of metalloproteinase-3 induce apoptosis of retinal pigment epithelial and MCF-7 cells. *FEBS letters* 529 (2-3), 281-285.

Mamalis, A., Garcha, M. and Jagdeo, J. (2015a) Light Emitting Diode-Generated Blue Light Modulates Fibrosis Characteristics: Fibroblast Proliferation, Migration Speed, and Reactive Oxygen Species Generation. *Lasers in surgery and medicine* 47 (2), 210-215.

Mamalis, A., Koo, E., Isseroff, R. R., Murphy, W. and Jagdeo, J. (2015b) Resveratrol Prevents High Fluence Red Light-Emitting Diode Reactive Oxygen Species-Mediated Photoinhibition of Human Skin Fibroblast Migration. *PLoS ONE* 10 (10), e0140628.

Martin, P. (1997) Wound Healing--Aiming for Perfect Skin Regeneration. *Science* 276 (5309), 75-81.

Mascre, G., Dekoninck, S., Drogat, B., Youssef, K. K., Brohee, S., Sotiropoulou, P. A., Simons, B. D. and Blanpain, C. (2012) Distinct contribution of stem and progenitor cells to epidermal maintenance. *Nature* 489 (7415), 257-62.

Masson-Meyers, D. S., Bumah, V. V. and Enwemeka, C. S. (2016) Blue light does not impair wound healing in vitro. *J Photochem Photobiol B* 160, 53-60.

Matsui, M. S., Pelle, E., Dong, K. and Pernodet, N. (2016) Biological Rhythms in the Skin. *Int J Mol Sci* 17 (6).

May, L. T., Leach, K., Sexton, P. M. and Christopoulos, A. (2007) Allosteric modulation of G Protein-Coupled Receptors *Annual review of pharmacology and toxicology* 47, 1-51.

Mendoza-Garcia, J., Sebastian, A., Alonso-Rasgado, T. and Bayat, A. (2015) Optimization of an ex vivo wound healing model in the adult human skin: Functional evaluation using photodynamic therapy. *Wound Repair Regen* 23 (5), 685-702.

Mignon, C., Botchkareva, N. V., Uzunbajakava, N. E. and Tobin, D. J. (2016) Photobiomodulation devices for hair regrowth and wound healing: a therapy full of promise but a literature full of confusion. *Exp Dermatol* 25 (10), 745-9.

Mignon, C., Uzunbajakava, N. E., Raafs, B., Botchkareva, N. V. and Tobin, D. J. (2017) Photobiomodulation of human dermal fibroblasts in vitro: decisive role of cell culture conditions and treatment protocols on experimental outcome. *Sci Rep* 7 (1), 2797.

Minatel, D. G., Frade, M. A., França, S. C. and Enwemeka, C. S. (2009) Phototherapy promotes healing of chronic diabetic leg ulcers that failed to respond to other therapies. *Lasers Surg Med* 41 (6), 433-41.

Montagna, W., Kligman, A. M. and Carlisle, K. S. (1992) *Atlas of normal human skin.* Springer

Morshedian, A. and Fain, G. L. (2017) Light adaptation and the evolution of vertebrate photoreceptors. *J Physiol* 595 (14), 4947-4960.

Motzkus, D., Loumi, S., Cadenas, C., Vinson, C., Forssmann, W. G. and Maronde, E. (2007) Activation of human period-1 by PKA or CLOCK/BMAL1 is conferred by separate signal transduction pathways. *Chronobiol Int* 24 (5), 783-92.

Nakashima, Y., Ohta, S. and Wolf, A. M. (2017) Blue light-induced oxidative stress in live skin. *Free Radical Biology and Medicine* 108, 300-310.

O'Neill, J. S., Maywood, E. S., Chesham, J. E., Takahashi, J. S. and Hastings, M. H. (2008) cAMP-dependent signaling as a core component of the mammalian circadian pacemaker. *Science* 320 (5878), 949-53.

Oh, P. S., Kim, H. S., Kim, E. M., Hwang, H., Ryu, H. H., Lim, S., Sohn, M. H. and Jeong, H. J. (2017) Inhibitory effect of blue light emitting diode on migration and invasion of cancer cells. *J Cell Physiol*.

Oplander, C., Deck, A., Volkmar, C. M., Kirsch, M., Liebmann, J., Born, M., van Abeelen, F., van Faassen, E. E., Kroncke, K. D., Windolf, J. and Suschek, C. V. (2013) Mechanism and biological relevance of blue-light (420-453 nm)-induced nonenzymatic nitric oxide generation from photolabile nitric oxide derivates in human skin in vitro and in vivo. *Free Radic Biol Med* 65, 1363-77.

Oplander, C., Hidding, S., Werners, F. B., Born, M., Pallua, N. and Suschek, C. V. (2011) Effects of blue light irradiation on human dermal fibroblasts. *J Photochem Photobiol B* 103 (2), 118-25.

Opländer , C., Deck, A., Volkmar, C. M., Kirsch, M., Liebmann, J., Born, M., van Abeelen, F., van Faassen, E. E., Kroncke, K. D., Windolf, J. and Suschek, C. V. (2013) Mechanism and biological relevance of blue-light (420-453 nm)-induced nonenzymatic nitric oxide generation from photolabile nitric oxide derivates in human skin in vitro and in vivo. *Free Radical Biology and Medicine* 65, 1363-77.

Opländer, C., Hidding, S., Werners, F. B., Born, M., Pallua, N. and Suschek, C. V. (2011) Effects of blue light irradiation on human dermal fibroblasts. *Journal of Photochemistry and Photobiology B: Biology* 103 (2), 118-125.

Panda, S., Sato, T. K., Castrucci, A. M., Rollag, M. D., DeGrip, W. J., Hogenesch, J. B., Provencio, I. and Kay, S. A. (2002) Melanopsin (Opn4) requirement for normal light-induced circadian phase shifting. *Science* 298 (5601), 2213-6.

Park, G.-H., Chang, S. E., Bang, S., Won, K. H., Won, C. H., Lee, M. W., Choi, J. H. and Moon, K. C. (2015) Usefulness of Skin Explants for Histologic Analysis after Fractional Photothermolysis. *Annals of Dermatology* 27 (3), 283-290.

Pastar, I., Stojadinovic, O., Yin, N. C., Ramirez, H., Nusbaum, A. G., Sawaya, A., Patel, S. B., Khalid, L., Isseroff, R. R. and Tomic-Canic, M. (2014) Epithelialization in Wound Healing: A Comprehensive Review. *Adv Wound Care (New Rochelle).* Vol. 3. United States: 445-464.

Patel, G. K., Wilson, C. H., Harding, K. G., Finlay, A. Y. and Bowden, P. E. (2006) Numerous Keratinocyte Subtypes Involved in Wound Re-Epithelialization. *Journal of Investigative Dermatology* 126 (2), 497-502.

Pfaff, S., Liebmann, J., Born, M., Merk, H. F. and von Felbert, V. (2015) Prospective Randomized Long-Term Study on the Efficacy and Safety of

UV-Free Blue Light for Treating Mild Psoriasis Vulgaris. *Dermatology* 231 (1), 24-34.
Pierce, K. L., Premont, R. T. and Lefkowitz, R. J. (2002) Seven-transmembrane receptors. *Nature reviews molecular cell biology* 3, 639-650.
Plikus, M. V., Van Spyk, E. N., Pham, K., Geyfman, M., Kumar, V., Takahashi, J. S. and Andersen, B. (2015) The Circadian Clock in Skin: Implications for Adult Stem Cells, Tissue Regeneration, Cancer, Aging, and Immunity. *J Biol Rhythms*.
Poletini, M. O., Ramos, B. C., Moraes, M. N. and Castrucci, A. M. (2015) Nonvisual Opsins and the Regulation of Peripheral Clocks by Light and Hormones. *Photochem Photobiol* 91 (5), 1046-55.
Pomari, E., Dalla Valle, L., Pertile, P., Colombo, L. and Thornton, M. J. (2015) Intracrine sex steroid synthesis and signaling in human epidermal keratinocytes and dermal fibroblasts. *FASEB J.* Vol. 29. United States: Faseb. 508-24.
Posten, W., Wrone, D. A., Dover, J. S., Arndt, K. A., Silapunt, S. and Alam, M. (2005) Low-level laser therapy for wound healing: mechanism and efficacy. *Dermatol Surg* 31 (3), 334-40.
Potten, C. S. (1974) The epidermal proliferative unit: the possible role of the central basal cell. *Cell Tissue Kinet* 7 (1), 77-88.
Poyton, R. O. and Ball, K. A. (2011) Therapeutic photobiomodulation: nitric oxide and a novel function of mitochondrial cytochrome c oxidase. *Discovery medicine* 11 (57), 154-159.
Prindeze, N. J., Moffatt, L. T. and Shupp, J. W. (2012) Mechanisms of action for light therapy: a review of molecular interactions. *Exp Biol Med (Maywood)* 237 (11), 1241-8.
QUIAGEN (2012) *RNeasy Mini Handbook.* https://www.qiagen.com/gb/resources/resourcedetail?id=14e7cf6e-521a-4cf7-8cbc-bf9f6fa33e24 Accessed 8th September 2015.
Rampersad, S. N. (2012) Multiple Applications of Alamar Blue as an Indicator of Metabolic Function and Cellular Health in Cell Viability Bioassays. *Sensors* 12 (9).
Regazzetti, C., Sormani, L., Debayle, D., Bernerd, F., Tulic, M. K., De Donatis, G. M., Chignon-Sicard, B., Rocchi, S. and Passeron, T. (2017) Melanocytes sense blue light and regulate pigmentation through the Opsin3. *J Invest Dermatol*.
Richmond, J. M. and Harris, J. E. (2014) Immunology and Skin in Health and Disease. *Cold Spring Harbor Perspectives in Medicine* 4 (12), a015339.
Rizzo, A. E., Beckett, L. A., Baier, B. S. and Isseroff, R. R. (2012) The linear excisional wound: an improved model for human ex vivo wound epithelialization studies. *Skin Res Technol* 18 (1), 125-32.
Rockey, D. C., Weymouth, N. and Shi, Z. (2013) Smooth muscle α actin (Acta2) and myofibroblast function during hepatic wound healing. *PLoS One* 8 (10), e77166.
Romani, N., Clausen, B. E. and Stoitzner, P. (2010) Langerhans cells and more: langerin-expressing dendritic cell subsets in the skin. *Immunological Reviews* 234 (1), 120-141.

Sancar, A. (2000) Cryptochrome: The Second Photoactive Pigment in The Eye and Its Role in Circadian Photoreception. *Annual Review of Biochemistry* 69 (1), 31-67.

Sandu, C., Dumas, M., Malan, A., Sambakhe, D., Marteau, C., Nizard, C., Schnebert, S., Perrier, E., Challet, E., Pévet, P. and Felder-Schmittbuhl, M. P. (2012) Human skin keratinocytes, melanocytes, and fibroblasts contain distinct circadian clock machineries. *Cell Mol Life Sci* 69 (19), 3329-39.

Schneider, M. R., Schmidt-Ullrich, R. and Paus, R. (2008) The hair follicle as a dynamic miniorgan. *Current biology* 19 (3), R132-R142.

Schäfer, M. and Werner, S. (2008) Oxidative stress in normal and impaired wound repair. *Pharmacological Research* 58 (2), 165-171.

Seery, J. P. and Watt, F. M. (2000) Asymmetric stem-cell divisions define the architecture of human oesophageal epithelium. *Curr Biol* 10 (22), 1447-50.

Senoo, M. (2013) Epidermal Stem Cells in Homeostasis and Wound Repair of the Skin. *Adv Wound Care (New Rochelle)* 2 (6), 273-282.

Sharma, R., Fu, S. M. and Ju, S.-T. (2011) IL-2: a two-faced master regulator of autoimmunity. *Journal of autoimmunity* 36 (2), 91-97.

Shaw, T. J. and Martin, P. (2016) Wound repair: a showcase for cell plasticity and migration. *Current Opinion in Cell Biology* 42 (Supplement C), 29-37.

Shi, S.-q., Ansari, T., McGuinness, O. P., Wasserman, D. H. and Johnson, C. H. (2013) Circadian disruption leads to insulin resistance and obesity. *Current biology : CB* 23 (5), 372-381.

Sikka, G., Hussmann, G. P., Pandey, D., Cao, S., Hori, D., Park, J. T., Steppan, J., Kim, J. H., Barodka, V., Myers, A. C., Santhanam, L., Nyhan, D., Halushka, M. K., Koehler, R. C., Snyder, S. H., Shimoda, L. A. and Berkowitz, D. E. (2014) Melanopsin mediates light-dependent relaxation in blood vessels. *Proceedings of the National Academy of Sciences of the United States of America* 111 (50), 17977-17982.

Singh, S. K., Kurfurst, R., Nizard, C., Schnebert, S., Perrier, E. and Tobin, D. J. (2010) Melanin transfer in human skin cells is mediated by filopodia—a model for homotypic and heterotypic lysosome-related organelle transfer. *The FASEB Journal* 24 (10), 3756-3769.

Slominski, A., Tobin, D. J., Shibahara, S. and Wortsman, J. (2004) Melanin pigmentation in mammalian skin and its hormonal regulation. *Physiol Rev* 84 (4), 1155-228.

Sorg, H., Tilkorn, D. J., Hager, S., Hauser, J. and Mirastschijski, U. (2017) Skin Wound Healing: An Update on the Current Knowledge and Concepts. *European Surgical Research* 58 (1-2), 81-94.

Spörl, F., Schellenberg, K., Blatt, T., Wenck, H., Wittern, K.-P., Schrader, A. and Kramer, A. (2011) A Circadian Clock in HaCaT Keratinocytes. *Journal of Investigative Dermatology* 131 (2), 338-348.

St John, P. C., Hirota, T., Kay, S. A. and Doyle, F. J., 3rd (2014) Spatiotemporal separation of PER and CRY posttranslational regulation in the mammalian circadian clock. *Proc Natl Acad Sci U S A* 111 (5), 2040-5.

Stadelmann, W. K., Digenis, A. G. and Tobin, G. R. (1998) Physiology and healing dynamics of chronic cutaneous wounds. *The American Journal of Surgery* 176 (2, Supplement 1), 26S-38S.

Stenn, K. S. and Paus, R. (2001) Controls of hair follicle cycling. *Physiol Rev* 81 (1), 449-494.

Stephens, P., Caley, M. and Peake, M. (2013) Alternatives for Animal Wound Model Systems. In Gourdie, R. G. and Myers, T. A. (editors) *Wound Regeneration and Repair: Methods and Protocols.* Totowa, NJ: Humana Press. 177-201. https://doi.org/10.1007/978-1-62703-505-7_10

Stojadinovic, O. and Tomic-Canic, M. (2013) Human ex vivo wound healing model. *Methods Mol Biol* 1037, 255-64.

Strader, C. D., Fong, T. M., Graziano, M. P. and Tota, M. R. (1995) The family of G-protein-coupled receptors. *The FASEB Journal* 9 (9), 745-754.

Sun, T. T., Eichner, R., Nelson, W. G., Tseng, S. C., Weiss, R. A., Jarvinen, M. and Woodcock-Mitchell, J. (1983) Keratin classes: molecular markers for different types of epithelial differentiation. *J Invest Dermatol* 81 (1 Suppl), 109s-15s.

Syrovatkina, V., Alegre, K. O., Dey, R. and Huang, X. Y. (2016) Regulation, Signaling, and Physiological Functions of G-Proteins. *J Mol Biol* 428 (19), 3850-68.

Taflinski, L., Demir, E., Kauczok, J., Fuchs, P. C., Born, M., Suschek, C. V. and Oplander, C. (2014) Blue light inhibits transforming growth factor-beta1-induced myofibroblast differentiation of human dermal fibroblasts. *Exp Dermatol* 23 (4), 240-6.

Tanaka, T., Narisawa, Y., Misago, N. and Hashimoto, K. (1998) The innermost cells of the outer root sheath in human anagen hair follicles undergo specialized keratinization mediated by apoptosis. *J Cutan Pathol* 25 (6), 316-21.

Tarafder, A. K., Bolasco, G., Correia, M. S., Pereira, F. J., Iannone, L., Hume, A. N., Kirkpatrick, N., Picardo, M., Torrisi, M. R., Rodrigues, I. P., Ramalho, J. S., Futter, C. E., Barral, D. C. and Seabra, M. C. (2014) Rab11b mediates melanin transfer between donor melanocytes and acceptor keratinocytes via coupled exo/endocytosis. *J Invest Dermatol* 134 (4), 1056-66.

Terakita, A. (2005) The opsins. *Genome Biology* 6 (3), 213-213.

Toh, P. P., Bigliardi-Qi, M., Yap, A. M., Sriram, G. and Bigliardi, P. (2016) Expression of peropsin in human skin is related to phototransduction of violet light in keratinocytes. *Exp Dermatol* 25 (12), 1002-1005.

Tsutsumi, M., Ikeyama, K., Denda, S., Nakanishi, J., Fuziwara, S., Aoki, H. and Denda, M. (2009) Expressions of rod and cone photoreceptor-like proteins in human epidermis. *Exp Dermatol* 18 (6), 567-70.

Vauquelin, G. and Van Liefde, I. (2005) G protein-coupled receptors: a count of 1001 conformations. *Fundamental & Clinical Pharmacology* 19 (1), 45-56.

Velnar, T., Bailey, T. and Smrkolj, V. (2009) The Wound Healing Process: An Overview of the Cellular and Molecular Mechanisms. *Journal of International Medical Research* 37 (5), 1528-1542.

Vitaterna, M. H., Selby, C. P., Todo, T., Niwa, H., Thompson, C., Fruechte, E. M., Hitomi, K., Thresher, R. J., Ishikawa, T., Miyazaki, J., Takahashi, J. S. and Sancar, A. (1999) Differential regulation of mammalian period genes and circadian rhythmicity by cryptochromes 1 and 2. *Proc Natl Acad Sci U S A* 96 (21), 12114-9.

Wanet, A., Arnould, T., Najimi, M. and Renard, P. (2015) Connecting Mitochondria, Metabolism, and Stem Cell Fate. *Stem Cells and Development* 24 (17), 1957-1971.

Wang, Y., Huang, Y. Y., Lyu, P. and Hamblin, M. R. (2016) Photobiomodulation (blue and green light) encourages osteoblastic-differentiation of human adipose-derived stem cells: role of intracellular calcium and light-gated ion channels. *Sci Rep* 6, 33719.

Waugh, A. and Grant, A. (2010) *Anatomy and physiology in health and ilness.* 11th edition. Edinburgh: Churchill Livingstone Elsevier.

Webb, A. R. (2006) Who, what, where and when-influences on cutaneous vitamin D synthesis. *Prog Biophys Mol Biol* 92 (1), 17-25.

Webb, C. and Dyson, M. (2003) The effect of 880 nm low level laser energy on human fibroblast cell numbers: a possible role in hypertrophic wound healing. *Journal of Photochemistry and Photobiology B: Biology* 70 (1), 39-44.

Webb, C., Dyson, M. and Lewis, W. H. P. (1998) Stimulatory Effect of 660 nm Low Level Laser Energy on Hypertrophic Scar-derived Fibroblasts: Possible Mechanisms for Increase in Cell Counts. *Lasers in Surgery and Medicine* 22, 294-301.

Weinstabl, A., Hoff-Lesch, S., Merk, H. F. and von Felbert, V. (2011) Prospective randomized study on the efficacy of blue light in the treatment of psoriasis vulgaris. *Dermatology* 223 (3), 251-9.

Werner, S., Krieg, T. and Smola, H. (2007) Keratinocyte–fibroblast interactions in wound healing. *Journal of Investigative Dermatology* 127 (5), 998-1008.

White, J. H., Chiano, M., Wigglesworth, M., Geske, R., Riley, J., White, N., Hall, S., Zhu, G., Maurio, F., Savage, T., Anderson, W., Cordy, J., Ducceschi, M., Vestbo, J. and Pillai, S. G. (2008) Identification of a novel asthma susceptibility gene on chromosome 1qter and its functional evaluation. *Hum Mol Genet* 17 (13), 1890-903.

Whiting, D. A. (2004) *The structure of the human hair follicle. Light microscopy of vertical and horizontal sections of scalp biopsies.* Fairfield: Pfizer Inc.

Wicks, N. L., Chan, J. W., Najera, J. A., Ciriello, J. M. and Oancea, E. (2011) UVA phototransduction drives early melanin synthesis in human melanocytes. *Curr Biol* 21 (22), 1906-11.

Wong-Riley, M. T., Liang, H. L., Eells, J. T., Chance, B., Henry, M. M., Buchmann, E., Kane, M. and Whelan, H. T. (2005) Photobiomodulation directly benefits primary neurons functionally inactivated by toxins: role of cytochrome c oxidase. *J Biol Chem* 280 (6), 4761-71.

Xue, Y., Liu, P., Wang, H., Xiao, C., Lin, C., Liu, J., Dong, D., Fu, T., Yang, Y., Wang, Z., Pan, H., Chen, J., Li, Y., Cai, D. and Li, Z. (2017) Modulation of Circadian Rhythms Affects Corneal Epithelium Renewal and Repair in Mice. *Invest Ophthalmol Vis Sci* 58 (3), 1865-1874.

Yadav, A. and Gupta, A. (2017) Noninvasive red and near-infrared wavelength-induced photobiomodulation: promoting impaired cutaneous wound healing. *Photodermatology Photoimmunology and Photomedicine* 33 (1), 4-13.

Yamashita, T., Ohuchi, H., Tomonari, S., Ikeda, K., Sakai, K. and Shichida, Y. (2010) Opn5 is a UV-sensitive bistable pigment that couples with Gi subtype of G protein. *Proc Natl Acad Sci U S A* 107 (51), 22084-9.

Ye, J., Coulouris, G., Zaretskaya, I., Cutcutache, I., Rozen, S. and Madden, T. L. (2012) Primer-BLAST: a tool to design target-specific primers for polymerase chain reaction. *BMC Bioinformatics* 13, 134.

Yoo, S.-H., Mohawk, J. A., Siepka, S. M., Shan, Y., Huh, S. K., Hong, H.-K., Kornblum, I., Kumar, V., Koike, N., Xu, M., Nussbaum, J., Liu, X., Chen, Z., Chen, Z. J., Green, C. B. and Takahashi, J. S. (2013) Competing E3 Ubiquitin Ligases Determine Circadian Period by Regulated Degradation of CRY in Nucleus and Cytoplasm. *Cell* 152 (5), 1091-1105.

Young, A. R. (1996) Chromophores in human skin. *Physics in Medicine and Biology* 42, 789-802.

Yu, H. S., Chang, K. L., Yu, C. L., Chen, J. W. and Chen, G. S. (1996) Low-energy helium-neon laser irradiation stimulates interleukin-1 alpha and interleukin-8 release from cultured human keratinocytes. *J Invest Dermatol* 107 (4), 593-6.

Yurchenco, P. D. (2011) Basement membranes: cell scaffoldings and signaling platforms. *Cold Spring Harb Perspect Biol* 3 (2).

Zaidel-Bar, R., Itzkovitz, S., Ma'ayan, A., Iyengar, R. and Geiger, B. (2007) Functional atlas of the integrin adhesome. *Nature cell biology* 9 (8), 858-867.

Zanello, S. B., Jackson, D. M. and Holick, M. F. (2000) Expression of the circadian clock genes clock and period1 in human skin. *J Invest Dermatol* 115 (4), 757-60.

Zhao, X., Cho, H., Yu, R. T., Atkins, A. R., Downes, M. and Evans, R. M. (2014) Nuclear receptors rock around the clock. *EMBO Reports* 15 (5), 518-528.

Zouboulis, C. C. (2004) The human skin as a hormone target and an endocrine gland. *Hormones (Athens)* 3 (1), 9-26.